DESIGN AND SYNTHESIS OF NANOPARTICLE *"PAINT-BRUSH"* LIKE MULTI-HYDROXYL CAPPED POLY (ETHYLENE GLYCOL) CONJUGATES FOR CANCER NANOTHERAPY

A Thesis

Presented to

The Graduate Faculty at The University of Akron

In Partial Fulfillment

of the Requirements for the Degree

Master of Science

Vinu Krishnan

August, 2008

DESIGN AND SYNTHESIS OF NANOPARTICLE *"PAINT-BRUSH"* LIKE MULTI-HYDROXYL CAPPED POLY (ETHYLENE GLYCOL) CONJUGATES FOR CANCER NANOTHERAPY

Vinu Krishnan

Thesis

Approved:	Accepted:
Advisor Dr. Stephanie T. Lopina	Department Chair Dr. Daniel B. Sheffer
Committee Member Dr. Amy Milsted	Dean of the College Dr. G.K. Haritos
Committee Member Dr. Daniel B. Sheffer	Dean of the Graduate School Dr. G.R. Newkome
Committee Member Dr. Daniel Ely	Date

ABSTRACT

Statistical figures outline the five-year survival rate for all cancers diagnosed between 1996 and 2002 as 66%, which depicts a marked rise from the 51% that survived in 1975-1977[1]. However, cancer still remains the second leading cause of death in the United States, following heart disease. An American Cancer Society report estimated that in 2007, there will be over 1.4 million new cancer cases and over half a million cancer deaths in the United States[1]. Although significant oncology drug discoveries have been made during the past 30 years, conventional chemotherapeutic agents exhibit poor specificity in reaching the tumor site and are often restricted by toxicity factors. The lack of a uniform biodistribution leads to harmful side-effects to healthy tissues and the need for administration of a larger than necessary drug dosage with a higher repetitive rate so as to elicit a satisfactory pharmacological response.

Wide interest in cancer nanotherapy has led to the development of nanoparticle based "smart drugs" that have not only improved pharmacological and therapeutic properties of anticancer drugs, but also offer a less invasive alternative enhancing the patient's life expectancy and quality of life as well. Dendrimers, due to their unique architecture and macromolecular characteristics are currently used extensively in research of nanoparticles for targeted and controlled drug delivery. The research objective was to design, synthesize and

characterize a novel nanoparticle based "PAINT-BRUSH" like multi-hydroxyl capped poly (ethylene glycol) (PEG) conjugate using the dendron – bishomotris that may have a potential use in targeted cancer nanotherapy.

Characterization of the conjugates suggested that the synthesis was successful; resulting in the formation of nanoparticle "PAINT-BRUSH" conjugates. It was also found that these conjugates remain stable under normal physiological conditions but would activate in response to an acidic pH (*a characteristic trait of target cancer cells*) so as to release the anticancer drug. The research also presents the relative cell viability of the human epithelial carcinoma cell line (*HeLa S3*) with respect to *in-vitro* characterization of the conjugate to determine its suitability as a drug delivery vector. The study demonstrated that bishomotris was cytotoxic in nature evidently due to the interaction of positively charged amine group with the surface of HeLa cells. It was also evident that surface modification by PEGylation has led to a distinct reduction in toxicity levels thus laying foundations for further research to realize a promising new scaffold for cancer nanotherapy.

ACKNOWLEDGEMENTS

First and foremost, I wish to thank my advisor Dr. Stephanie T. Lopina, for her constant support, words of encouragement and guidance throughout the course of my graduate studies at the Department of Biomedical Engineering of the University of Akron. Her unceasing patience and experience truly formed the basis for my confidence that motivated me to overcome each and every obstacle I encountered in this research. I feel truly proud and honored to state that my years at the University of Akron under her mentorship has truly opened the doors of my career into the world of cancer research. As I look forward to the next stage of my career, I will forever cherish the memories of my life here at The University of Akron, and hope to be in touch with Dr. Lopina for a long time.

I would like to thank Dr. Amy Milsted (Professor - Department of Biology) for being part of my graduate committee and for her valuable suggestions towards the successful realization of cytotoxicity studies of this project. No words can do justice to the gratitude I feel for her and her team, Dr. Jeffrey J. Dunmire (Research Associate-Biology), Mr. Adam Underwood and Ms. Helen for providing facilities and training in cell culture.

I would like to thank Dr. Daniel B. Sheffer (Associate Professor and Department Chair - Biomedical Engineering) for being part of my graduation committee and for having provided his expertise in the statistical analysis of this project. I would also like to thank Dr. Richard L. Einsporn (Associate Professor - Department of Statistics) for his patience and his time in helping me plan and perform a successful statistical analysis of this study. Additionally, I would like to thank Dr. Daniel Ely (Professor - Department of Biology) for serving in my committee and for providing valuable pointers towards the project. I also wish to thank Dr. Suresh K. Jewrajka (Sr. Research Scholar - Institute of Polymer Science) for his patience and support during the preliminary phase of this project and for being a good friend. Again, I specially thank Dr. Yang H. Yun, Assistant Professor of the Department of Biomedical Engineering for allowing the liberal use of his fluorescent microscope facility. On the whole, the important people mentioned above were a source of encouragement and motivation during the course of this work.

I also extend my sincere appreciation and gratitude to Mrs. Sara E. Whitson at the Mass Spectrometry Lab for being such a wonderful friend and for training me on the ESI-MS as part of my Integrated Bioscience course project. I would like to acknowledge Ms. Sarah Robenstine for having taught me the basics of LIVE/DEAD® assay.

Mere words can never sum up the overwhelming gratitude I have towards all the members (present and former included) of my research group for their suggestions with my work and for being such great friends. In particular, I would like to thank Dr. Debanjan Sarkar, Senthilram Subramanian and Parth N. Shah for their invaluable support throughout my thesis and for taking the time to answer a lot of my questions pertaining to research. Without their help my research work would not have been possible. I wish them all the best of luck in their endeavors. I also extend my thanks to Peter and Nancy for all the fun times we had together and for creating a great atmosphere at work.

I am extremely grateful to all of my friends, for without their support, I would not have been able to work here miles away from home. It would not be possible for me to list all of their names and the memories they have provided over the last few years in the acknowledgments but I would have to at least mention the following: Rohit, Adarsh, Mithun, Subash, Narayanan, Srujana, Rajesh, Vidya, Dr. Niketa, Dr. Santosh, Sajal and Sowmya. I express my sincere thanks to them for being such true friends, whom I could always count on.

Finally, I would like to thank my parents and my sister for their unconditional love and encouragement throughout my life. Without their sacrifices and prayers, I would not have had the opportunity to pursue my dreams. Thank you so much

DEDICATION

To my loving family, teachers and my dearest friends

TABLE OF CONTENTS

Page

LIST OF FIGURES

Figure Page

LIST OF SCHEMES

Scheme Page

CHAPTER I

INTRODUCTION

The five-year survival rate for all cancers diagnosed between 1996 and 2002 was 66%, which is a marked rise from the 51% that survived in 1975-1977 [1]. However, cancer still remains the second leading cause of death in the United States, following heart disease. It's been estimated that around 1,444,920 new cases of cancer were diagnosed in 2007 and another 559, 560 Americans died of cancer as well [1]. The National Institutes of Health had estimated the overall costs of cancer treatment in 2006 to be at $206.3 billion, even with a declining death rate [1]. Although significant oncology drug discoveries have been made during the past 30 years, conventional chemotherapeutic agents exhibit poor specificity in reaching the tumor site and are often restricted by toxicity factors that may limit the dosage rates as well. The lack of uniform bio-distribution leads to harmful side-effects to the healthy tissues and the need for administration of a larger than necessary drug dosage with a higher repetitive rate designed to elicit a satisfactory pharmacological response.

Since Ehrlich proposed the idea of the "magic bullet" in 1906, where concept of targeting a drug to a desired region in a controlled fashion was outlined [2], research in drug delivery has witnessed exponential progress. The focus is on developing controlled/targeted drug delivery systems that may act as a more efficient and less toxic mode of treatment. Thus, a wide array of drug delivery systems has been designed and explored over the years. Polymeric drug delivery systems based on synthetic and natural polymers have attracted attention and established themselves as pharmaceutical excipients in drug formulations [3]. The past decade has witnessed the rise of polymeric drug-delivery systems in oncology, especially with advent of biocompatible and biodegradable polymeric implants. The ability of polymers, both natural and synthetic in origin, to alter favorably the biological properties of the conjugated drugs attributes positively to the increasing interest in designing and developing polymer conjugates in drug-delivery [4-9]. These conjugates have been found to be extremely useful for the following reasons:

1) An increase in half-life in the circulatory system, increase in solubility of the conjugated drug and most importantly a reduced level of toxicity [10]

2) Polymeric conjugates with their high molecular weight exhibit enhanced accumulation in tumor tissues in contrast to normal tissues. This property is referred to as the enhanced permeation and retention effect (EPR) effect [11].

Among biodegradable polymeric implants, noteworthy examples include Zoladex ® (www.zoladex.net) and Lupron Depot® (www.lupron.com) that are capable of releasing agonists of the luteinizing hormone-releasing hormone (LHRH) and are commonly used for treatment of prostrate and other hormone-dependant cancers [12]. Another example of a biodegradable polymeric implant used post-surgery is the Gliadel ®Wafer (www.gliadel.com) that provides local delivery of chemotherapy to treat brain cancer [13]. Thus, it would be appropriate to introduce the term "polymer therapeutics" at this point [14] which refers to polymers that incorporate therapeutic agents.

Wide interest in using nanotechnology for cancer therapy has led to the development of nanoparticle based "smart drugs" that have not only improved pharmacological and therapeutic properties of anticancer drugs, but also offer a less invasive alternative for enhancing the patient's life expectancy and quality of life. These nanoscale drug delivery systems are capable of releasing chemotherapeutic agents directly inside the tumor cells by readily interacting with biomolecules on surface of the targeted cell and within them noninvasively [15]. With a size range varying from 10-100 nm, nanoparticles offer more surface area and a host array of functional groups that can be linked to therapeutic

agents, including tumor-targeting ligands such as monoclonal antibodies, and also optical, radio isotopic, or magnetic diagnostic agents. Organic and inorganic dendrimers, due to their unique architecture and well defined macromolecular characteristics have emerged as widely promising nanoparticles for drug-delivery. These are synthetic molecules characterized by a highly branched, spherical, monodispersed macromolecular structure that offers a high level of control over shape, size, branching length, and surface functionality [16, 17]. Thus, it is possible to design drug delivery systems based on tunable architectures and molecular weights so as to optimize tumor accumulation.

This research primarily focuses on bishomotris, a dendritic building block for a higher generation Newkome-type polyamide dendrimer [18] and the aim is to investigate the nature of bishomotris as a suitable drug carrier. The research goal includes synthesis of a novel conjugate with a model drug, 4-phenylbutyric acid; cytotoxicity studies of the modified carrier and an analysis of the conjugate's release characteristics. The research aims in laying a solid foundation for developing a complete multiple carrier system by exploiting the fact that macromolecules have been traditionally employed as suitable drug carriers due to their selective accumulation in malignant tissues compared to the healthy tissues by passive/active targeting, hence bypassing any undesirable side effects generated by a free drug.

1.1 Objectives of the study

The primary objective of this study is to design, synthesize and characterize a novel nanoparticle based drug carrier system based on bishomotris, which may have a potential use as a safer drug delivery system and produce more effective pharmaceutical effect than conventional chemotherapeutics. The attempt is to prove that synthesis of a PEGylated bishomotris "PAINT-BRUSH" conjugate is possible as a drug delivery scaffold. Further objectives include a comparative analysis of the in-vitro release profiles in normal physiological pH and acidic pH (a characteristic trait of cancer cells) and biocompatibility studies on the scaffold in an attempt to confirm that the novel conjugate can be used for biological applications. To achieve these primary objectives, the following studies shall be performed.

1) Design, synthesis and characterization of the PEGylated bishomotris "PAINT-BRUSH" conjugate using 4-phenylbutyric acid as a model anticancer agent. Characterization results of the compound synthesized would validate the structure of the conjugate envisioned.

2) Release studies: To measure and quantify drug release from the conjugate due to hydrolytic degradation of the ester linkages between the carrier and the model drug molecule in normal physiological buffer (7.4) and acidic buffer (5.5).

3) In-vitro cytotoxicity studies: To compare the biocompatibility properties of the dendron and its PEGylated form.

Based on the above-mentioned objectives, the following hypotheses were framed for this work.

1.2 Hypotheses

Research Hypothesis 1: *The PEGylated bishomotris "PAINT-BRUSH" conjugate can be synthesized using 4-phenylbutyric acid as a model anticancer agent for controlled and targeted drug delivery applications.*

It is hypothesized that a PEGylated bishomotris "PAINT-BRUSH" conjugate can be synthesized using 4-phenylbutyric acid as a model anticancer drug. The conjugate synthesized thus, would act as a platform for controlled and targeted drug delivery applications. The first phase of the synthesis involves the PEGylation of the dendron bishomotris where the amine group would be masked completely. The second phase involves the conjugation of the model drug, 4-phe with PEGylated bishomotris through its hydroxyl groups thus forming ester linkages between the PEGylated carrier and the model drug.

Research Hypothesis 2: *A sustained release rate can be obtained at physiological conditions; while a remarkable burst release shall be induced in an acidic condition that simulates a tumor environment using the synthesized conjugate.*

It is hypothesized that by coupling the drug to the PEGylated dendron a controlled release profile shall be attained at physiological pH 7.4 while a burst release shall be induced at pH 5.5 which corresponds to endosomal pH within the cell due to hydrolytic degradation of the ester linkage.

Null Hypothesis 1 (H_{10}): *There is no significant difference in cell viability between bishomotris and PEGylated bishomotris.*

There is no statistically significant difference in cell viability for samples treated with bishomotris and PEGylated bishomotris.

Alternate Hypothesis 1 (H_{1a}): *There is a significant difference in cell viability between bishomotris and PEGylated bishomotris.*

There exists a statistically significant difference in cell viability for samples treated with bishomotris and PEGylated bishomotris.

Null Hypothesis 2 (H_{II0}): *There is no significant difference in cell viability in a dose-response study of the PEGylated bishomotris.*

There is no statistically significant difference in cell viability for samples treated with variant concentrations of PEGylated bishomotris for different incubation periods.

Null Hypothesis 2 (H_{IIa}): *There is a significant difference in cell viability in a dose-response study of the PEGylated bishomotris.*

There exists a statistically significant difference in cell viability for samples treated with variant concentrations of PEGylated bishomotris for different incubation periods.

CHAPTER II

SIGNIFICANCE AND BACKGROUND OF STUDY

In view of all existing applications in nanotechnology, its medical application i.e. nanomedicine holds enormous potential in drug delivery to improve life expectancy and quality of life of the patient. The past three decades have witnessed evolution of formulations that control rate and period of drug delivery (time-release medications). The advent in knowledge of the human body and discovery of bioactive molecules and gene therapies has led to an explosion of new and potential treatments [19]. Yet obstacles like lack of cancer/tumor target specificity, lack of an effective delivery system both at cellular and intracellular level, lack of an efficient predictive preclinical model, and the gradual development of drug resistance have hindered the very progress of developing effective treatment modalities. Hence, researchers are currently focused on overcoming obstacles that prevent them from optimizing mechanisms that can deliver these treatments in the most effective manner.

2.1 Drug Delivery – Targeted and Controlled

Drug delivery, in essence refers to delivery of a pharmaceutical compound to humans or animals. As outlined earlier, efforts are on to develop - 1) targeted drug delivery in which drug is only active in the targeted area of the body (for example, in cancerous tissues) thus, bypassing harmful side-effects that cause damage to healthy tissues and 2) controlled drug delivery (sustained release formulations) in which the drug is released over a period of time in a controlled manner from a formulation. Targeted drug delivery can be achieved by exploiting the fact that a typical malignant tissue is characterized by an amplified expression of certain proteins or receptors. For instance, the surface of colorectal and various forms of lung and ovarian cancer are characterized by the presence of a carcinoembryonic antigen [20]. Drug targeting can thus be achieved by functionalizing the parent drug with structural moieties such as specific ligands (antibodies, peptides, nucleic acid aptamers, carbohydrates, and small molecules) that would lead to signal based preferential accumulation of the therapeutic agent at the target tissue.

The underlying advantage of a controlled drug delivery system can be understood from the figure below (Figure 2.1) [21]. The figure depicts change in concentration of drug in blood plasma as a function of time in a conventional drug delivery system following the administration of a single dose of therapeutic agent. On administering the first dose, there occurs a sudden rise of drug

concentration levels in blood plasma, which reaches the maximum peak value; and then undergoes an exponential decay when the drug metabolizes and gets eliminated from the body. The cycle continues in a similar fashion for subsequent doses. The drug concentration cycles can also be mapped onto a therapeutic window of activity, called the therapeutic index which is defined as a prescribed set of concentration limits for the drug to be effective. If the level of drug concentration goes above the maximum prescribed limit, the effect can be toxic in nature; while a level below would render it ineffective. Any attempt to limit the dosage rate to a single administration and to maintain the drug concentration above the minimum effective limit would only propel the blood plasma concentrations into the toxic region since this can be made possible only by increasing the dose-size. The alternative then is to administer safe doses at periodic intervals so as to ensure optimum drug levels in the blood plasma which is in fact inconvenient and not at all advisable from the patient's safety point of view.

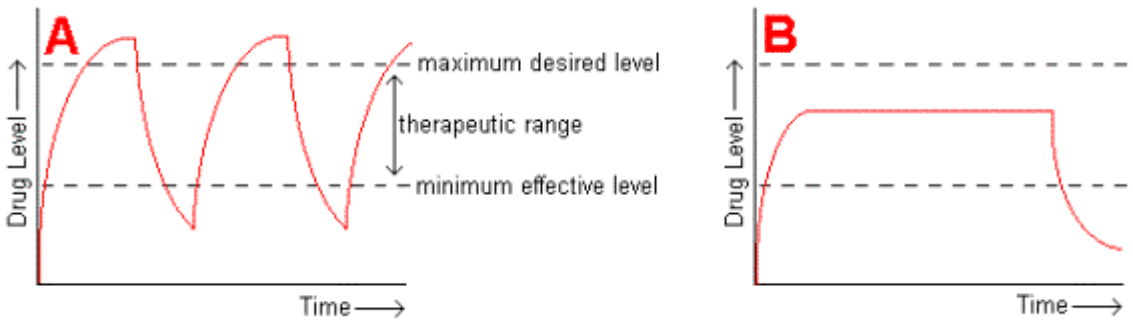

Figure 2.1 Drug level profiles achieved by conventional (A) and controlled release (B) drug delivery systems [21]

The lack of uniform bio-distribution of drugs leads to harmful side-effects to healthy tissues and the need for administration of a larger than necessary drug dosage with a higher repetitive rate so as to elicit a satisfactory pharmacological response. Thus, it is imperative that researchers develop a combination of targeted drug delivery and controlled-release technologies in order to safely shepherd drugs through specific areas of the body; for instance, a healthy bone or tissue that might be adversely affected. The objective is to provide a highly efficient and less harmful solution to overcome limitations that exist in conventional chemotherapy. Research at an interdisciplinary level between polymer chemistry and biomedical sciences has evolved a new class of chemotherapeutic agents termed polymer therapeutics. Polymer therapeutics refers to polymers incorporated with therapeutic agents. These therapeutic

agents can be in the form of polymeric drugs, polymeric micelles to which the drug is bound covalently or as components of water-soluble polymer-drug conjugates.

2.2 Polymer Therapeutics

Polymer therapeutics uses design principles based on advanced polymer chemistry and molecular level precision engineering along with knowledge of pathophysiology of normal and diseased tissues to help realize a full therapeutic potential. The importance and feasibility of using polymer therapeutics has been widely demonstrated by initial polymer-drug conjugation and characterization studies carried out by Ringsdorf [22], Shen and Ryser [23], Chu with coworkers [24] and Blair and Ghose with collaborators [25]. They also demonstrated conjugate retention in serum, its endocytotic cell entry, elevated intracellular levels of the conjugate, and the cytotoxicity nature as well. Langer stated that polymeric drug delivery systems are expected to (i) maintain constant drug levels in a therapeutically desirable range, (ii) reduce potentially harmful side effects (iii) decrease amount of drug needed (iv) facilitate easy administration of the drug for pharmaceuticals with short in vivo half-lives (e.g., proteins and peptides) and finally (v) provide a less invasive method of dosing and an improved patient compliance in accordance with the prescribed drug regimen

[26]. Thus, polymer therapeutics undoubtedly play an important role in optimizing an effective drug delivery system.

The emergence of these polymer-drug conjugates is an extension of Ringsdorf's vision for an ideal drug delivery system (Figure 2.2) which is based on the covalent link between the drug and a polymeric backbone through a physiologically labile bond.

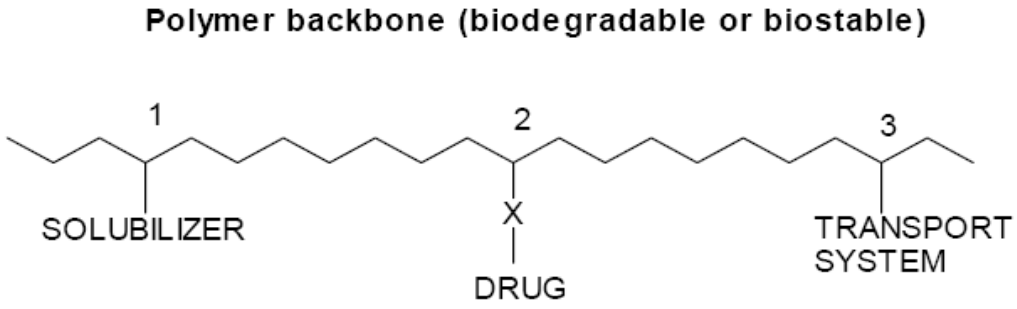

Figure 2.2 Ringsdorf's model drug delivery system [27]

The model is characterized by the presence of a solubilizer, polymer-drug covalent linker, and a biocompatible polymeric carrier (transport system) [28]. The solubilizer may be a functional group that imparts high solubility to the entire system. Thus, drug conjugation to a water-soluble polymer system restricts cellular uptake to the endocytic pathway, making way for tumor-specific targeting of low-molecular weight anti-cancer agents. Simultaneously, polymer-drug conjugation improves the therapeutic index of a toxic drug and reduces the

necessity for repeated high doses. Also a decreased clearance rate is observed giving rise to an increased circulation time for the conjugate to arrive and accumulate at the target. In addition, a solubilizer would also enable solubilization of hydrophobic drugs, thus enhancing the possibility of an intravenous administration of the system which is more convenient than conventional chemotherapy.

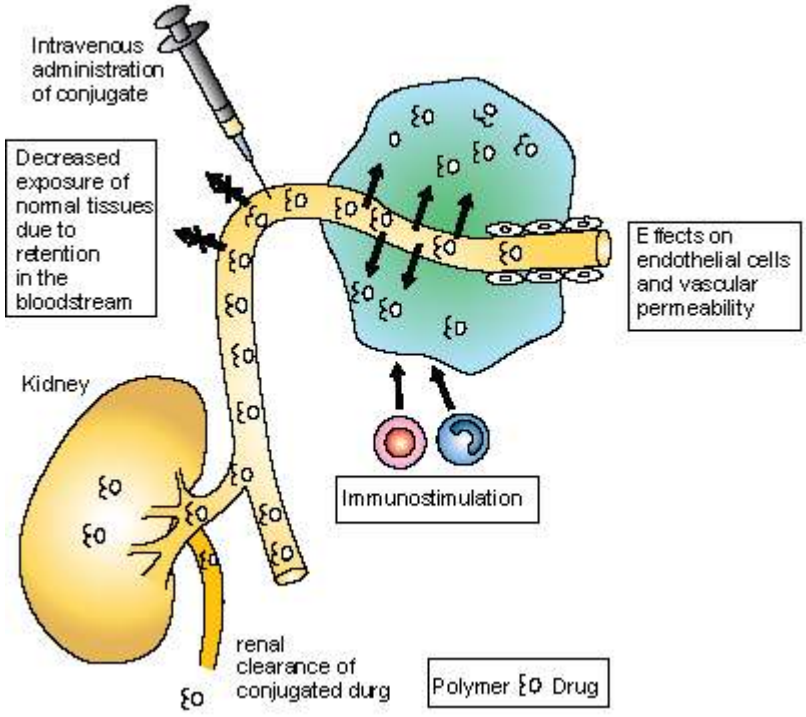

Figure 2.3 Mechanism of action of polymer-drug conjugates [29]

The mechanism of action of polymer-drug conjugates is as outlined in figure 2.3. The polymer-drug linker is typically a covalent linkage created as a result of attachment of drug molecule to the polymeric carrier. The linkage has assumed different forms such as ester [30], carbonate [30], amide [31], malonate [32], or disulfide [33] linkers ever since Ringsdorf proposed his model. Apart from these, pH-sensitive cis-aconityl, hydrazone and acetal linkages have also been used [34]. The linker can act as a site-specific/rate specific release mechanism. In other words, it would act as a bioresponsive system that remains stable during transportation to the tumor and would commence drug release at an optimum rate once ingested within tumor cells by cell mediated endocytosis or enhanced permeability and retention effect (explained in section 2.3) when they get hydrolyzed due to acidic pH (6.5-4.0) within endosomes and lysosomes. The targeting moiety, e.g. an antibody, is a protein that directs the entire conjugate to the targeted site based on its affinity towards the amplified expression of proteins or receptors characteristic to cancer/tumor cells. Antibodies or immunoglobulins are proteins found in blood or other body fluids of vertebrates used by the immune system to identify and neutralize foreign bodies such as bacteria and viruses. The polymeric carrier that forms the structural framework of the entire system is the last component of Ringsdorf's ideal drug delivery system [29]. A specific water-soluble polymer is selected and designed to be the bioactive agent. Since the focus is to facilitate drug, protein or

gene delivery selection of a suitable polymer carrier is a critical factor in designing an effective delivery system. The molecular mass and physico-chemical properties of the carrier act as drivers governing biodistribution, elimination and metabolism of a complete conjugate. Other factors to be kept in mind while selecting a carrier is its non-toxicity and non-immunogenic properties. A wide range of polymeric carriers including Poly (ethylene glycol) (PEG) [35, 36], polyglutamicacid (PGA) [37, 38] and N-(2-hydroxypropylmethacrylamide) (HPMA) [39, 40] copolymers is being investigated currently for use as a suitable carrier.

2.3 Cancer Nanotherapy

Targeted cancer nanotherapy offers a potentially safe and effective mode of treatment for patients. It enhances quality of life and life-expectancy rates as well. The advantage of using nanotechnology in tumor targeting can be outlined by the fact that a typical human cell size spans in the range of 10-20μm and cell organelles range from a few nanometers to a few hundred nanometers in diameter. This provides a solid platform for nanosized delivery vehicles to readily interact with characteristic proteins and receptors present on target cell surface in a noninvasive manner. At the same time, the devices ensure that surrounding normal cells are left intact.

Generally, a chemotherapeutic agent is combined with a natural or synthetic polymer of nanoscale dimensions in such a way that the agent is completely encompassed within the polymer system. Subsequently release takes place in a predetermined manner leading to what is known as a controlled-release mechanism. The polymer system works by releasing drugs as a result of modifications it undergoes in response to tumor characteristics such as acidic pH and high temperature [41]. These nanosized delivery systems are novel entities that resort to chemical conjugation rather than entrapping or solubilizing drug molecules in conventional chemotherapeutics. On nanotechnology levels in polymer therapeutics the primary objective would be to design and develop better defined polymer structures rather than a heterogeneous, random-coiled polymeric carrier. Hence, researchers are presently focused on developing delivery systems of nanoscale dimensions (5-100) nm that are capable of targeting and controlling release rate of anti-cancer drugs directly inside the tumor cells.

Thus, use of nanoparticles as a potential targeted/controlled drug delivery system offer significant advantages such as the ability to target specific locations in the body, the reduction of drug quantity needed to attain a particular concentration in target vicinity, a reduced dosage rate, and finally a reduced drug concentration at the non-targeted sites (e.g. Abraxane, a recent FDA approved albumin nanoparticle based drug delivery system to treat breast, lung,

ovarian, and neck cancers) [42]. Nanoparticles offer vast surface areas with multiple sites possessing functional groups that can be manipulated and correspondingly linked to therapeutic agents and tumor-targeting ligands such as monoclonal antibodies. The programmed nanoparticles can be used to target tumor antigens (biomarkers) and tumor vasculature with high affinity and specificity as well. In essence, two primary targeting schemes could be outlined for nanoscale drug delivery vehicles, passive targeting and active targeting schemes.

2.3.1 Passive Targeting

The passive targeting scheme generally takes advantage of a tumor tissue's permeability. With a diffusion-limited size of about $2mm^3$ [43, 44], tumor tissues would remain at this size until angiogenesis initiates so as to grant access to an increased rate of blood circulation [45]. Further the tumor site develops into a leaky, defective architecture with an impaired lymphatic drainage as a result of rapid vascularization to permit more blood flow to the fast growing cancerous tissues. The enhanced permeability and retention (EPR) effect comes into play in this context. EPR is basically the property by which molecules of variant sizes, typically liposomes or macromolecular drugs, tend to accumulate in tumor cells more than they do in normal tissues. Presence of vascular endothelial growth factor (VEGF) in solid tumors stimulates the production of

blood vessels so as to facilitate rapid growth of tumor cells. Generally, tumor cells aggregate in sizes as small as 150-200μm and depend on blood circulation carried out by the newly developed vasculature for their nutritional and oxygen supply needs. The newly formed tumor vessels have a leaky, defective architecture characterized by the lack of smooth muscle layer, innervations with wider lumen and impaired functional receptors for angiotensin II. They also possess a line of poorly aligned defective endothelial cells along with an ineffective lymphatic drainage system. These contribute to abnormal molecular and fluid transport dynamics that lead to rapid accumulation of macromolecular drugs within the cells [46]. To ensure proper passive targeting by the EPR scheme, it is essential to control size and surface properties of drug delivery nanoparticles. This is to prevent any uptake by the reticuloendothelial system (RES), a part of the immune system where phagocytic macrophages may get rid of the nano-conjugates without permitting a proper effective action [47]. For effective delivery, it is important that circulation times and target specificity should be maximized. Hence, the optimum diameter should be less than100 nm and surface should be preferably hydrophilic in nature. The hydrophilic nature of the surface would prevent the particle from getting adsorbed onto plasma proteins. This can be achieved by coating the surface with PEG tails or poloxamines, polysaccharides and poloxamers etc [48, 49].

An alternative passive targeting scheme is employing a tumor-activated prodrug therapy where characteristics unique to tumor environment play a vital role in ensuring proper delivery. The anticancer agent is conjugated to a polymeric carrier through a characteristic spacer or linker which remains inactive until it reaches the target [50]. This is followed by subsequent hydrolysis or degradation of the spacer or linker by the acidic pH, high temperature or cancer-specific enzymes at the tumor site as a result of which the nanoparticle releases the drug [51, 52]. Direct local delivery of anticancer agents to tumors is yet another passive targeting scheme where the drug can be excluded from systemic circulation. The process however is highly invasive and painful as it involves injections or surgical procedures. Passive tumor targeting's primary limitation is its failure to achieve an optimum level of drug concentration at the tumor site. This results in low therapeutic efficacy and elicits undesirable side effects as well [53].

2.3.2 Active Targeting

Active targeting is usually achieved by conjugating a targeting moiety to the nanoparticle so as to provide a preferential accumulation at the tumor site (organs, individual cancer cells, intracellular organelles etc.) The approach is primarily based on specific interactions such as antibody-antigen and ligand-receptor. The amplified expression of antigens or receptors in numerous cancer

cells leads to a characteristic affinity as a result of which the entire conjugate is ingested within the targeted cell via receptor-mediated endocytosis [54]. For instance, the large number of folate receptors present on the surface of various cancers, including breast, lung malignancies, brain, ovary, and kidney often organize themselves in clusters and bind preferably to the targeting ligand attached to the nanoparticulate carrier. Studies using surface plasma resonance have revealed that folate-conjugated PEGylated cyanoacrylate nanoparticles possess ten-fold higher affinity for folate receptors than free folate [55]. Confocal microscopy studies have also demonstrated selective uptake and endocytosis of folate-conjugated nanoparticles by tumor cells bearing folate receptors [49, 55]. Engineered antibody based tumor-targeting is still in its infancy but holds real potential for an effective targeting system. Subsequent release of anticancer agents takes place either due to the action of lysosomal enzymes that come into play once the cells ingest the nanoparticles or due to hydrolysis of the spacer or linkers that hold the agents to the carrier molecule. The active targeting mechanism acts an alternative route for overcoming multiple drug resistance (MDR) a major challenge in chemotherapy where overexpression of the plasma membrane P-glycoprotein (Pgp) acts as an efflux pump to throw positively charged anticancer drugs out of the cell [56, 57]. For instance, studies have been performed with regards to doxorubicin to develop poly (cyanoacrylate) nanoparticles to overcome multiple drug resistance [58]. Doxorubicin, a widely

used DNA-interacting chemotherapeutic agent, is highly resisted by many tumor cells and is a Pgp substrate as well. Adsorption of these doxorubicin loaded cyanoacrylate nanoparticles onto the plasma membrane, and subsequent release of the drug, would lead to saturation of Pgp with positively charged doxorubicin. Subsequent neutralization of these positive charges takes place by negatively charged degradation products of the polymer i.e. poly (cyanoacrylate) nanoparticles that form an ion pair [58]. This enhances the diffusion of the drug across the plasma membrane. Another way of overcoming the MDR effect is to selectively kill resistant tumor cells. The approach here as explained by Blagosklonny, et al. [59] is based on a temporary increase in resistance of sensitive cells to certain drugs by using protectors that act as pharmacological inhibitors of cell death. For instance, vinblastine, an anticancer drug that acts as substrate for a protein encoded by the human gene ABCC2 appears to contribute to drug resistance in normal mammalian cells. Thus by increasing the resistance in sensitive cells that do not posses active drug efflux pumps, the MDR cells pump out the protectors. This paves the way for chemotherapeutic agents to act on unprotected MDR cells while leaving protected sensitive cells untouched. The strategy of selective killing can be implemented in treating aggressive and resistant cancers while abolishing simultaneously dose-limiting side-effects of chemotherapy [60].

2.4 Dendrimers

Dendrimers, an emerging class of drug encapsulating nanoparticles (NPs) have found wide attraction as an option to deliver antitumor drugs due to their unique architecture and well defined macromolecular characteristics. Extensive reviews have been carried out regarding the pharmaceutical and biomedical applications of dendrimers [61-64]. These are synthetic molecules, characterized by a highly branched, spherical, monodispersed macromolecular structure with an average diameter of 1.5-14.5 nm making it an ideal platform for controlled/targeted drug delivery. Early synthesis of dendrimers was pioneered by Tomalia [65] and Newkome [66] in the 1980s.

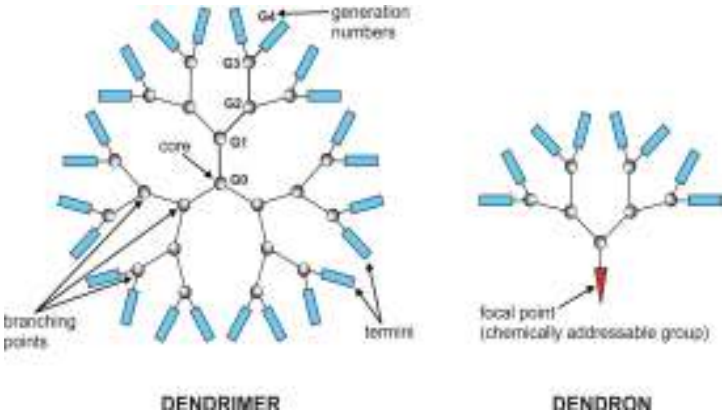

Figure 2.4 a Typical Dendrimer and a Dendron

(Adapted with permission from Oleg Lukin; email id:olukin@ccmsi.us)

The dendrimer consists of an initiator core with highly branched layers of repeating units possessing multiple active terminal groups that can be functionalized with the drugs that need to be delivered. A typical dendron molecule is a building block towards a fully grown dendrimer (Figure 2.4). The advantage a dendrimer offers over traditional linear polymers is high level of control over its shape, size, branching length, and surface functionality. These NPs offer multiple sites for covalent attachment of therapeutic agents with a suitable spacer, targeting ligands and water-solubilizers as well depicting the complete agreement with Ringsdorf's vision of an ideal drug delivery system. Thus, it is possible to design drug delivery systems based on tunable architectures and molecular weights so as to optimize tumor accumulation and treatment. One of the most widely used commercially available dendrimers in biological research is the Starburst polyamidoamine (PAMAM) dendrimers manufactured by Dendritech (Midland, MI, USA). PAMAM dendrimers are built by polyamide branches with tertiary amines as focal points. Another commercially available dendrimer is the "Poly (Propylene Imine)"; the PPI dendrimers with propyl amine spacer moieties and primary amines as end groups. The interior of PPI dendrimers are characterized by the presence of numerous tertiary tris-propylene amines [67].

Despite the promise dendrimers have shown as drug carriers; further *in vitro* and *in vivo* evaluations are necessary to study the biocompatibility, cytotoxicity and biodistribution of dendrimers and dendrimer based delivery systems. Roberts et al. [68] found that PAMAM toxicity is dose and generation dependent in vitro. His results demonstrated that low generation dendrimers were not as toxic as compared to the higher ones. Malik et al. [69] found that cationic dendrimers characterized by the presence of amine end groups caused haemolysis and cytotoxicity. The toxicity effect is attributed to cell membrane disruption caused through initial adhesion by electrostatic attraction to the cell surface groups which are negatively charged followed by formation of a hole or endocytosis that caused the cell to lyse [70]. Although the exact mechanism of plasma membrane destabilization has not been elucidated in detail the cytotoxicity profile of cationic dendrimers seem to be governed to a great extent by the primary amine surface groups, e.g. melamine based dendrimers characterized by amine surface groups have in vitro toxicity identical to amino PPI and PAMAM dendrimers [71]. Malik et al. stated that unsuitable dendrimers such as cationic PAMAM dendrimers may be used biologically as long as the surface was characterized by presence of anionic or neutral groups. Amino terminated G4-PAMAM dendrimers were shown to be more toxic towards muscle cells compared to cationic liposomes and proteins. Studies also

demonstrated that lysis of neuroblastoma cells occurred following one-week of exposure to amino-terminated PAMAM and PPI dendrimers [72].

One way to combat this issue of cytotoxicity is to encapsulate or "quench" the charged surface amines with another functional group that would shield the basic nitrogen atoms from interacting with the surroundings [73]. It has been shown that a dendrimer's cytotoxicity is highly dependent on the degree of substitution on the surface amine. Hence, primary amines are more toxic in nature as compared to secondary and tertiary alkyl amines. In a highly substituted amine, the positive charge on the nitrogen atom is shielded from interacting with its surroundings by the alkyl substituents that have a larger size compared to the hydrogen atoms present on a primary amine [74, 75]. In addition, presence of anionic surface groups promote non-adhesion to negatively charged cell membranes thus diminishing lysis to a great extent. Studies have also demonstrated that dendrimers with hydroxyl surface functionalities show less cytotoxicity when compared with those with carboxy-terminated groups [76]. A prominent way of quenching the charged surface amine is the introduction of uncharged PEG chain on the dendrimer surface. One reason that can be attributed to the inertness imparted may be due to the ability of PEG to uphold a sufficient hydration of the surface along with charge neutrality and also suppressing hydrophobic or ionic interactions with cell membrane [77].

The research here involves the use of a dendritic building block bishomotris, for a higher generation Newkome-type polyamide dendrimer as a polymeric carrier. The primary advantage of using such a dendrimer apart from being highly soluble in water is the presence of anionic functionalities which makes it potentially less cytotoxic as compared with PAMAM dendrimers. The other major advantage is, it is characterized by the presence of a single primary amine group that can be shielded completely by alkyl substitution. The research here involves the use of a poly (ethyleneglycol) (PEG) tail as the substituent. In addition, PEG is also used as a solubilizer and the presence of a biofissionable ester linkage acts as the vital polymer-drug linker for the novel system. Ester hydrolysis or degradation takes place in an acidic environment which is a characteristic feature of tumor sites. As a result of hydrolysis, subsequent release of the drug molecule also takes place [78]. PEG is a highly favored entity in drug delivery applications because of the wide array of biological traits it possess including non-toxicity and non-immunogenicity. PEG being highly soluble in water imparts solubility to hydrophobic drugs. The one another advantage of using PEG in the conjugate is the ease of manipulation of its hydroxyl end group in various ways so as to facilitate the covalent attachment of different molecules or targeting ligands to it. Since it is absolutely essential that an increased in vivo circulation time should exist in targeted drug delivery compared to conventional dosing, attachment of a PEG tail to the carrier would shield the entire conjugate

from being cleared by the reticuloendothelial system's phagocytic cells and from a rapid renal clearance rate as well. Finally, the PEGylated carrier is conjugated with a model anticancer drug 4-phenylbutyirc acid so as to form a complete "PAINT-BRUSH" conjugate (Figure 2.5). 4-phenylbutyric acid (Figure 2.6) is selected as the model anticancer drug since its structure is in complete agreement with the antitumor agent chlorambucil (Figure 2.7) with the exception that the nitrogen mustard group vital to inhibit DNA proliferation in cancerous cells is absent.

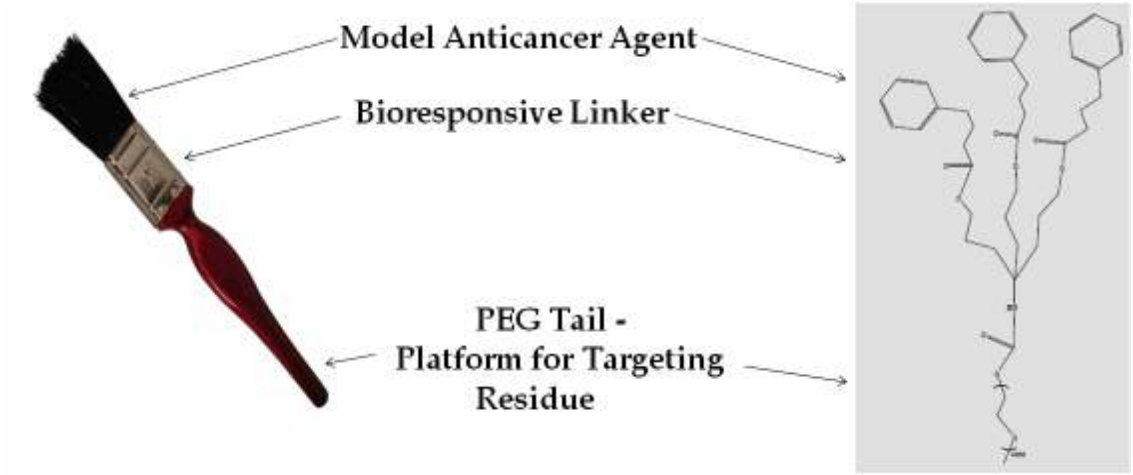

Figure 2.5 The "PAINT-BRUSH" Conjugate

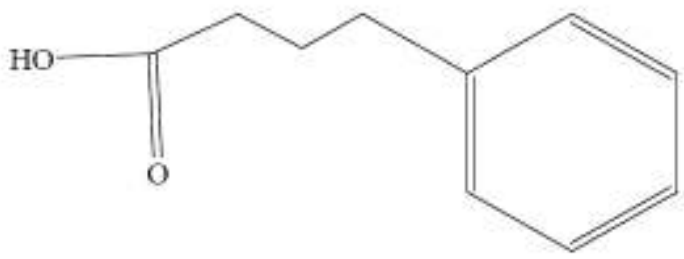

Figure 2.6 - 4-phenylbutyric acid

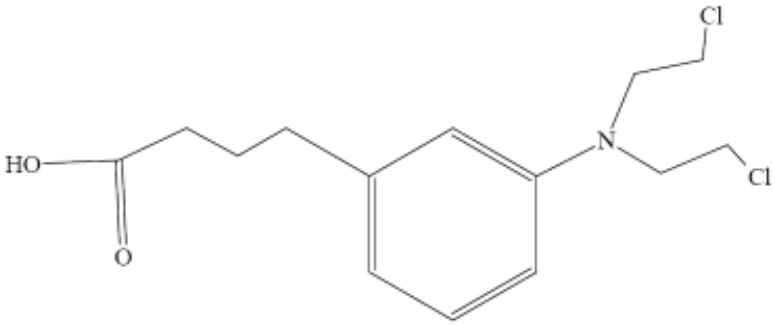

Figure 2.7 Chlorambucil

The uniqueness in the "PAINT-BRUSH" model envisioned lies in the fact that the structure can be exploited in more than one way to develop novel hybrids that may have the ability to carry antibody; enzymes or even additional PEO/PEG linkages that may serve to the system's biocompatibility, along with its purpose as a targeted drug delivery system for malignancies. Thus, the research aims in laying a solid foundation for the development of a complete multiple carrier system by exploiting the fact that macromolecules have been traditionally employed as suitable drug carriers due to their selective accumulation in malignant tissues compared to the healthy tissues by passive/active targeting, thus bypassing harmful side-effects.

CHAPTER III

SYNTHESIS AND CHARACTERIZATION OF NOVEL NANOPARTICLE *"PAINT-BRUSH"* LIKE MULTI-HYDROXYL CAPPED – POLY (ETHYLENE GLYCOL) CONJUGATES

3.1 Introduction

Ongoing efforts among drug delivery researchers worldwide to enhance the therapeutic efficacy of chemotherapeutic agents have led to a significant thrust to explore dendrimers as a potential drug delivery scaffold. A dendrimer with an initiator core is generally composed of multiple branching layers with numerous sites for the covalent attachment of chemotherapeutic agents with a suitable spacer, targeting ligands and water-solubilizers thus confirming Ringsdorf's vision of an ideal drug delivery system (Figure 2.2). A dendron molecule is a building block towards a fully grown dendrimer (Figure 2.4).

Our primary research hypothesis involves the use of a dendron bishomotris, for a higher generation Newkome-type polyamide dendrimer as a polymeric carrier. The dendron characterized by hydroxyl surface functionalities also possess a single primary amine group that can be shielded completely by the

use e of a poly (ethyleneglycol) (PEG) tail as the substituent which also acts as a solubilizer. The formation of a biofissionable ester linkage as a result of conjugation with a model anticancer drug 4 phenylbutyric acid to the dendron's hydroxyl functionalities acts as the vital polymer-drug linker that may undergo hydrolysis or degradation in an acidic environment (a characteristic feature of tumor sites) so as to facilitate the subsequent release of the drug molecule as well [78]. 4-phenylbutyric acid (Figure 2.6) is selected as the model anticancer drug since its structure is in complete agreement with the antitumor agent chlorambucil (Figure 2.7) with the exception that the nitrogen mustard group vital to inhibit DNA proliferation in cancerous cells is absent. Apart from providing an increased *in-vivo* circulation half life, PEG also facilitates the ease of manipulation of its hydroxyl end group for the attachment of targeting ligands. Thus, the pegylated carrier is conjugated with the model anticancer drug so as to form a complete "PAINT-BRUSH" conjugate (Figure 2.5).

The vision is to utilize this novel dendrimer based nanodevice in cancer nanotherapy. In this chapter, we describe the synthesis and structural characterization of these novel devices.

3.2 Materials and Methods

Details pertaining to materials required for synthesis of novel "PAINT-BRUSH" conjugates are disclosed herewith. The corresponding schematic procedures involved are also discussed.

3.2.1 Materials

Methoxy poly (ethylene glycol) (mPEG) (MW=2000), *p*-nitrophenyl chloroformate (4-NPC), triethylamine (TEA), acetonitrile, bishomotris (MW=205.29), dicyclohexylcarbodiimide (DCC), dimethylaminopyridine (4-DMAP), phenylbutyric acid (4-phe) (MW=164.2), and all solvents including diethyl ether, dimethyl sulfoxide (DMSO), dimethylformamide (DMF), dichloromethane (DCM), hexane and phosphate buffered saline (PBS (10x; pH 7.4 & pH 5.5) were purchased from Sigma-Aldrich (St. Louis, MO) and used directly without further purification.

3.2.2 Synthesis of "PAINT-BRUSH" conjugate

The initial part of this study involves the design and synthesis of PEGylated bishomotris "PAINT-BRUSH" conjugate using 4-phenylbutyirc acid as a model anticancer agent. The synthesis of the "PAINT-BRUSH" conjugate involves three phases –

- Preparation of activated methoxy poly (ethylene glycol) (mPEG: M.W= 2000)
- Preparation of pegylated bishomotris
- Conjugation of PEGylated bishomotris with model anticancer drug 4-phenylbutyric acid (4-phe)

3.2.2.1 Preparation of activated mPEG-2000

Activated mPEG-2000s were obtained by using the procedure described elsewhere [79]. 1.8 g of mPEG 2000 (0.9 mmol) was dissolved in acetonitrile (12.5 ml) and 0.5 ml triethylamine (TEA). This was added drop wise to a solution of 4-nitrophenylchloroformate (0.36 g) in 25 ml of acetonitrile. The mixture was continuously stirred for the first 3 hours at 5°C and then for 24 hours at room temperature. The by-product triethylamine-HCL salt was removed overnight by crystallization from a saturated solution of acetonitrile at a low temperature. The residual 4-NPC was removed by washing the saturated solution with diethyl ether. Activated mPEGS or mPEG p-nitrophenylcarbonate was recovered by

evaporation under reduced pressure. The formation of activated mPEGS was confirmed by ^{1}H NMR analysis.

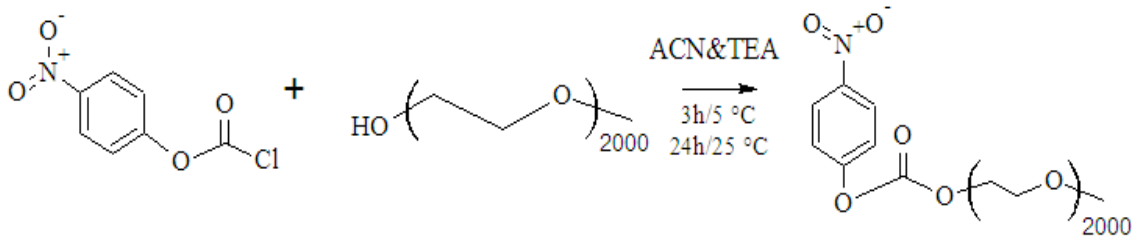

Scheme 3.2.2.1 Synthesis of activated mPEG 2000

3.2.2.2 Preparation of PEGylated bishomotris

PEGylation of bishomotris was carried out as described in Hu Yang et al. 2004 [79]. A solution of 0.226 g bishomotris (1.1 mmol) in 10ml of dimethyl sulfoxide (DMSO) was prepared and to this were added 1mmol of activated mPEGs. The solution was stirred for 72 hours at room temperature and was evaporated to dryness by rotary evaporation. Purification was carried out by column chromatography method using a silica-gel packed column with a mixture of dichloromethane and hexane solvents as eluent (1: 3). Structure confirmation was validated by ^{1}H NMR characterization.

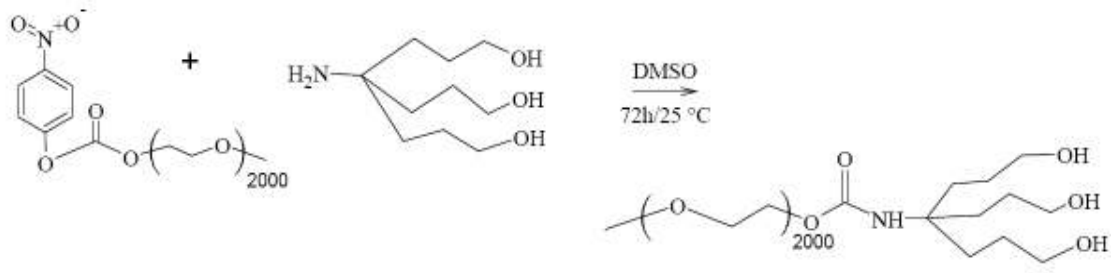

Scheme 3.2.2.2 Synthesis of PEGylated bishomotris

3.2.2.3 Conjugation of PEGylated bishomotris with model drug 4-phenylbutyric acid (4-phe)

To a stirred solution of 2.2 g of PEGylated bishomotris (1 mmol) in 10 ml dimethylformamide (DMF), 0.64 g DCC (3.1 mmol) and a pinch of DMAP were added. The mixture was stirred for 10 minutes following which 0.5 g of 4-Phe (3.1 mmol) was added and the solution was continuously stirred for 48 hours at room temperature. The DCC urea byproducts formed were removed by reprecipitation from a mixture of hexane-dichloromethane solvents, followed by filtration. The filtrate obtained was evaporated to dryness by rotary evaporation so as to obtain the final product. The final product was purified by column chromatography method using a silica-gel packed column with a mixture of dichloromethane and hexane solvents as eluent (1: 3). Structure confirmation of the paint-brush conjugate was validated by ^{1}H NMR characterization.

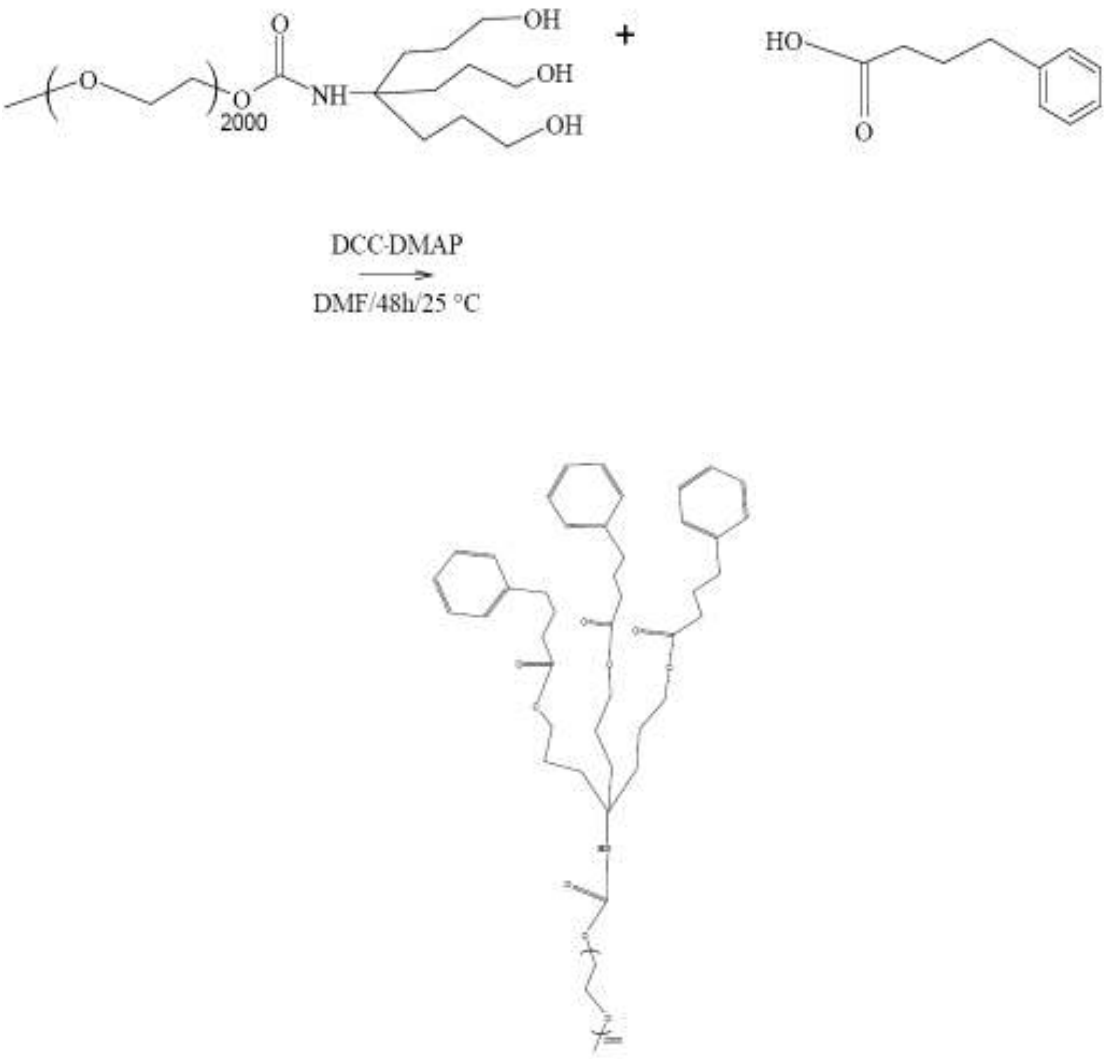

Scheme 3.2.2.3 Synthesis of "PAINT-BRUSH" conjugates

3.3 Chemical Characterization

The products derived at each phase during the synthesis of "PAINT-BRUSH" conjugates were characterized by recording their corresponding ^{1}H-NMR spectra on the Varian Gemini 300 MHz spectrometer with the solvent proton signal as the standard. The solvent used in NMR characterization was Chloroform-d ($CDCl_3$, 99.8%) which was obtained from Cambridge Isotope Laboratories, Inc. 5mg of each sample was dissolved in deuterated solvent before measurement. The chemical shift of $CDCl_3$ is 7.26 ppm.

The typical chemical shifts for 1) 4-NPC (Figure 3.1): ^{1}H-NMR (300 MHz, $CDCl_3$): δ 8.35 and 7.46 ppm (characteristic doublets) - 2) Activated mPEG (Figure 3.2): ^{1}H-NMR (300 MHz, $CDCl_3$): δ 8.29 and 7.37 (shift in doublets); 3.64 ppm (PEG-CH_2-); 3.37 ppm (PEG-OCH_3) - 3) PEGylated bishomotris (Figure 3.3): ^{1}H-NMR (300 MHz, $CDCl_3$): δ 6.97 ppm (-NH-); 3.64 ppm (PEG-CH_2-); 3.37 ppm (PEG-OCH_3); 2.64 ppm, 2.17 ppm, 1.43 ppm (-CH_2- in BH) - 4) The "Paint-Brush" Conjugate (Figure 3.4): ^{1}H-NMR (300 MHz, $CDCl_3$): δ 7.28 ppm, 7.23 ppm & 7.19 ppm (-C_6H_5); 6.69 ppm (-NH-); 3.72-4.12 ppm (-CH_2-O-CO); 3.64 ppm (PEG-CH_2-); 3.38 ppm (PEG-OCH_3); 3.24 ppm, 1.57 ppm, 1.25 ppm (-CH_2- in BH)

NMR of 4-Nitrophenyl Chloroformate (4-NPC)

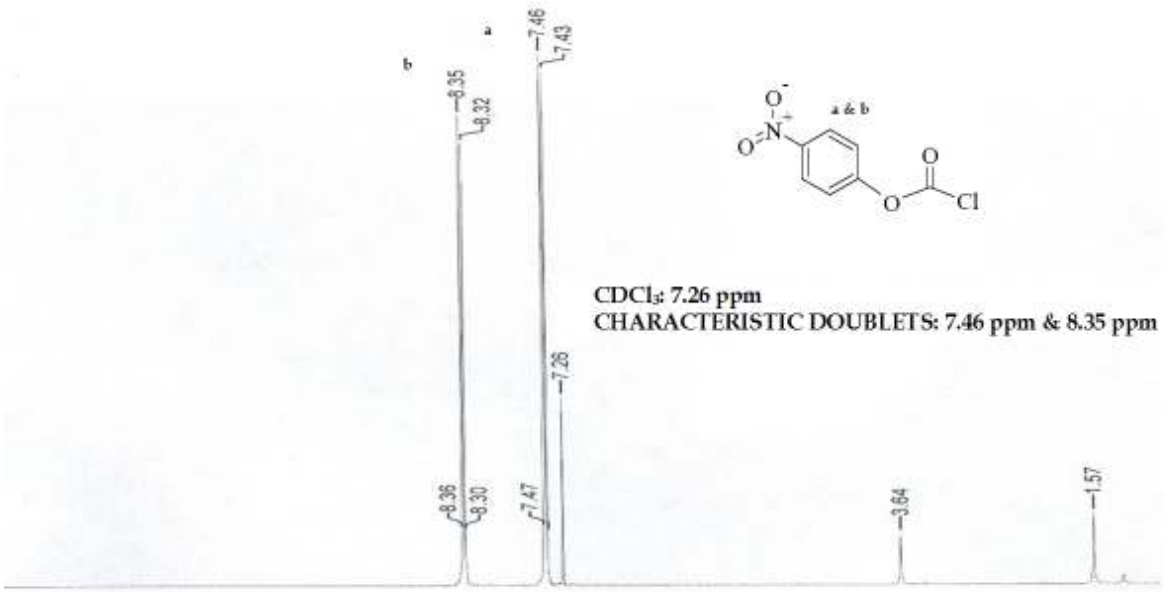

Figure 3.1 A 300 MHz ^{1}H NMR spectrum of 4-nitrophenyl chloroformate ($CDCl_3$: 7.26 ppm; doublets at 7.46 ppm & 8.35 ppm)

NMR of Activated mPEG2000 (4-nitrophenyl carbonate-mPEG)

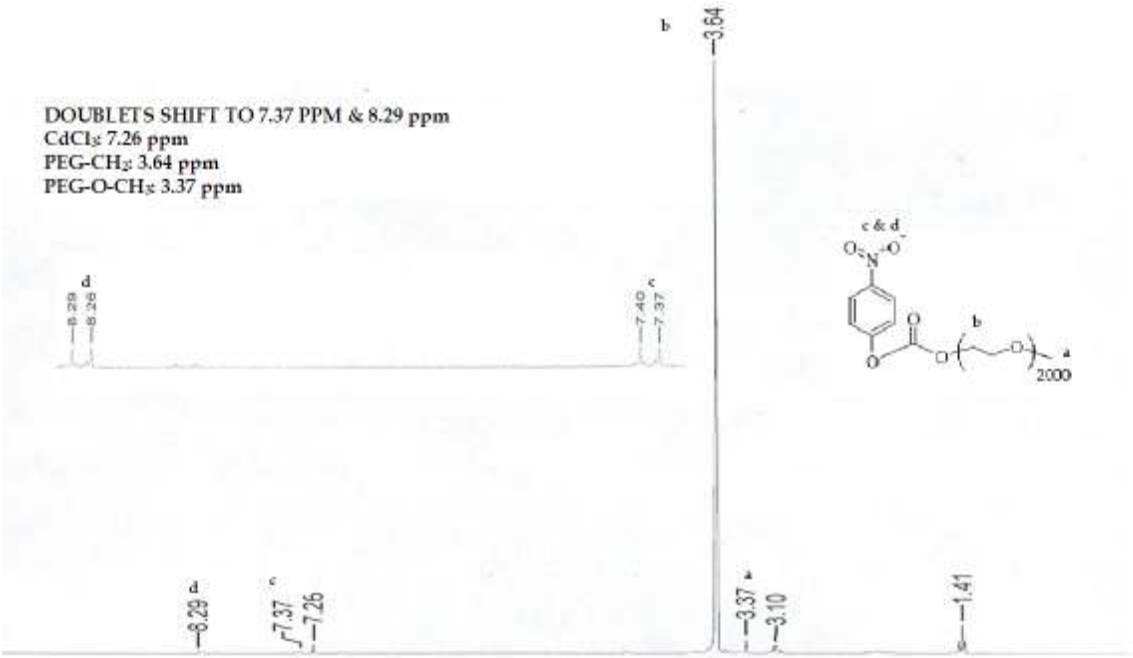

Figure 3.2 A 300 MHz ^{1}H NMR spectrum of activated PEG2000 (4-nitrophenyl carbonate PEG) (PEG-OCH_3: 3.37 ppm; PEG-CH_2: 3.64 ppm; $CDCl_3$: 7.26 ppm; doublets shift to 7.37 & 8.29 ppm)

NMR of PEGylated bishomotris

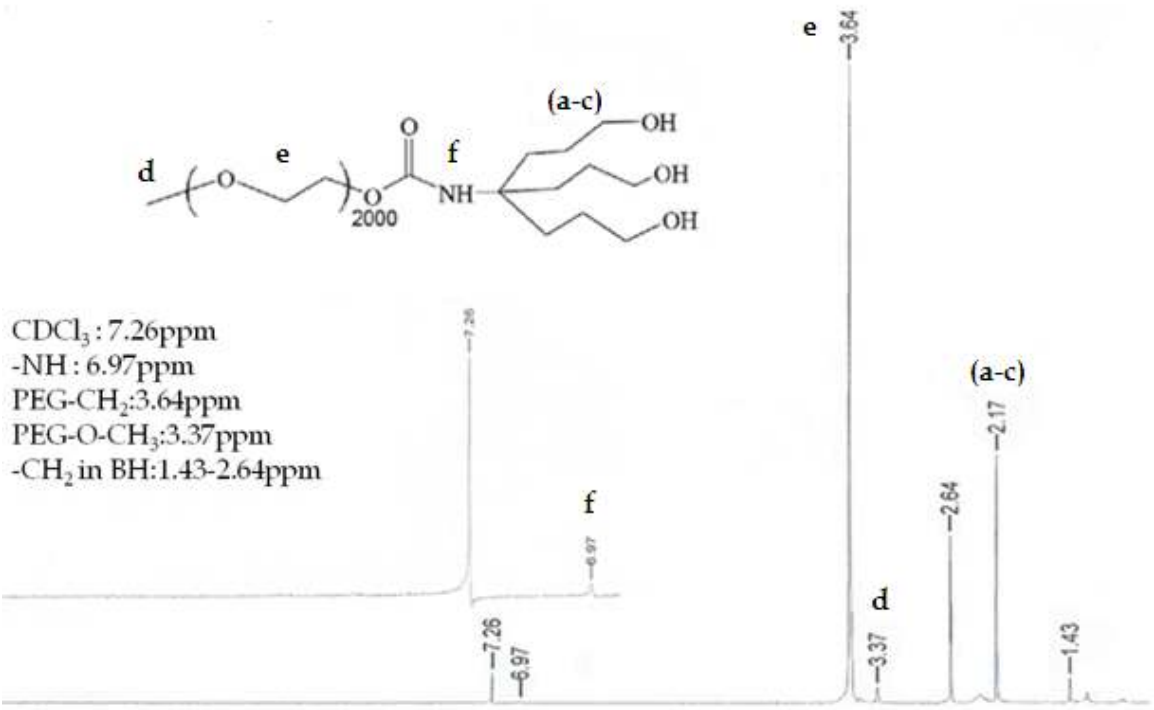

Figure 3.3 A 300 MHz ^{1}H NMR spectrum of PEGylated bishomotris (-CH_2 in BH: 1.43-2.64 ppm; PEG-OCH_3: 3.37 ppm; PEG-CH_2: 3.64 ppm; -NH: 6.97 ppm; $CDCl_3$: 7.26 ppm)

NMR of the "Paint-Brush" Conjugate

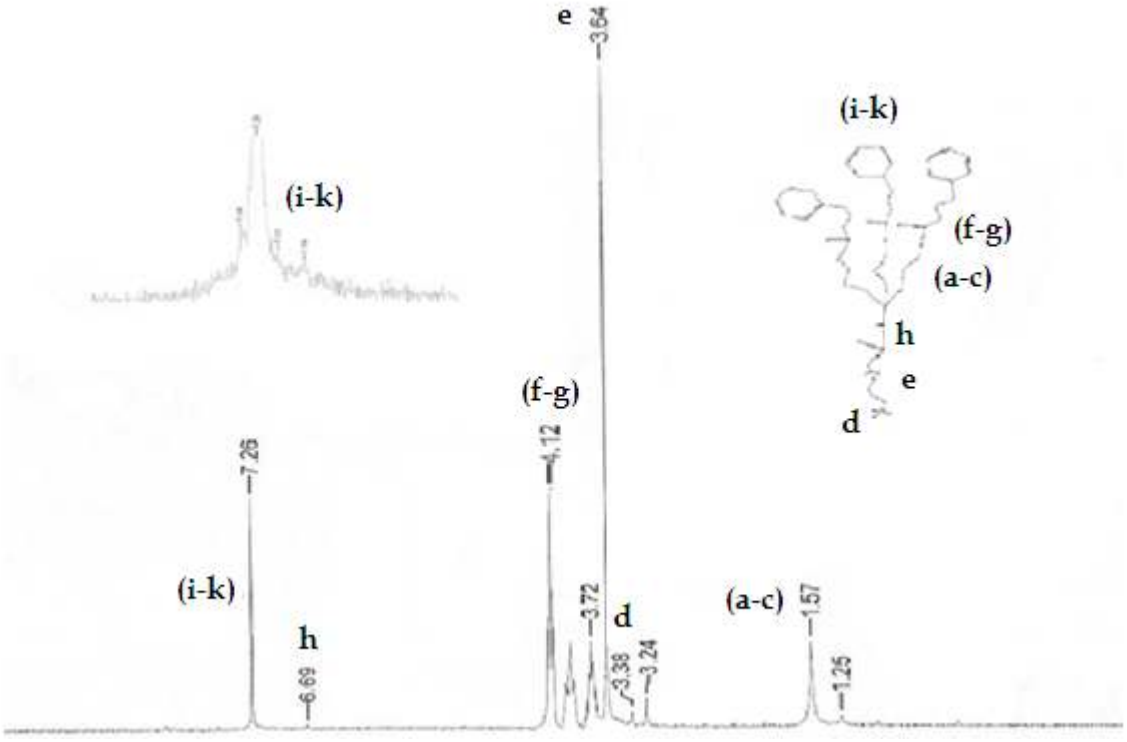

Figure 3.4 A 300 MHz ^{1}H NMR spectrum of the "PAINT-BRUSH" conjugate (-CH_2 in BH: 1.25-3.24 ppm; PEG-OCH_3: 3.38 ppm; PEG-CH_2: 3.64 ppm; (-CH_2-O-CO): 3.72 ppm-4.12 ppm; -NH: 6.69 ppm; Benzene: 7.19 ppm, 7.23 ppm & 7.28 ppm; $CDCl_3$: 7.26 ppm)

3.4 Results and Discussion

Details pertaining to synthesis and structural characterization of "PAINT-BRUSH" polymeric structures are discussed herewith.

The study here is primarily focused on creating an ester linkage between the polymeric carrier and the model drug molecule. For this purpose, carboxylate functionality of the model drug is utilized to attach to the hydroxyl functionalities present in the modified polymeric carrier molecule (mPEG-bishomotris conjugate). Such an ester is obtained readily by reaction of the free carboxylic acid of the model drug with the hydroxyl groups of the PEGylated bishomotris conjugate under standard DCC coupling conditions. As outlined earlier, 4-phenyl butyric acid was selected as the model drug for this coupling. The attachment reaction was carried out in dichloromethane using DMAP as catalyst. The final "PAINT-BRUSH" structure of the conjugate was confirmed by ^{1}H NMR.

The completeness of the coupling reaction between the PEGylated bishomotris conjugate and the model drug, 4-phenylbutyric acid can be observed clearly from figure 3.4. The expansion of the spectra depicts the appearance of new peaks at 7.19 ppm, 7.23 ppm and 7.28 ppm that pertain to methylene protons of benzyl rings associated with the model drug molecule. A set of peaks formed between 3.72 ppm and 4.12 ppm corresponds to protons associated with newly formed ester linkages between the model drug molecule's carboxylate

group and PEGylated-bishmotris's hydroxyl functionalities. The peak's low intensity could be attributed to the dominance of the intensity of the signal formed corresponding to methylene protons of the long mPEG chain of molecular weight 2000. Thus, it can be seen that the respective NMR spectral recordings attained at each phase are in complete agreement with the proposed structure of the "PAINT-BRUSH" conjugate.

^{1}H NMR Characterization

^{1}H NMR is highly essential in the monitoring of the transformations of the various functional groups. Figure 3.1 shows the proton spectra of 4-NPC starting material which can be identified by the presence of characteristic doublet peaks at 7.46 and 8. 35ppm. Figure 3.2 shows the proton spectra of 4-nitrophenyl carbonate-PEG, the formation of which can be identified and validated by the shift of the doublet peaks to 7.37 and 8.29ppm. The large peak at 3.64ppm is due to methylene protons from the mPEG chain. The peak at 3.37ppm pertains to methyl protons associated with methoxy group in mPEG. Figure 3.3 shows the proton spectra of PEGylated bishomotris. It can be seen that characteristic doublets for 4-nitrophenyl carbonate-PEG disappear completely following coupling of bishomotris with mPEG. A new peak is formed at 6.97ppm representing the newly derived –NH linkage between mPEG and bishomotris. Also, a new set of peaks appear between 1.43-2.64ppm that correspond to

methylene protons from bishomotris. The remaining peaks seen in the previous recorded spectra still stand depicting the presence of mPEG in the newly formed mPEG-bishomotris conjugate. The completeness of the coupling reaction between mPEG-bishomotris conjugate and the model drug, 4-phenylbutyric acid can be observed clearly from figure 3.4. The expansion of the spectra depicts the appearance of new peaks at 7.19, 7.23 and 7.28ppm that pertain to methylene protons of benzyl rings associated with the model drug molecule. Peaks formed between 3.72-4.12 ppm correspond to protons associated with newly formed ester linkages between the model drug molecule's carboxylate group and PEGylated-bishmotris's hydroxyl functionalities. The peak's low intensity could be attributed to the dominance of the intensity of the signal formed corresponding to methylene protons of the long mPEG chain of molecular weight 2000. Thus, it can be seen that the respective NMR spectral recordings attained at each phase are in complete agreement with the proposed structure of the "PAINT-BRUSH" conjugate.

3.5 Conclusion

In this chapter, we have successfully demonstrated the synthesis of PEGylated bishomotris "PAINT-BRUSH" conjugates using 4-phenylbutyric acid as a model anticancer drug. We, thereby accept our research hypothesis 1. The

conjugate synthesized thus, would act as a platform for controlled and targeted drug delivery applications.

CHAPTER IV

pH-CONTROLLED ACTIVATION OF NOVEL NANOPARTICLE "PAINT-BRUSH" POLYMERIC CONJUGATES AS ANTICANCER NANOMEDICINES

4.1 Introduction

The concept of drug delivery refers to an optimum delivery of a pharmaceutical compound to humans or animals. Its evolution into formulations that control rate and period of release (time-release medications) has been on an increase during the last few decades. Current focus is to develop a combination of targeted and controlled drug delivery systems which would activate drug release in the targeted area of the body (for example, in cancerous tissues) so as to bypass all harmful side-effects that cause damage to healthy tissues and to maintain drug concentration levels in the blood plasma well within permissible limits.

Dendrimer based nano-scaled drug delivery systems are of wide interest to cancer nanotechnologists as an option to deliver antitumor drugs on account of their unique architecture and well defined macromolecular characteristics. The high level of control over its shape, size, branching length, and surface functionality offers it a significant advantage over traditional linear polymers. Dendrimers offer vast surface areas with multiple surface functionalities that may be programmed accordingly with therapeutic agents and tumor-targeting ligands so as to target tumor antigens (biomarkers) and tumor vasculature with high affinity and specificity.

In accordance with Ringsdorf's vision for an ideal drug delivery system (Figure 2.2) dendrimer- drug conjugates posses a physiologically labile bond that may be an ester [30], carbonate [30], amide [31], malonate [32], or disulfide [33] bond. The linker can act as a bioresponsive system that shall remain stable during transportation to the tumor and would take advantage of the characteristic acidic pH (6.5-4.0) within endosomal and lysosomal vesicles following receptor mediated endocytosis of conjugates to undergo hydrolysis thus initiating drug release at an optimum rate

Here, we describe and compare the release profiles of a novel nanoparticle "PAINT-BRUSH" polymeric conjugate (Figure 2.5) in which a model anticancer drug 4-phenylbutyirc acid (Figure 2.6) is conjugated via simple ester bonds with the PEGylated derivative of bishomotris, a dendritic building

block for a higher generation Newkome-type polyamide dendrimer that may have a potential application as a cancer drug carrier. We hypothesize that coupling the drug to the PEGylated dendron a controlled release profile shall be attained at physiological pH 7.4 while a burst release shall be induced at pH 5.5 which corresponds to the endosomal pH within cancer cells due to hydrolytic degradation of the ester linkage. While the ester linkage is expected to undergo hydrolysis at a controlled rate to release 4-phe in normal pH (7.4), we expect activation to occur promoting rapid hydrolysis on exposure to an acidic pH (5. 5), that corresponds to the endosomal pH within tumor cells.

4.2 Materials and Methods

Details for synthesizing the novel "PAINT-BRUSH" conjugates are as earlier in Chapter III. The corresponding *in vitro* drug release studies are here.

4.2.1 Materials

Methoxy poly (ethylene glycol) (mPEG) (MW=2000), *p*-nitrophenyl chloroformate (4-NPC), triethylamine (TEA), acetonitrile, bishomotris (MW=205.29), dicyclohexylcarbodiimide (DCC), dimethylaminopyridine (4-DMAP), phenylbutyric acid (4-phe) (MW=164.2), and all solvents including diethyl ether, dimethyl sulfoxide (DMSO), dimethylformamide (DMF), dichloromethane (DCM), hexane and phosphate buffered saline (PBS (10x; pH

7.4 & pH 5.5) were purchased from Sigma-Aldrich (St. Louis, MO) and used directly without further purification.

4.2.2 In vitro release study

The drug-loaded conjugates at a concentration of 3 mg/mL were transferred into two closed containers; one filled with 0.1M PBS buffer of pH 7.4 and the other containing 0.1M PBS buffer of pH 5.5. The entire system in turn was placed in an incubator maintained at 37°C. At each pre-determined interval, 3 ml of drug release medium was taken out from the bulk solution and analyzed by a Hewlett Packard 8453 UV-Visible spectrophotometer at 227nm (detection wavelength of 4-phe at pH 7.4) and 212 nm (detection wavelength of 4-phe at pH 5.5) so as to measure the concentration of drug released. Three replicates were run at predetermined time intervals. Since the rate of ester hydrolysis in these conjugates was unknown, care was taken to ensure that all conjugated drug molecules were accounted for. Hence, the drug release medium was put back immediately into the bulk solution after measurement.

4.3 Results and Discussion

Details pertaining to synthesis and structural characterization of "PAINT-BRUSH" polymeric structures were discussed in the previous chapter. A comprehensive study of the *in vitro* drug release follows herewith.

In-vitro release studies were carried out in pH 7.4 and pH 5.5 PBS medium at 37°C. The amount of model drug released in the bulk solution was analyzed at 227nm (detection wavelength of 4-phe at pH 7.4) and 212 nm (detection wavelength of 4-phe at pH 5.5) using a Hewlett Packard 8453 UV-Visible spectrophotometer at pre-determined time intervals. Release profile obtained (Figure 4.1) as a result of hydrolysis of "PAINT-BRUSH" conjugates in pH 7.4 PBS medium indicated drug release in a sustained manner, i.e. only 40 % of the conjugated drug molecules were released at the end of 40 hours. Hydrolysis study of "PAINT-BRUSH" conjugates in pH 5.5 PBS medium indicated a 10 % release of drug molecules within 10 minutes. This could be attributed to the burst effect in acidic media. Thus, 100 % of the model drug was released in less than 2 hours. The rate of drug release in acidic buffer (5.5μg/min) was definitely higher than the rate in normal physiological buffer (0.017μg/min).

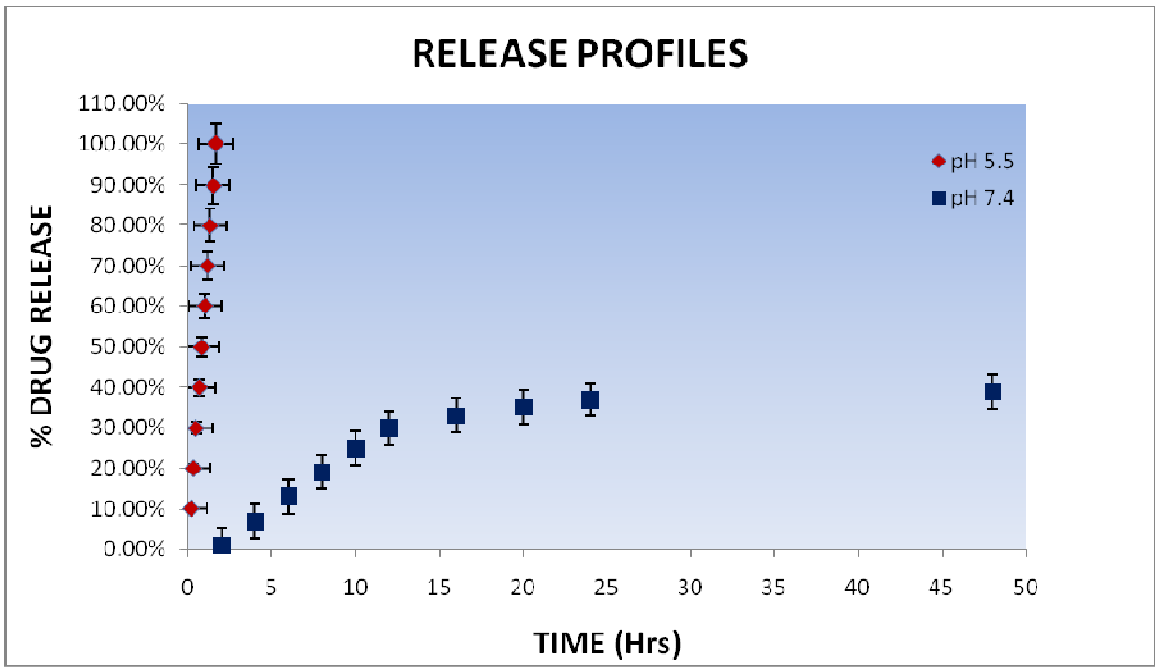

Figure 4.1 In vitro hydrolysis of "PAINT-BRUSH" conjugates in PBS at 37°C

The fact that a polymer-drug linker is expected to remain stable during transport to the tumor, but would release drug at an optimum rate on arrival within tumor cells forms one of the primary rationale for anticancer activity of nanoscaled polymer drug conjugates. The drug molecules may be released from the polymer carrier due to lysosomal enzymatic hydrolysis or due to hydrolysis of acid-labile bonds such as an ester or hydrazone linker. Under optimum conditions, the conjugate is expected to remain stable during its circulation in the blood (pH 7.4). The "PAINT-BRUSH" conjugates are based on pH-labile polymeric systems containing ester linked model drug entities that undergo

hydrolysis variably in response to pH of the buffer solutions. The breakage of bonds that link drug molecules to the PEGylated carrier may be attributed to ester hydrolysis that easily occurs in acid environment reverting back to the primary carrier with hydroxyl groups.

The release profiles as shown in the figure above depict the susceptibility of "PAINT-BRUSH" conjugates to hydrolysis post incubation in buffers of pH 7.4 and 5.5 respectively. The results uphold the fact that rate of drug release can indeed be controlled to an extent due to the presence of an acid-labile bond such as an ester linker and a PEG polymeric chain conjugated along with it which would also enhance the conjugates in-vivo circulation time. The results corroborate our hypothesis on stability of the linkage with respect to pH. Thus, polymeric "PAINT-BRUSH" conjugates tend to remain stable or release drugs at a controlled rate under normal physiological conditions but would be activated to release at a higher rate when exposed to acidic conditions (pH~5.5); a characteristic trait of cancer cells.

Further study will be required to synthesize "PAINT-BRUSH" conjugates that limit the amount of drug release to less than 5% under normal physiological conditions and to increase it further under acidic conditions. This may be achieved synthesizing the next generation dendrimers using bishomotris and conjugating a higher molecular weight polymeric carrier such as PEG to the entire system.

4.4 Conclusions

In this chapter, we have described the release properties of novel nanoscaled polymeric "PAINT-BRUSH" conjugates that may have a potential application as a drug delivery scaffold in cancer nanotherapy. Hydrolytic studies demonstrate that the novel conjugates are relatively stable at normal physiological pH (pH of blood~7.4), but are activated to release drug molecules at a rapid rate under acidic conditions (pH~5.5) simulating endosomal and lysosomal environment within tumor cells which confirms our initial hypothesis.

CHAPTER V

THE EFFECT OF SURFACE MODIFICATION ON CYTOTOXICITY OF NANOPARTICLE "PAINT-BRUSH" LIKE MULTI-HYDROXYL CAPPED POLYETHYLENE GLYCOL CONJUGATES

5.1 Introduction

The past decade has witnessed an increasing focus on cancer nanotherapy, which offers a potentially safe and effective mode of treatment for patients. The fact that a typical human cell size spans 10-20μm in diameter and cell organelles range from a few nanometers to a few hundred nanometers in diameter uphold the advantage of using nanotechnology in tumor targeting. Thus nanosized drug delivery vehicles readily interact with characteristic proteins and receptors present on target cell surface and within them in a noninvasive manner leaving the surrounding normal cells intact.

Apart from functionalizing nanoparticles with targeting ligands, selection of an appropriate nanocarrier that can act as a drug delivery scaffold is also vital. Liposomes made of amphiphilic unilamellar/multilamellar

membranes of natural or synthetic lipids are widely used to encapsulate drug molecules, both hydrophobic and hydrophilic in nature. Doxil, the doxorubicin-encapsulated liposome that targets a wide range of cancers including Kaposi's sarcoma and ovarian cancer was the first liposomal drug carrier to gain the FDA approval in 1995. Despite the fact that liposomal carriers were a major clinical success, they are limited by suboptimal stability and short half-life on the basis of the drug release profiles in vivo [80]. The drawback associated with liposomes may be overcome by using dendrimer based nano-scaled drug delivery systems. Extensive reviews have been carried out regarding the pharmaceutical and biomedical applications of dendrimers [61-64].

In spite of dendrimers showing promise as drug carriers, further in vitro and in vivo evaluations are necessary to study the biocompatibility, cytotoxicity and biodistribution of these nanosized delivery systems. Malik et al. [69] found that cationic dendrimers characterized by the presence of amine end groups caused haemolysis and cytotoxicity. This could be overcome as long as the surface was characterized by presence of anionic or neutral groups such as PEG that promote non-adhesion to negatively charged cell membranes thus diminishing haemolysis to a great extent.

Our interest is to use bishomotris (BH), a dendritic building block for a higher generation Newkome-type polyamide dendrimer that may have a potential application as a cancer drug carrier. The primary advantage of using

such a dendrimer apart from being highly soluble in water is the presence of hydroxyl surface functionalities which makes it potentially less cytotoxic. It is also characterized by the presence of a single primary amine group that can be shielded completely by PEGylation. In this preliminary study, cytotoxicity of the polymeric carrier (bishomotris – BH) and its modified form (PEGylated bishomotris - PEG-BH) at variant concentrations for different incubation periods was evaluated. We hypothesize that there is a significant difference in cell viability between BH and PEG-BH and also at different doses of the modified polymer. The primary intent is to observe the effect of modified bishomotris on HeLa cells and to ascertain that cancer cells are killed primarily by the drug and not due to the modified carrier. The human epithelial cervical cancer cell line (HeLa S3) was cultured for the in-vitro characterization of bishomotris and PEGylated bishomotris.

5.2 Materials and Methods

Details of materials and methods pertaining to synthesis of surface modified nano-conjugates are as earlier in Chapter III. The corresponding *in vitro* characterization studies of these novel conjugates for various incubation periods are here.

5.2.1 Materials

Human epithelial cervical cancer cell lines (HeLa S3) were purchased from ATCC. 10% HAMS F-12K media purchased from SIGMA® was supplemented with 10mM HEPES, 10% fetal bovine serum (ATLANTA biologicals®) and 1% HyQ antibiotic/antimycotic solution (100x HyQ antibiotic/antimycotic solution from HyClone : 10,000 U/mL PenicillinG, 10,000 µg/mL Streptomycin and 25 µg/mL Amphotericin). LIVE/DEAD® cell vitality assay kit was purchased from Molecular Probes (Invitrogen detection technologies).

5.2.2 Cell Culture & In-Vitro Characterization

The HeLa S3 cells were cultured in 10% HAMS F-12K media supplemented with 10mM HEPES, 10% fetal bovine serum (FBS) and 1% HyQ antibiotic/antimycotic at 37°C, in a humidified, 5% CO_2 atmosphere in a NAPCO Model 6500 Water Jacketed CO_2 incubator. Cells were then passaged twice a week. Cell passages were restricted to 7 in order to retain the original morphologic and phenotypic characteristics of the cells. Further, the HeLa S3 cells were seeded at 20,000 cells per well in 24 well plates and cultured to subconfluence in complete medium at 37°C, in a humidified, 5% CO_2 atmosphere

in a NAPCO Model 6500 Water Jacketed CO_2 incubator for 48 hours. The medium in each well was then aspirated and subject to the following treatment. While wells designated as the positive control were treated with hydrogen peroxide, the negative control wells were treated with fresh growth medium containing no polymer. The remaining wells were treated with three different concentrations (1 mg/mL, 2 mg/mL and 3 mg/mL) of bishomotris, PEGylated bishomotris (PEG-BH) and PEG alone. There were 3 replicates for each condition. Each 24-well cell culture plate was then subjected to four incubation time-periods (6 hour, 12 hour, 24 hour and 36 hour) with polymers at 37°C in a humidified 5% CO_2 atmosphere.

Post incubation cell viability assessment was carried out by staining the cells with the LIVE/DEAD® cell vitality assay kit. The two-color fluorescence assay distinguishes metabolically active cells from injured and dead cells. The fluorescence microscope used for observing the stained cells at a total magnification of 100x was the Zeiss Axiovert 200 Microscope (Carl Zeiss Inc, Thornwood NY). The camera used to capture the fluorescent images was a Zeiss AxioCam HRm (Carl Zeiss Inc). The stained cell culture samples were viewed under phase contrast light, FITC (fluorescein isothiocyanate) filtered light (ex. 488 nm: blue; em. 520 nm: green) and rhodamine red filtered light (ex. 540 nm: green; em. 565 nm: red). The assay is based on the reduction of C_{12} resazurin to red-fluorescent C_{12} resosurfin in metabolically active cells and the uptake of cell-

impermeable, green-fluorescent nucleic acid stain, SYTOX Green dye, in cells with compromised plasma membranes. Thus, while dead cells would emit green fluorescence, the healthy, metabolically active cells emit mostly red fluorescence. The injured cells of lower metabolic activity emit a reduced red fluorescence.

5.2.3 Statistical Analysis

Statistical evaluation of data expressed as means was performed by a three-way analysis of variance (3-way ANOVA) based on General Linear Model (GLM) followed by Tukey's test for pair wise comparison of subgroups. Differences among means were considered statistically significant at a P value of ≤ 0.05.

5.3 Results & Discussion

Cytotoxicity of bishomotris and the effect of PEG on cytotoxicity reduction of bishomotris are discussed below.

In-vitro efficacy of the dendron and its PEGylated form was determined by performing toxicity experiments *in vitro* with human epithelial cervical carcinoma cells (HeLa S3). Variant concentrations (1mg/mL, 2mg/mL and 3mg/mL) of all polymers were incubated for 6 h, 12 h, 24 h and 36 h with HeLa S3 cells. It was clearly evident that PEG-BH demonstrated a reduced level of cytotoxicity as compared to BH.

Observation with regards to cytotoxicity of BH characterized by presence of an amine group was expected since extensive studies pertaining to toxicity of cationic dendrimers have already been documented. The cell viability versus the polymer concentrations at different incubation periods are shown in Figures 5.1 and 5.2. A significant three way interaction among time, polymer and concentration was observed as a result of statistical evaluation of cell viability measurements which were significantly different for BH and PEG-BH. Cell viability was significantly higher for all groups of PEG-BH than that of BH with P=0.0001.

On the basis of a two way interaction between time and concentration, the results of cell viability obtained (Figure 5.3) on exposure to unmodified bishomotris (BH) exhibited significant cytotoxicity towards HeLa cells at higher concentrations for 12 h, 24 h, and 36 h (P=0.0001). Morphological changes in cell structure induced by lysis occurred at 36 h for 3mg/mL since they lacked a definite membrane and depicted a burst appearance as well (Figure 5.9 A). In contrast BH treatment showed no morphological changes up to a concentration of 2 mg/mL. A marked decrease in the cytotoxicity was observed when cells were exposed to PEG-BH conjugates. The low viability of the tested cells seen after 6 h incubation may be attributed to the cells being shocked by the polymers when they were first added. However, high viability was achieved after longer incubation when the cells appeared to have adapted to the polymers. This was

evident in the 12 h and 24 h viability measurements. The difference in cytotoxicity was more distinct for higher concentrations of BH and PEG-BH.

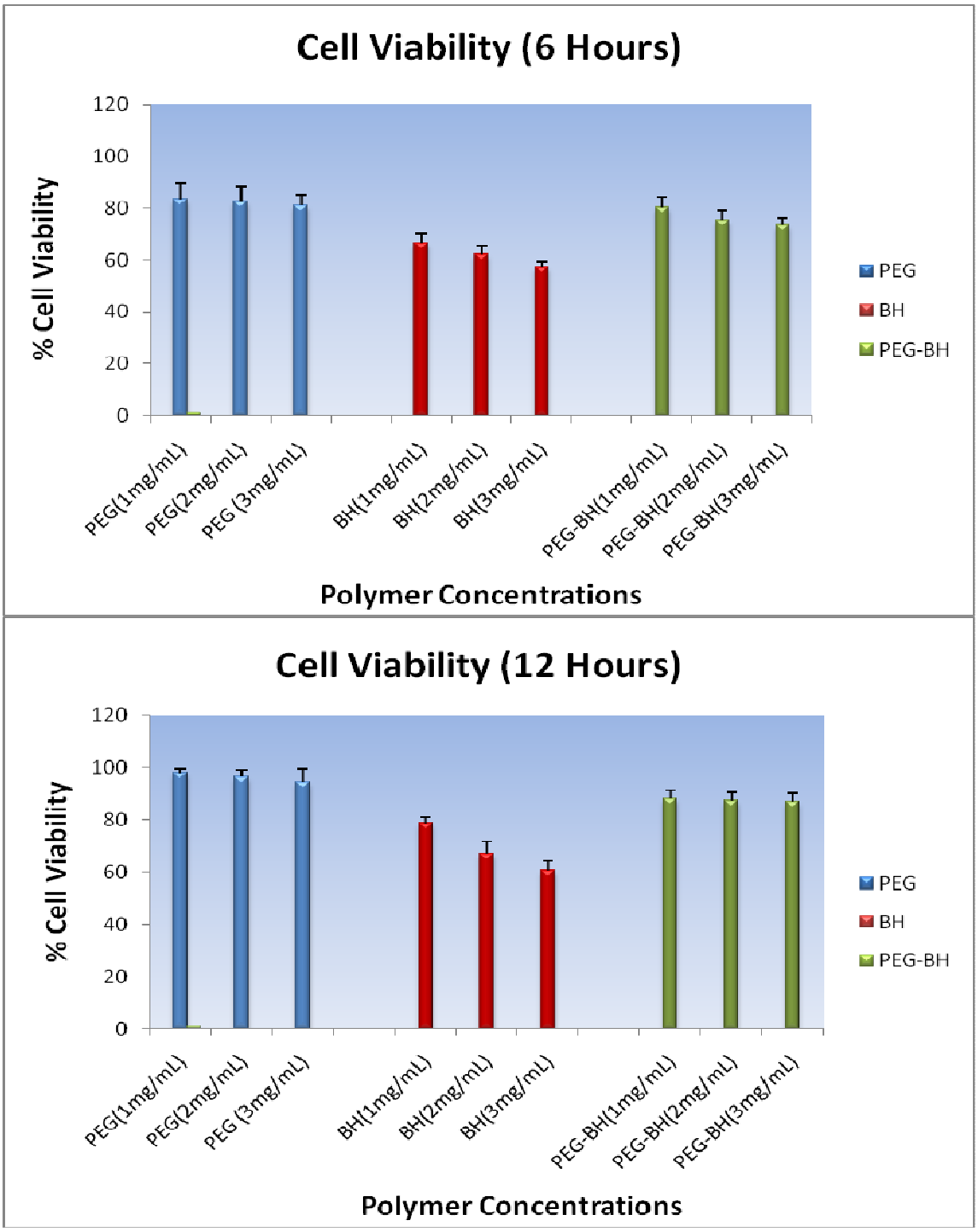

Figure 5.1 Cell Viability by PEG, bishomotris (BH) and surface modified bishomotris (PEG-BH) at 6 and 12 h (n=3)

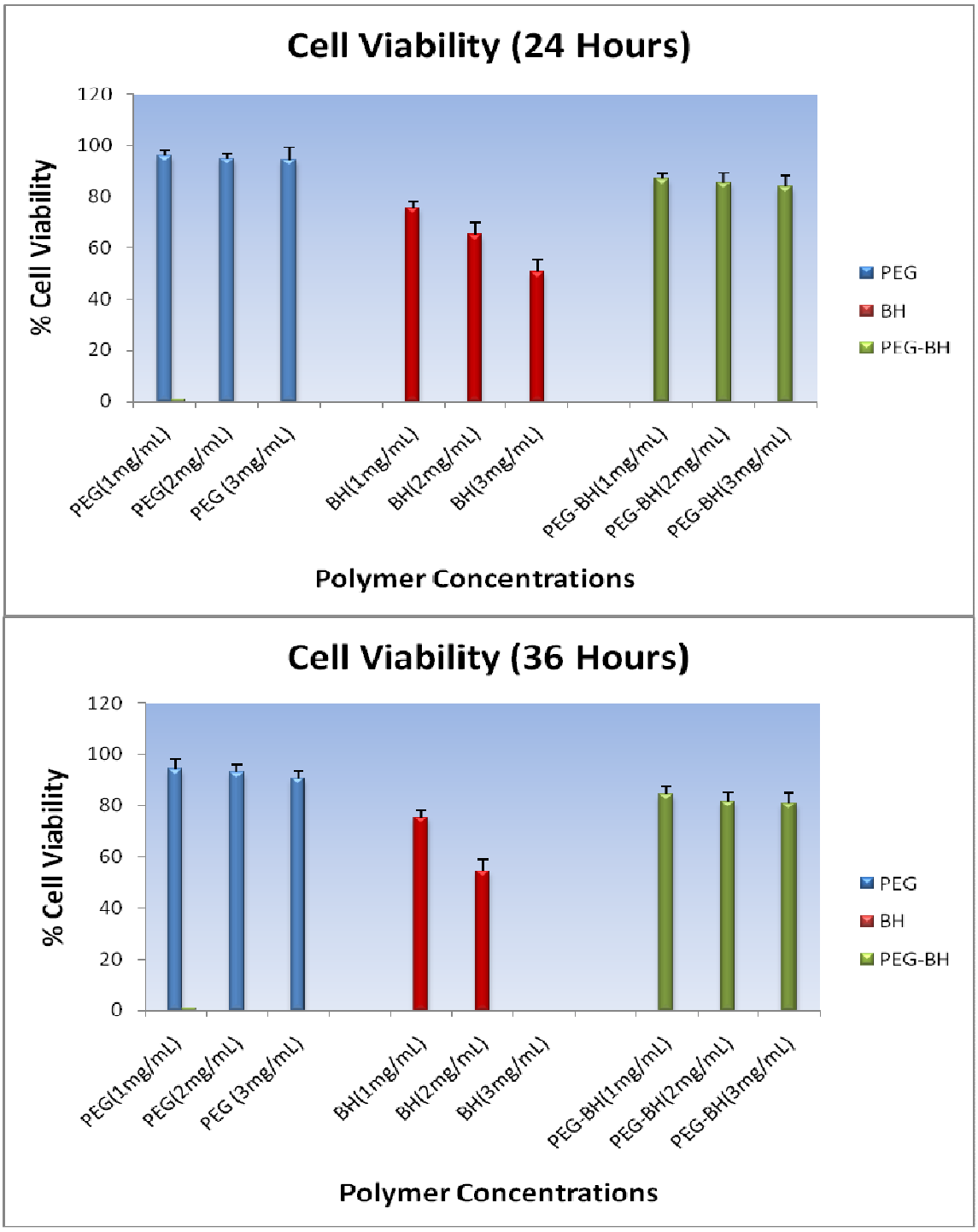

Figure 5.2 Cell Viability by PEG, bishomotris (BH) and surface modified bishomotris (PEG-BH) at 24 & 36 hours (n=3)

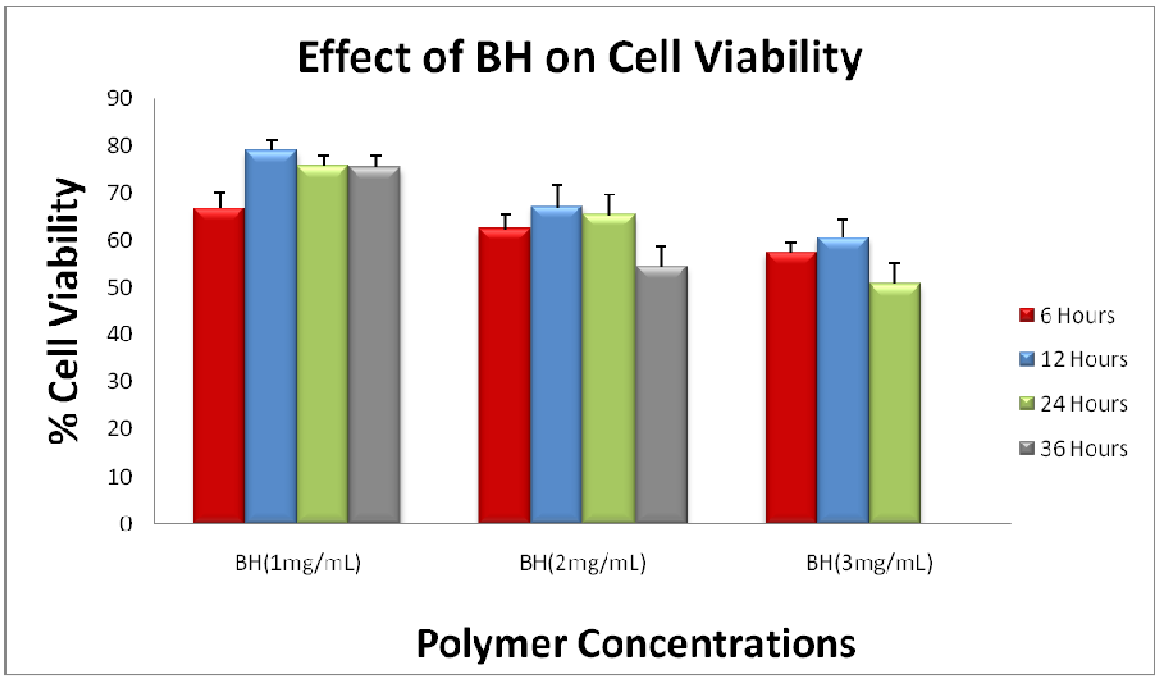

Figure 5.3 Effect of BH on viability of HeLa cells at 6, 12, 24 and 36 h. Dose increase from left to right: 1, 2 and 3 mg/mL (n=3)

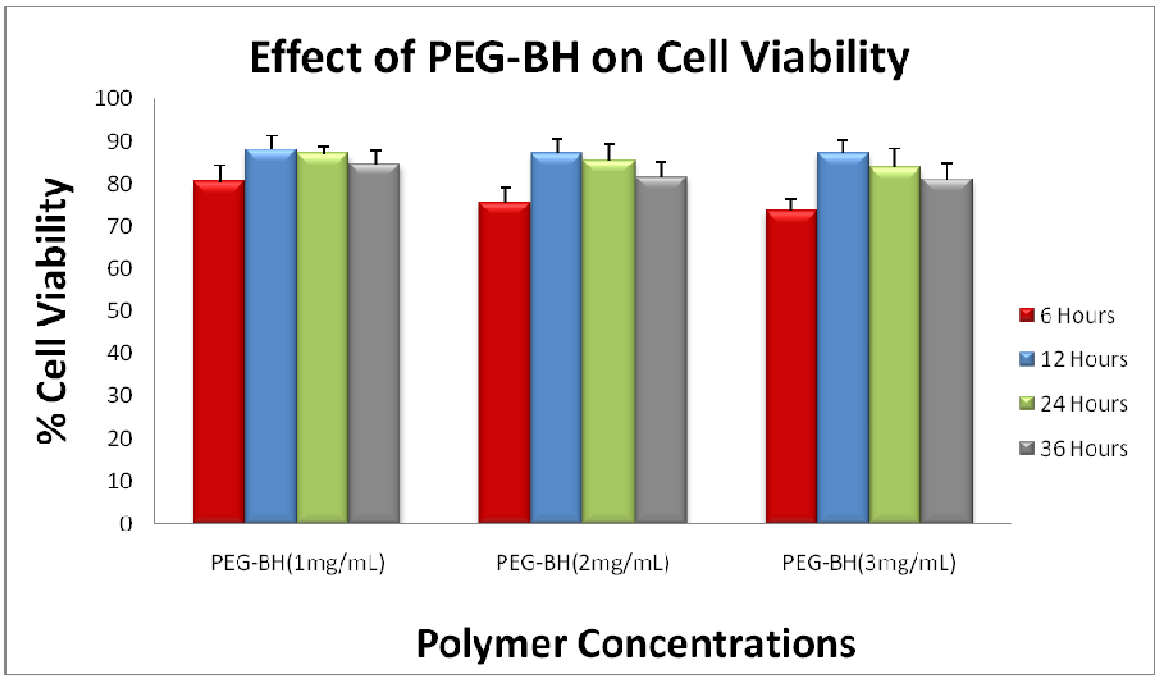

Figure 5.4 Effect of PEG-BH on viability of HeLa cells at 6, 12, 24 and 36 h. Dose increase from left to right: 1, 2 and 3 mg/mL (n=3)

On basis of dose-response and time-course plots (Figures 5.3 and 5.4), the effect of BH and surface modified BH on cell viability could be analyzed. Fluorescence images of stained HeLa cells were obtained post incubation and representative images are shown in Figures 5.5, 5.6, 5.7, 5.8 and 5.9 for respective concentrations and time-periods. HeLa cells treated with PEG alone emitted a higher rate of red fluorescence thus asserting once again its biocompatibility. In contrast, HeLa cells treated with various concentrations of BH and PEG-BH displayed a marked difference in the emission of red and green fluorescence thus

confirming that there was indeed an effect of polymer surface modification on the cytotoxicity of bishomotris alone.

The results of cell viability obtained on exposure to surface modified bishomotris (PEG-BH) were not significantly different on account of a two way interaction between time and concentration. Statistical evaluation depicted differences in cell viability as insignificant for all three concentrations at 12 h, 24 h and 36 h. Though cell viability measurements for all three concentrations at 12 h was significantly higher than that at 6 h (1mg/mL : P=0.0086; 2mg/mL : P=0.0001; 3mg/mL : P=0.0001), there existed no significant differences when compared with groups at 24 h and 36 h. It was also evident that cell viability measurements for all concentrations at 24 h was significantly higher than that at 6 h (1mg/mL : P=0.0273; 2mg/mL : P=0.0001; 3mg/mL : P=0.0001) and there were no significant differences when compared with groups at 36 h. While no significant difference existed in cell viability for all three concentrations at 36h; cell viability was significantly higher than that at 6 h for the concentration at 3mg/mL (P=0.0184). Thus, a significant difference in cell viability does not exist due to differences in concentration and exposure time as well.

A major limitation associated with LIVE/DEAD® cell vitality assay kit is the unaccounted estimate of dead cells that may get removed while aspirating the treatment media post incubation before we commence the staining procedure. The estimate may further be affected due to wash-out with 1x PBS

before we add the dyes to the cell suspension. Although consideration of this estimate would affect the cell viability data obtained, the overall trend would remain unchanged. One way of overcoming this handicap is to obtain an estimate of the total count in each well before the treatment media is removed and use this count to normalize the data obtained from the fluorescent image of the stained cells. One another way is to normalize the observed cell viability data with the control cell viability. Data normalization for cell number makes results more comparable well-to-well and day-to-day. In addition, bioluminescence and plate counting (other methods to assess viability) may also be used as reference procedures.

Hence, PEGylation of bishomotris resulted in higher viability as compared to unmodified bishomotris when applied to HeLa cells for 12 h, 24 h and 36 h incubation periods. PEG, apart from being a highly water soluble polymer is less toxic in nature and highly biocompatible and hence, is widely accepted for use in drug formulations. Studies have shown that PEG-coated carriers demonstrate a reduced uptake by liver and also possess a prolonged circulation half-life in the bloodstream when compared with non-PEG coated carriers. The toxicity effect of bishomotris may be attributed to cell membrane disruption caused through initial adhesion by electrostatic attraction of the amine group to the cell surface groups which is negatively charged, followed by formation of a hole or endocytosis that caused the cell wall to lyse. Thus,

introducing PEG would encapsulate or "quench" the charged surface and promote non-adhesion to negatively charged cell membranes thus diminishing cell lysis to a great extent. Another reason that can be attributed to the inertness imparted may be due to the ability of PEG to uphold a sufficient hydration of the surface along with charge neutrality and also suppressing hydrophobic or ionic interactions with cell membrane [77].

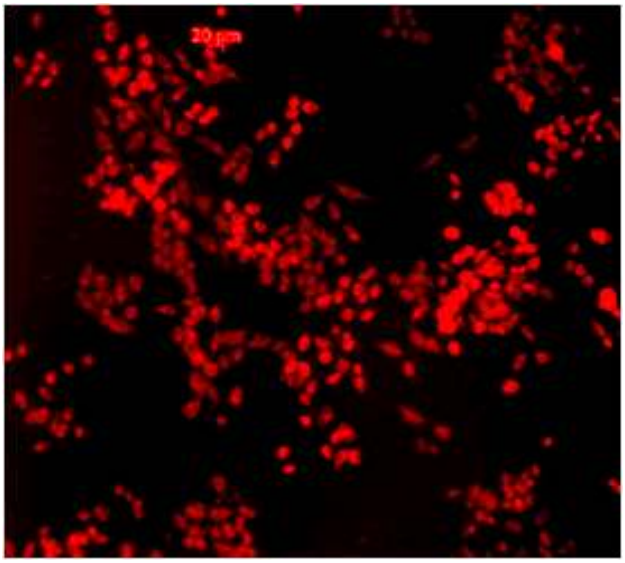

(A)

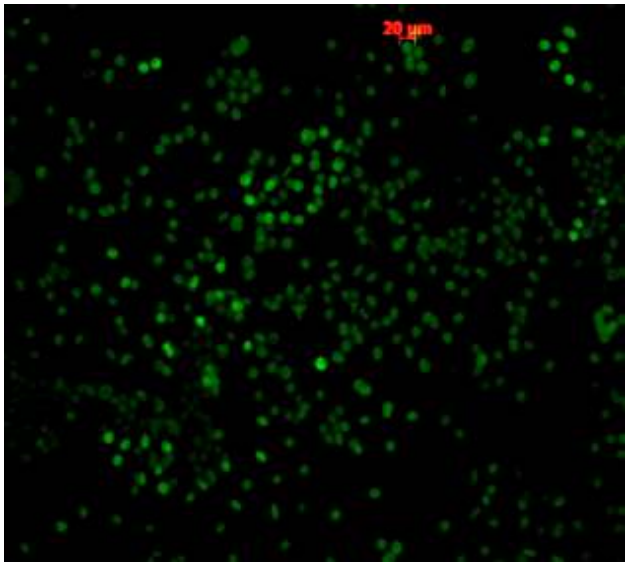

(B)

Figure 5.5 Fluorescence images of HeLa cells treated with growth media alone (negative control) – (A), Hydrogen Peroxide (H_2O_2 – positive control) – (B)

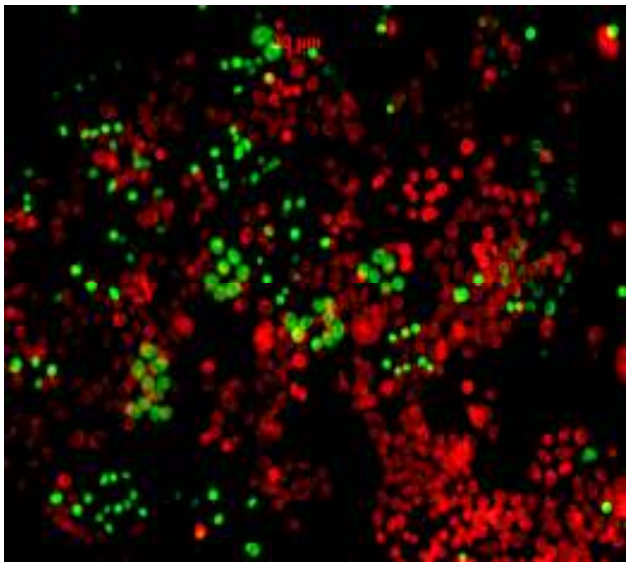

(A)

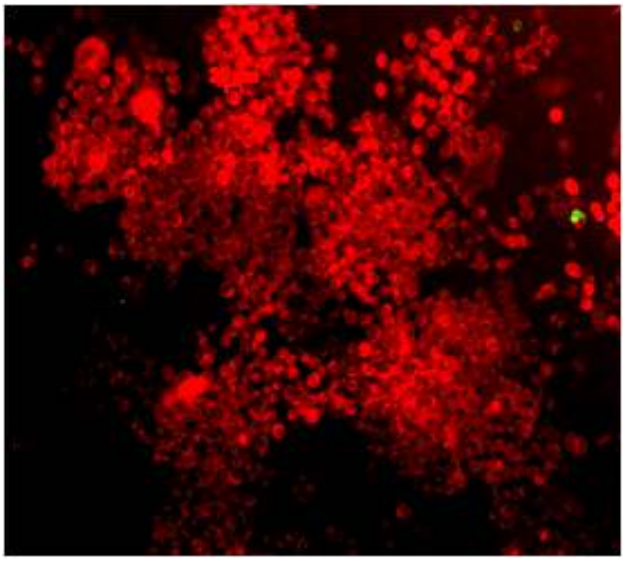

(B)

Figure 5.6 12 h fluorescence images of HeLa cells treated with BH (1mg/mL) – (A), PEG-BH (1mg/mL) – (B)

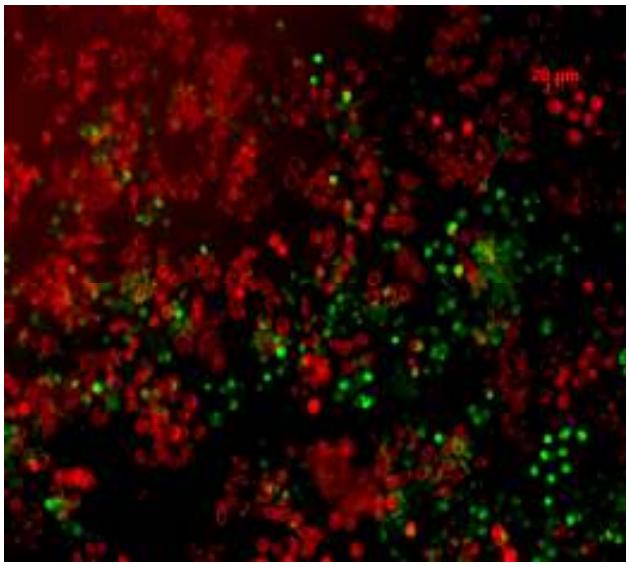

(A)

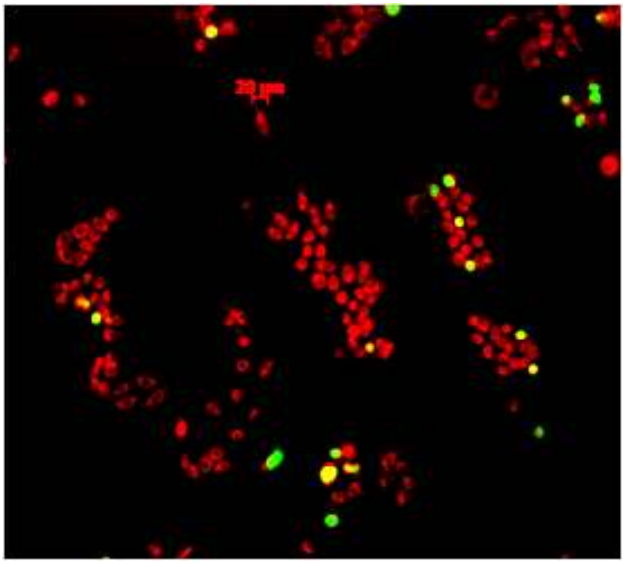

(B)

Figure 5.7 12 h fluorescence images of HeLa cells treated with BH (3mg/mL) – (A), PEG-BH (3mg/mL) – (B)

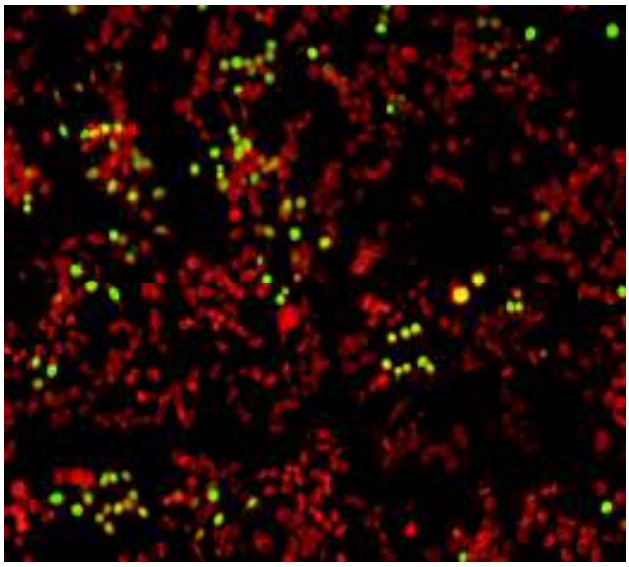

(A)

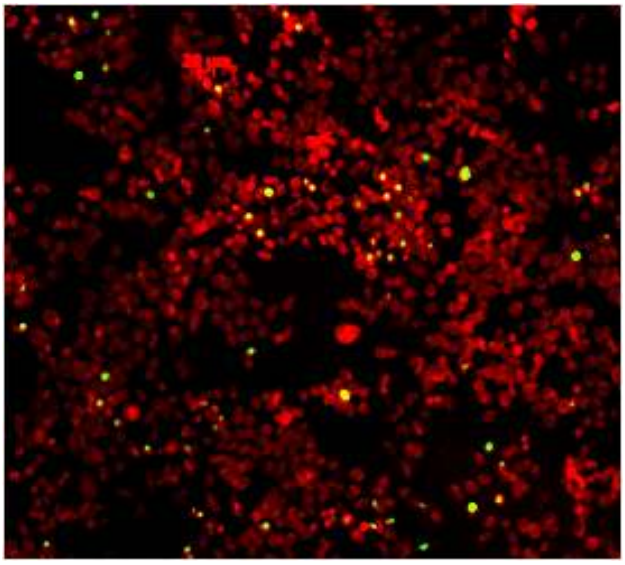

(B)

Figure 5.8 36 h fluorescence Images of HeLa cells treated with BH (1mg/mL) – (A), PEG-BH (1mg/mL) – (B)

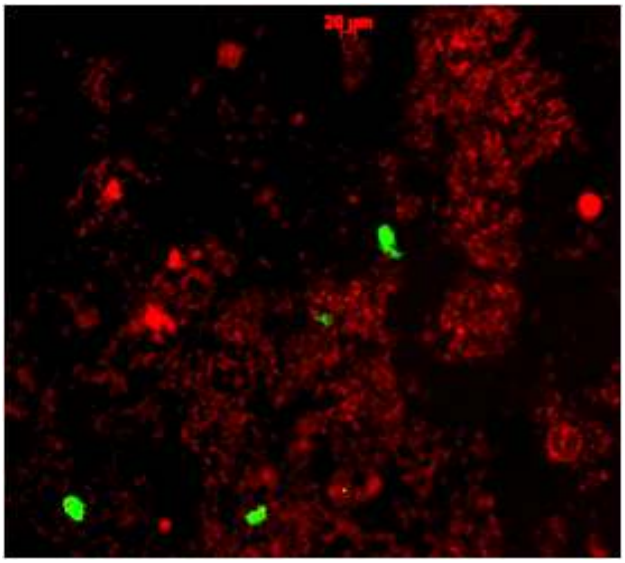

(A)

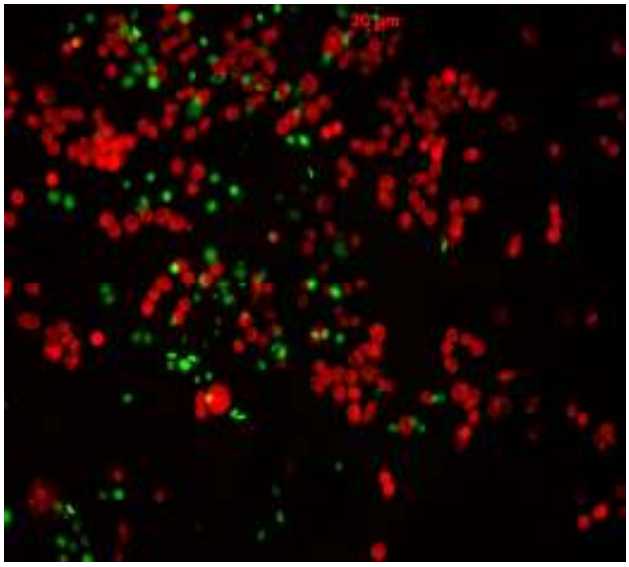

(B)

Figure 5.9 36 h fluorescence Images of HeLa cells treated with BH (3mg/mL) – (A), PEG-BH (3mg/mL) – (B)

5.4 Conclusions

In this chapter, PEG-BH "Paint-Brush" polymers were studied as a potential cancer drug delivery scaffold. The results obtained have vital implications for the fact these nanocarriers may have a potential application as parental drug carriers. The study demonstrated that bishomotris was cytotoxic in nature due to the interaction of positively charged amine group with the HeLa cells. It was also evident that surface modification by PEGylation has led to a distinct reduction in toxicity levels thus laying foundations for further research to realize a promising new scaffold for cancer nanotherapy. Future work shall focus on the application of these novel polymers as carriers of anticancer drugs.

CHAPTER VI

CONCLUSIONS AND FUTURE WORK

Cascade dendritic molecules and polymers are attractive because of their versatile iterative stepwise synthesis that comprises of amide formation followed by surface polarity reversal via reduction or facile hydrolysis so as to yield the desired polyalcohol or polyacid at each generation. Thus, the synthesis provides excellent control of surface functionality. This makes it possible to conjugate selectively several different moieties like drug molecules, solubilizing groups and targeting ligands on the same dendritic molecule. The modus operandi is to take advantage of this versatility of surface chemistry so as to design and synthesize a novel drug delivery system exploiting surface functionalities for attachment of model drugs and solubilizing groups as well. Since most drugs are hydrophobic in nature, especially when their hydrophilic functional groups are used to conjugate with polymeric carriers, the attachment of solubilizing groups like PEG would definitely render an increase in its solubility. The reason why PEG was selected as the solubilizer in this research is PEG, apart from being a highly water soluble polymer it is less toxic in nature and highly biocompatible

and hence, is widely accepted for use in drug formulations. Studies have shown that PEG-coated carriers demonstrate a reduced uptake by liver and also possess a prolonged circulation half-life in the bloodstream when compared with non-PEG coated carriers.

Our primary research hypothesis stated that a PEGylated Bishomotris "PAINT-BRUSH" conjugate can be synthesized using 4-phenylbutyric acid as a model anticancer drug. To test this hypothesis, structural validation was performed by NMR characterization, which depicted successful synthesis of the conjugate accepting research hypothesis 1.

Research Hypothesis 2 stated that by coupling the drug to the PEGylated dendron a controlled release profile shall be attained at physiological pH 7.4 while a remarkable burst of release shall be induced at pH 5.5 which corresponds to the endosomal pH within cancer cells due to hydrolytic degradation of the ester linkage. Hence, having accepted our primary research hypothesis, the next step was to monitor *in-vitro* release of the model drug molecule by the conjugate in a normal and an acidic PBS buffer, maintained at 37°C so as to simulate and validate the conjugate's stability in normal physiological conditions, while it breaks down to initiate drug release in an acidic environment, which is a characteristic trait of tumor sites. In-vitro release profiles depicted a controlled drug release for more than 80 h in physiological

buffer while a 100% drug release was observed in less than 2 h in an acidic buffer thus enabling us to accept research hypothesis 2.

Our null hypothesis 1 (H_{10}) stated that there is no significant difference in cell viability for samples treated with bishomotris and PEGylated bishomotris. To test this hypothesis, we used an in vitro cell culture study performed on human epithelial carcinoma cells (HeLa cells) where cytotoxicity of the polymeric carrier (bishomotris – BH) and its modified form (PEGylated bishomotris - PEG-BH) at various concentrations (1 mg/mL, 2 mg/mL and 3 mg/mL) for different incubation periods (6 h, 12 h, 24 h and 36 h) was evaluated. The primary intent was to observe the effect of modified bishomotris on HeLa cells and to ascertain that cancer cells are killed primarily by the drug and not due to the modified carrier. Statistical analysis on live/dead cell counts indicated a significant difference in cell viability confirming our justification of proposing the use of modified bishomotris for drug delivery applications. Thus, we fail to accept our null hypothesis 1(H_{10}) and thereby reject it.

Finally we test our null hypothesis 2 (H_{II0}) which stated that there is no significant difference in cell viability for samples treated with various concentrations (1 mg/mL, 2 mg/mL and 3 mg/mL) of PEGylated bishomotris for different incubation periods (6 h, 12 h, 24 h and 36 h). The results of cell viability obtained on exposure to surface modified bishomotris (PEG-BH) were

not significantly different on account of a two way interaction between time and concentration. Thus, a significant difference in cell viability does not exist due to differences in dosage rate and exposure time as well. Hence, we fail to reject our null hypothesis 2 (H_{II0}) and thereby accept it.

The outcome of the cell culture study did indicate the safety of using this newly created nanoparticle system within biological systems. The presence of a PEG tail on bishomotris definitely brought about a reduction in toxicity level associated with bishomotris alone which is no doubt encouraging and provides further motivation in proceeding to the next level of this research. Although the model study did demonstrate encouraging results, we should also point out that these are just preliminary results since further optimization of the "PAINT-BRUSH" conjugate is required.

Future work shall focus on the synthesis and structural characterization of a higher generation conjugate with increased surface functionalities wherein the original anti-cancer drug, chlorambucil shall be conjugated along with targeting ligands and moieties. The 1st Generation "PAINT-BRUSH" may be thus exploited in more than one way to develop novel hybrids that would carry antibodies, enzymes or even additional PEG linkages that may enhance the system's biocompatibility alongwith its purpose as a targeted drug delivery system for malignancies. Further study will be required to synthesize conjugates

that limit the amount of drug release to less than 5% under normal physiological conditions and to increase it further under acidic conditions. This may be achieved synthesizing the next generation dendrimers using bishomotris and conjugating a higher molecular weight polymeric carrier such as PEG to the entire system. Further in-vitro characterization study is required to optimize the dosage rate for targeting before proceeding to animal model experiments so as to determine the conjugate's effectiveness.

REFERENCES

1) *Cancer Facts and Figures 2007*, American Cancer Society, Atlanta, 2007

2) P. Ehrlich, *Studies in immunity*, Plenum Press, New York, 1906

3) P. Baldrick, Pharmaceutical excipient development: The need for preclinical guidance. *Regul. Toxico. Pharmacol.* (2000) 32: 210-218

4) E.K Rowinsky, Signal events: cell signal transduction and its inhibition in cancer. *Oncologist* (2003) 8(Suppl 3): 5-17

5) Y. Cao, Antiangiogenic cancer therapy. *Sem. Cancer Biol.* (2004) 14: 139-145

6) M. Cristofanilli, C. Charnsangavej, G. N Hortobagyi. Angiogenesis modulation in cancer research: novel clinical approaches. *Nat. Rev. Drug Discov.* (2002) 1: 415-426

7) P.S Steeg, Metastasis suppressors alter the signal transduction of cancer cells. *Nat. Rev. Cancer* (2003) 3: 55-63

8) J.J Alam, Apoptosis: target for novel drugs. *Trends Biotechnol.* (2003) 21: 479-483

9) M. Ranson, Epidermal growth factor receptor tyrosine kinase inhibitors. *Br. J. Cancer.* (2004) 90: 2250-2255

10) D. Putnam, J. Kopecek, Polymer conjugates with anticancer activity. *Adv. Polym. Sci.* (1995) 122: 55-123

11) Y. Matsumura, H. Maeda, A new concept for macromolecular therapeutics in cancer chemotherapy: mechanism of tumoritropic accumulation of proteins and the antitumor agent smancs. *Cancer Res.* (1986) 46: 6387-6392

12) M. Bolla, L. Collette, L. Blank, P. Warde, J. B Dubois, R. O Mirimanoff, G. Storme, J. Bernier, A. Kuten, C. Sternberg, J. Mattelaer, J. Lopez Torecilla, J. R Pfeffer, C. Lino Cutajar, A. Zurlo, M. Pierart, Long term results with immediate androgen suppression and external irradiation in patients with locally advanced prostrate cancer (an EORTC study): a phase III randomized trial. *Lancet* (2002) 360: 103-108

13) C. Guerin et al. Recent advances in brain tumor therapy: local intracerebral drug by polymers. *Invest. New Drugs* (2004) 22:27-37

14) R. Duncan, The dawning era of polymer therapeutics. *Nat. Rev. Drug Discov.* (2003) 2:347-360

15) Garber K., Improved Paclitaxel formulation hints at new chemotherapy approach. *J. Natl. Cancer Inst.* (2004), 96(2):90-91

16) T.L Andresen, S.S Jensen, K. Jorgensen, Advanced strategies in liposomal cancer therapy: Problems and prospects of active and tumor specific drug release. *Prog. Lipid Res.* (2005), 44(1): 68-97

17) A.K Patri, I.J Majoros, R.J Baker Jr., Dendritic polymer macromolecular carriers for drug delivery. *Curr. Opin. Chem. Biol*, (2002), 6 (4):466-471

18) Dr. G. R. Newkome, Dr. C. N. Moorefield, Dr. F. Vögtle, *Dendrimers and Dendrons: concepts, syntheses & applications*, Weinheim; New York: Wiley-VCH, c2001, Dendrimers Derived by Divergent Procedures Using 1→3 Branching Motifs: Chapter 4.6-4.14

19) J.H Atkins, L.J Gershell, Selective anticancer drugs. *Nat. Rev. Drug Discov.*, (2002) 1: 491-492

20) M.H Chun, Serum signaling factors and spheroids. *Critical Reviews in oncology/hematology*, (2000) 36(2-3): 89-98)

21) http://www.ul.ie/elements/Issue6/Polymeric%20gels.htm *(accessed Dec 2007)*

22) M. Przybylski, E. Fell, H. Ringsdorf, D.S Zaharko, *Makromol Chem* (1978) 179: 1719

23) W.C Shen, B. Ballou, H. J.P Ryser, T.R Hakala, Targeting, internalization and cytotoxicity of methotrexate-monoclonal anti-stage-specific embryonic antigen-1 conjugates in cultured F-9 teratocarcinoma cells. *Cancer Res.* (1986) 46: 3912

24) B. C. F Chu, S. B Howell, Differential toxicity of carrier-bound methotrexate toward human lymphocytes, marrow and tumor cells *Biochem Pharmacol.* (1981) 30: 2545

25) T. Ghose, S. Ferrone, A.H Blair, Y. Kralovec, M. Temponi, M. Singh, M. Mammen, Regression of human melanoma xenografts in nude mice injected with methotrexate linked to monoclonal antibody 225.28 to human high molecular weight-melanoma associated antigen. *Cancer Immunol Immunother.* (1991) 34: 90

26) R. Langer, Drug delivery and targeting. *Nature* (1998) 392: 5-10

27) C. Elvira, A. Gallardo, J. S Roman, A. Cifuentes, Covalent Polymer- Drug Conjugates. *Molecules* (2005) 10: 114-125

28) H. Ringsdorf, Structure and properties of pharmacologically active polymers. *J. Polym. Sci., Polym. Symp.* (1975) 51: 135-153

29) R. Duncan, Polymer conjugates as anticancer nanomedicines. *Nature Reviews*, (2006) 6: 688-701

30) S. Zalipsky, C. Gilon, A. Zilkha, Attachment of drugs to polyethylene glycols. European Polymer Journal, (1983) 19(12): 1177-83

31) R Duncan et al. Fate of N-(2-hydroxypropyl) methacrylamide copolymers with pendant galactosamine residues after intravenous administration to rats. *Biochim. Biophys. Acta* (1986) 880: 62-71

32) E Gianasi, RG Buckley, J Latigo, M Wasil, R Duncan, HPMA copolymers palatinates containing dicarboxylato ligands. Preparation, characterization and in vitro and in vivo evaluation. *J. Drug Targeting* (2002) 10: 549-556

33) W.C. Shen, H. J. Ryser, L. LaManna, Disulfide spacer between methotrexate and poly(D-lysine). A probe for exploring the reductive process in endocytosis. *Journal of Biological Chemistry* (1985) 260 (20): 10 905-8

34) K. Ulbrich, V. Subr Polymeric anticancer drugs with pH-controlled activation. *Adv. Drug Deliv. Rev.* (2004) 23: 1023-1050

35) J. M Harris, R. B Chess, Effect of PEGylation on pharmaceuticals. *Nat. Rev. Drug Discov.* (2003) 2: 214-221

36) G. Pasut, A. Guiotto, F.M Veronese, Protein, peptide and non-peptide drug PEGylation for therapeutic application. *Expert Opin. Therap. Patents* (2004) 14: 859-894

37) J.W Singer, S. Shaffer, B. Bake, A. Bernareggi, S. Stromatt, D. Nienstedt, M. Besman, Paclitaxel poliglumex (XYOTAX; CT-2103): an intracellularly targeted taxane. *Anti-cancer Drugs* (2005) *16(3): 243-254*

38) G. M. Springett, C. Takimoto, M. McNamara, J. H. Doroshow, S. Syed, E. Eastham, D. Spriggs, S. Pezzulli, G. Michelson and J. Dupont, Phase 1 study of CT-2106 (polyglutamate camptothecin) in patients with advanced malignancies. *J. Clin. Oncol.* (2004) 22: 3127

39) R. Duncan, Polymer-Drug Conjugates. *In Handbook of Anticancer Drug Development* (D. Budman et al., eds) (2003) 239-260, Lipincott Williams & Wilkins.

40) R. Duncan, N-(2-hydroxypropyl) methacrylamide copolymer conjugates. *In Polymeric Drug Delivery Systems (G.S Kwon, ed.)*, (2005) 1-92, Marcel Dekker

41) V.P Torchilin, Drug targeting. *Bull. Tech. Gattefosse* (2000) 93: 101-114

42) J. Crown, M. O'Leary, The Taxanes: an update. *Lancet* (2000) 355: 1176

43) G. D Grossfeld, P. R Carroll, N. Lindeman, M. Meng, S. Groshen, A-C. Feng, D. Hawes and R. J Cote, Thrombospondin-1 expression in patients with pathologic stage T3 prostate cancer undergoing radical prostatectomy: association with p53 alterations, tumor angiogenesis, and tumor progression. *Urology*, 59(1): 97-102

44) G. Storm, S. O Belliot, T. Daemen and D.D Lasic, Surface modification of nanoparticles to oppose uptake by the mononuclear phagocyte system. *Adv. Drug Deliv. Rev.* (1995) 17(1): 31-48

45) R. K Jain, Transport of Molecules, Particles, and Cells in Solid Tumors. *Annu. Rev Biomed Eng.* (1999) 1: 241-263

46) H. Maeda, Y. Matsumura, Tumoritropic and lymphotropic principles of macromolecular drugs. *Crit Rev Ther Drug Carrier Syst* (1989) 6: 193

47) R. Gref, Y. Minamitake, M.T Peracchia, V. Trubetskoy, V. Torchilin, and R. Langer, Biodegradable long-circulating polymeric nanospheres. *Science* (1994) 263(5153): 1600 – 1603

48) S.M Moghimi, A.C Hunter, Poloxamers and poloxamines in nanoparticle engineering and experimental medicine. *Trends Biotechnol.* (2000) 18(10): 412

49) E.K Park, S.B Lee, Y.M Lee, Preparation and characterization of methoxy poly(ethylene glycol)/poly(ε-caprolactone) amphiphilic block copolymeric nanospheres for tumor-specific folate-mediated targeting of anticancer drugs. *Biomaterials* (2005) 26(9): 1053-1061

50) R.V Chari, Targeted delivery of chemotherapeutics: tumor-activated prodrug therapy. *Adv. Drug Delivery Rev.* (1998) 31(1-2): 89-104

51) A.M Mansour, J. Drevs, N. Esser, F. M Hamada, O. A Badary, C. Unger, I. Fichtner, F. Kratz, A New Approach for the Treatment of Malignant Melanoma: Enhanced Antitumor Efficacy of an Albumin-binding Doxorubicin Prodrug That Is Cleaved by Matrix Metalloproteinase 2. *Cancer Res.* (2003) 63(14): 4062-4066

52) X. Guo, F. C Szoka Jr., Chemical approaches to triggerable lipid vesicles for drug and gene delivery. *Acc. Chem. Res.* (2003) 36(5): 335-341

53) I. Brigger, C. Dubernet, P. Couvreur, Nanoparticles in cancer therapy and diagnosis. *Adv. Drug Delivery Rev.* (2002) 54: 631-651

54) S. Bennis, C. Chapey, J. Robert, P. Couvreur, Enhanced cytotoxicity of doxorubicin encapsulated in polyisohexylcyanoacrylate nanospheres against multidrug-resistant tumour cells in culture. *Eur. J. Cancer* (1994) 30(1): 89-93

55) B. Stella, S. Arpicco, M. T Peracchia, D. Desmaele, J. Hoebeke , M. Renoir , J. D'Angelo , L. Cattel , P. Couvreur, Design of folic acid-conjugated nanoparticles for drug targeting. *J Pharm Sci.* (2000) 89(11): 1452-1464

56) R Brown, M Links, Clinical relevance of the molecular mechanisms of resistance to anti-cancer drugs. *Expert Reviews in Molecular Medicine*, (2004) 1:1-21

57) R Krishna, LD Mayer, Multidrug resistance (MDR) in cancer Mechanisms, reversal using modulators of MDR and the role of MDR modulators in influencing the pharmacokinetics of anticancer drugs. *European Journal of Pharmaceutical Sciences* (2000) 11(4): 265-283

58) C. Vauthier C. Dubernet, C. Chauvierre, I. Brigger, P. Couvreur Drug delivery to resistant tumors: the potential of poly(alkyl cyanoacrylate) nanoparticles. *Journal of Controlled Release* (2003) 93(2): 151-160

59) MV Blagosklonny Targeting cancer cells by exploiting their resistance. *Trends in Molecular Medicine* (2003) 9(7): 307-312

60) A. K Larsen, A. E Escargueil, A. Skladanowski, Resistance mechanisms associated with altered intracellular distribution of anticancer agents. *Pharmacol. Ther.* (2000) 85(3): 217-229

61) R. Esfand, D. A Tomalia, Poly(amidoamine) (PAMAM) dendrimers: from biomimicry to drug delivery and biomedical applications. *Drug Discov. Today* (2001) 6: 427-436

62) Y. Kim, S. C Zimmerman, Applications of dendrimers in bio-organic chemistry. *Curr. Opin. Chem. Biol.* (1998) 2: 733-742

63) R. Duncan, Dendrimers: novel carriers for oral and parenteral drug delivery. *Polym. Mater. Sci. Eng.* (2001) 84: 214

64) M. Liu, J. M. J Frechet, Designing dendrimers for drug delivery. *Pharm. Sci. Technol. Today* (1999) 2: 393-401

65) D. A Tomalia, H. Baker, J. Dewald, M. Hall, G. Kallos, S. Martin, J. Roeck, J. Ryder, P. Smith, A new class of polymer : starburst-dendritic macromolecules. *Polym. J.* (1985) 17: 117-132

66) G. R Newkome, Z. Yao, G. R Baker, V. K Gupta, Micelles. Part 1. Cascade molecules: a new approach to micelles. A [27]-arborol. *J. Org. Chem.* (1985) 50: 2003-2004

67) E. Buhleier, W. Wehner, F. Vogtle, "Cascade" and nonskidchain-like synthesis of molecular cavity topologies *Synthesis* (1978) 155-158

68) J. C Roberts, M. K Bhalgat, R. T Zera, Preliminary biological evaluation of polyamidoamine (PAMAM) Starburst™ dendrimers. *J. Biomed. Mater. Res.* (1996) 30: 53-65

69) N. Malik, R. Wiwattanapatapee, R. Klopsch, K. Lorenz, H. Frey, J. W Weener, E. W Meijer, W. Paulus, R. Duncan, Dendrimers: Relationship between structure and biocompatibility in vitro, and preliminary studies on the biodistribution of ^{125}I-labelled polyamidoamine dendrimers in vivo. *J. Controlled Release* (2000) 65: 133-142

70) S. Hong, A. U Bielinska, A. Mecke, B. Keszler, J. L Beals, X. Shi, L. Balogh, B.G Orr, J. R Baker, M. M. B Holl, Interaction of poly (amidoamine) dendrimers with supported lipid bilayers and cells: hole formation and the relation to transport. *Bioconjugate Chem.* (2004) 15: 774-782

71) M. F Neerman, W. Zhang, A. R Parrish, E. E Simanek, In vitro and in vivo evaluation of a melamine dendrimer as a vehicle for drug delivery. *Int. J. Pharm.* (2004) 281: 129-132

72) G. A Brazeau, S. Attia, S. Poxon, J. A Hughes, In vitro myotoxicity of selected cationic macromolecules used in non-viral gene delivery *Pharmacol. Res.* (1998) 15: 680-684

73) P. Ferruti, S. Knobloch, E. Ranucci, R. Duncan, E. Giansi, A novel modification of poly(L-lysine) leading to a soluble cationic polymer with reduced toxicity and with potential as a transfection agent. *Macromol. Chem. Phys.* (1998) 199: 2565

74) D. Fischer, Y. Li, B. Ahlemeyer, J. Krieglstein, T. Kissel, In vitro cytotoxicity testing of polycations: influence of polymer structure on cell viability and hemolysis. *Biomaterials* (2003) 24 (7): 1121-1131

75) P. Ferruti, S. Knobloch, E. Ranucci, E. Gainsi, R. Duncan, E. Giansi. *Proc. Int. Symp. Controlled Rel. Bioact. Mater.* (1997) 45

76) M. El-Sayed, M. Ginski, C. Rhodes, H. Ghandehari, Influence of surface chemistry of poly (amidoamine) dendrimers on Caco-2 cell monolayers. *Journal of Bioactive and Compatible Polymers* (2003) 18(1): 7-22

77) O. L Padilla de Jesus, H. R Ihre, L. Gagne, J. M Frechet and F. C Szoka Jr., Polyester Dendritic Systems for Drug Delivery Applications: In Vitro and In Vivo Evaluation. *Bioconjugate Chem.* (2002) 13: 453-461

78) H. Yang, S. T Lopina, Extended release of a novel antidepressant, venlafaxine, based on anionic polyamidoamine dendrimers and poly(ethylene glycol)-containing semi-interpenetrating networks. *J. Biomed. Mater. Res.* (2005) 72A: 107

79) H. Yang, J. J Morris, S. T Lopina, Polyethylene glycol-polyamidoamine dendritic micelle as solubility enhancer and the effect of the length of polyethylene glycol arms on the solubility of Pyrene in water. *J. Colloid and Interface Science* (2004) 273: 148-154

80) W. M Pardrige, Vector-mediated drug delivery to the brain. *Adv. Drug Delivery Reviews* (1999) 36(2-3): 299-321

APPENDICES

APPENDIX A

STATISTICAL ANALYSIS

A1. Statistical analysis of cell viability measurements using 3 Way ANOVA with MINITAB version 15

General Linear Model: CELL VIABILITY versus TIME, POLY, CONC

```
Factor  Type   Levels  Values
TIME    fixed       4  6, 12, 24, 36
POLY    fixed       3  BH, PEG, PEG-BH
CONC    fixed       3  1, 2, 3


Analysis of Variance for CELL VIABILITY, using Adjusted SS for Tests

Source           DF   Seq SS   Adj SS  Adj MS        F      P
TIME              3   2593.7   2593.7   864.6   200.95  0.000
POLY              2  19827.6  19827.6  9913.8  2304.31  0.000
CONC              2   3030.4   3030.4  1515.2   352.19  0.000
TIME*POLY         6   2506.3   2506.3   417.7    97.09  0.000
TIME*CONC         6   1528.3   1528.3   254.7    59.20  0.000
POLY*CONC         4   3442.1   3442.1   860.5   200.02  0.000
TIME*POLY*CONC   12   2892.6   2892.6   241.0    56.03  0.000
Error            72    309.8    309.8     4.3
Total           107  36130.7


S = 2.07420   R-Sq = 99.14%   R-Sq(adj) = 98.73%


Unusual Observations for CELL VIABILITY

          CELL
Obs  VIABILITY      Fit  SE Fit  Residual  St Resid
  1    87.0169  83.3363  1.1975    3.6807      2.17 R
  2    78.0943  83.3363  1.1975   -5.2419     -3.10 R
  5    78.7048  82.5595  1.1975   -3.8547     -2.28 R
 36    90.7792  94.5425  1.1975   -3.7632     -2.22 R
 71    47.1071  50.6242  1.1975   -3.5171     -2.08 R
 76    89.3354  85.2969  1.1975    4.0385      2.38 R
 77    81.3459  85.2969  1.1975   -3.9510     -2.33 R

R denotes an observation with a large standardized residual.
```

Tukey Simultaneous Tests
Response Variable CELL VIABILITY
All Pairwise Comparisons among Levels of TIME
TIME = 6 subtracted from:

TIME	Difference of Means	SE of Difference	T-Value	Adjusted P-Value
12	10.5450	0.5645	18.679	0.0000
24	7.8996	0.5645	13.993	0.0000
36	-0.7667	0.5645	-1.358	0.5295

TIME = 12 subtracted from:

TIME	Difference of Means	SE of Difference	T-Value	Adjusted P-Value
24	-2.65	0.5645	-4.69	0.0001
36	-11.31	0.5645	-20.04	0.0000

TIME = 24 subtracted from:

TIME	Difference of Means	SE of Difference	T-Value	Adjusted P-Value
36	-8.666	0.5645	-15.35	0.0000

Tukey Simultaneous Tests
Response Variable CELL VIABILITY
All Pairwise Comparisons among Levels of POLY
POLY = BH subtracted from:

POLY	Difference of Means	SE of Difference	T-Value	Adjusted P-Value
PEG	32.07	0.4889	65.59	0.0000
PEG-BH	23.44	0.4889	47.95	0.0000

POLY = PEG subtracted from:

POLY	Difference of Means	SE of Difference	T-Value	Adjusted P-Value
PEG-BH	-8.625	0.4889	-17.64	0.0000

Tukey Simultaneous Tests
Response Variable CELL VIABILITY
All Pairwise Comparisons among Levels of CONC
CONC = 1 subtracted from:

CONC	Difference of Means	SE of Difference	T-Value	Adjusted P-Value
2	-5.40	0.4889	-11.04	0.0000
3	-12.92	0.4889	-26.42	0.0000

CONC = 2 subtracted from:

CONC	Difference of Means	SE of Difference	T-Value	Adjusted P-Value
3	-7.518	0.4889	-15.38	0.0000

Tukey Simultaneous Tests
Response Variable CELL VIABILITY
All Pairwise Comparisons among Levels of TIME*POLY
TIME = 6
POLY = BH subtracted from:

TIME	POLY	Difference of Means	SE of Difference	T-Value	Adjusted P-Value
6	PEG	20.22	0.9778	20.68	0.0000
6	PEG-BH	14.24	0.9778	14.57	0.0000
12	BH	6.67	0.9778	6.82	0.0000
12	PEG	34.17	0.9778	34.94	0.0000
12	PEG-BH	25.27	0.9778	25.85	0.0000
24	BH	1.80	0.9778	1.84	0.7893
24	PEG	32.98	0.9778	33.73	0.0000
24	PEG-BH	23.38	0.9778	23.91	0.0000
36	BH	-18.85	0.9778	-19.28	0.0000
36	PEG	30.52	0.9778	31.21	0.0000
36	PEG-BH	20.49	0.9778	20.96	0.0000

TIME = 6
POLY = PEG subtracted from:

TIME	POLY	Difference of Means	SE of Difference	T-Value	Adjusted P-Value
6	PEG-BH	-5.98	0.9778	-6.11	0.0000
12	BH	-13.56	0.9778	-13.87	0.0000
12	PEG	13.94	0.9778	14.26	0.0000
12	PEG-BH	5.05	0.9778	5.16	0.0002
24	BH	-18.42	0.9778	-18.84	0.0000
24	PEG	12.76	0.9778	13.05	0.0000
24	PEG-BH	3.16	0.9778	3.23	0.0740
36	BH	-39.07	0.9778	-39.96	0.0000
36	PEG	10.30	0.9778	10.53	0.0000
36	PEG-BH	0.27	0.9778	0.28	1.0000

TIME = 6
POLY = PEG-BH subtracted from:

TIME	POLY	Difference of Means	SE of Difference	T-Value	Adjusted P-Value
12	BH	-7.58	0.9778	-7.75	0.0000
12	PEG	19.92	0.9778	20.37	0.0000
12	PEG-BH	11.03	0.9778	11.28	0.0000
24	BH	-12.44	0.9778	-12.73	0.0000
24	PEG	18.74	0.9778	19.16	0.0000
24	PEG-BH	9.14	0.9778	9.35	0.0000
36	BH	-33.09	0.9778	-33.84	0.0000
36	PEG	16.28	0.9778	16.64	0.0000
36	PEG-BH	6.25	0.9778	6.39	0.0000

TIME = 12
POLY = BH subtracted from:

TIME	POLY	Difference of Means	SE of Difference	T-Value	Adjusted P-Value
12	PEG	27.50	0.9778	28.12	0.0000
12	PEG-BH	18.61	0.9778	19.03	0.0000
24	BH	-4.86	0.9778	-4.97	0.0003
24	PEG	26.32	0.9778	26.92	0.0000
24	PEG-BH	16.72	0.9778	17.10	0.0000
36	BH	-25.51	0.9778	-26.09	0.0000
36	PEG	23.85	0.9778	24.40	0.0000
36	PEG-BH	13.83	0.9778	14.14	0.0000

TIME = 12
POLY = PEG subtracted from:

TIME	POLY	Difference of Means	SE of Difference	T-Value	Adjusted P-Value
12	PEG-BH	-8.89	0.9778	-9.10	0.0000
24	BH	-32.36	0.9778	-33.10	0.0000
24	PEG	-1.18	0.9778	-1.21	0.9866
24	PEG-BH	-10.78	0.9778	-11.03	0.0000
36	BH	-53.01	0.9778	-54.22	0.0000
36	PEG	-3.65	0.9778	-3.73	0.0182
36	PEG-BH	-13.67	0.9778	-13.98	0.0000

TIME = 12
POLY = PEG-BH subtracted from:

TIME	POLY	Difference of Means	SE of Difference	T-Value	Adjusted P-Value
24	BH	-23.47	0.9778	-24.00	0.0000
24	PEG	7.71	0.9778	7.89	0.0000
24	PEG-BH	-1.89	0.9778	-1.93	0.7352
36	BH	-44.12	0.9778	-45.12	0.0000
36	PEG	5.25	0.9778	5.37	0.0001
36	PEG-BH	-4.78	0.9778	-4.88	0.0004

TIME = 24
POLY = BH subtracted from:

TIME	POLY	Difference of Means	SE of Difference	T-Value	Adjusted P-Value
24	PEG	31.18	0.9778	31.89	0.0000
24	PEG-BH	21.58	0.9778	22.07	0.0000
36	BH	-20.65	0.9778	-21.12	0.0000
36	PEG	28.72	0.9778	29.37	0.0000
36	PEG-BH	18.69	0.9778	19.12	0.0000

TIME = 24
POLY = PEG subtracted from:

TIME	POLY	Difference of Means	SE of Difference	T-Value	Adjusted P-Value
24	PEG-BH	-9.60	0.9778	-9.82	0.0000
36	BH	-51.83	0.9778	-53.01	0.0000

36	PEG	-2.46	0.9778	-2.52	0.3448
36	PEG-BH	-12.49	0.9778	-12.77	0.0000

TIME = 24
POLY = PEG-BH subtracted from:

TIME	POLY	Difference of Means	SE of Difference	T-Value	Adjusted P-Value
36	BH	-42.23	0.9778	-43.19	0.0000
36	PEG	7.14	0.9778	7.30	0.0000
36	PEG-BH	-2.89	0.9778	-2.95	0.1452

TIME = 36
POLY = BH subtracted from:

TIME	POLY	Difference of Means	SE of Difference	T-Value	Adjusted P-Value
36	PEG	49.37	0.9778	50.49	0.0000
36	PEG-BH	39.34	0.9778	40.24	0.0000

TIME = 36
POLY = PEG subtracted from:

TIME	POLY	Difference of Means	SE of Difference	T-Value	Adjusted P-Value
36	PEG-BH	-10.02	0.9778	-10.25	0.0000

Tukey Simultaneous Tests
Response Variable CELL VIABILITY
All Pairwise Comparisons among Levels of TIME*CONC
TIME = 6
CONC = 1 subtracted from:

TIME	CONC	Difference of Means	SE of Difference	T-Value	Adjusted P-Value
6	2	-3.35	0.9778	-3.43	0.0439
6	3	-6.13	0.9778	-6.27	0.0000
12	1	11.45	0.9778	11.71	0.0000
12	2	6.77	0.9778	6.92	0.0000
12	3	3.94	0.9778	4.03	0.0072
24	1	9.69	0.9778	9.91	0.0000
24	2	4.93	0.9778	5.04	0.0002
24	3	-0.40	0.9778	-0.41	1.0000
36	1	8.32	0.9778	8.51	0.0000
36	2	-0.48	0.9778	-0.50	1.0000
36	3	-19.62	0.9778	-20.06	0.0000

TIME = 6
CONC = 2 subtracted from:

TIME	CONC	Difference of Means	SE of Difference	T-Value	Adjusted P-Value
6	3	-2.78	0.9778	-2.85	0.1832
12	1	14.80	0.9778	15.13	0.0000
12	2	10.12	0.9778	10.35	0.0000
12	3	7.29	0.9778	7.45	0.0000

24	1	13.04	0.9778	13.34	0.0000
24	2	8.28	0.9778	8.46	0.0000
24	3	2.95	0.9778	3.01	0.1259
36	1	11.67	0.9778	11.93	0.0000
36	2	2.87	0.9778	2.93	0.1525
36	3	-16.27	0.9778	-16.64	0.0000

TIME = 6
CONC = 3 subtracted from:

TIME	CONC	Difference of Means	SE of Difference	T-Value	Adjusted P-Value
12	1	17.58	0.9778	17.98	0.0000
12	2	12.90	0.9778	13.19	0.0000
12	3	10.07	0.9778	10.30	0.0000
24	1	15.83	0.9778	16.19	0.0000
24	2	11.06	0.9778	11.31	0.0000
24	3	5.73	0.9778	5.86	0.0000
36	1	14.45	0.9778	14.78	0.0000
36	2	5.65	0.9778	5.78	0.0000
36	3	-13.48	0.9778	-13.79	0.0000

TIME = 12
CONC = 1 subtracted from:

TIME	CONC	Difference of Means	SE of Difference	T-Value	Adjusted P-Value
12	2	-4.68	0.9778	-4.79	0.0005
12	3	-7.51	0.9778	-7.68	0.0000
24	1	-1.75	0.9778	-1.79	0.8157
24	2	-6.52	0.9778	-6.67	0.0000
24	3	-11.85	0.9778	-12.12	0.0000
36	1	-3.13	0.9778	-3.20	0.0796
36	2	-11.93	0.9778	-12.20	0.0000
36	3	-31.06	0.9778	-31.77	0.0000

TIME = 12
CONC = 2 subtracted from:

TIME	CONC	Difference of Means	SE of Difference	T-Value	Adjusted P-Value
12	3	-2.83	0.9778	-2.89	0.1657
24	1	2.93	0.9778	2.99	0.1323
24	2	-1.84	0.9778	-1.88	0.7656
24	3	-7.17	0.9778	-7.33	0.0000
36	1	1.55	0.9778	1.59	0.9089
36	2	-7.25	0.9778	-7.42	0.0000
36	3	-26.38	0.9778	-26.98	0.0000

TIME = 12
CONC = 3 subtracted from:

TIME	CONC	Difference of Means	SE of Difference	T-Value	Adjusted P-Value
24	1	5.75	0.9778	5.89	0.0000
24	2	0.99	0.9778	1.01	0.9970
24	3	-4.34	0.9778	-4.44	0.0018

36	1	4.38	0.9778	4.48	0.0016
36	2	-4.42	0.9778	-4.52	0.0014
36	3	-23.55	0.9778	-24.09	0.0000

TIME = 24
CONC = 1 subtracted from:

TIME	CONC	Difference of Means	SE of Difference	T-Value	Adjusted P-Value
24	2	-4.77	0.9778	-4.88	0.0004
24	3	-10.10	0.9778	-10.33	0.0000
36	1	-1.38	0.9778	-1.41	0.9583
36	2	-10.18	0.9778	-10.41	0.0000
36	3	-29.31	0.9778	-29.97	0.0000

TIME = 24
CONC = 2 subtracted from:

TIME	CONC	Difference of Means	SE of Difference	T-Value	Adjusted P-Value
24	3	-5.33	0.9778	-5.45	0.0001
36	1	3.39	0.9778	3.47	0.0390
36	2	-5.41	0.9778	-5.53	0.0001
36	3	-24.54	0.9778	-25.10	0.0000

TIME = 24
CONC = 3 subtracted from:

TIME	CONC	Difference of Means	SE of Difference	T-Value	Adjusted P-Value
36	1	8.72	0.9778	8.92	0.0000
36	2	-0.08	0.9778	-0.08	1.0000
36	3	-19.21	0.9778	-19.65	0.0000

TIME = 36
CONC = 1 subtracted from:

TIME	CONC	Difference of Means	SE of Difference	T-Value	Adjusted P-Value
36	2	-8.80	0.9778	-9.00	0.0000
36	3	-27.93	0.9778	-28.57	0.0000

TIME = 36
CONC = 2 subtracted from:

TIME	CONC	Difference of Means	SE of Difference	T-Value	Adjusted P-Value
36	3	-19.13	0.9778	-19.57	0.0000

Tukey Simultaneous Tests
Response Variable CELL VIABILITY
All Pairwise Comparisons among Levels of POLY*CONC
POLY = BH
CONC = 1 subtracted from:

POLY	CONC	Difference of Means	SE of Difference	T-Value	Adjusted P-Value
BH	2	-12.11	0.8468	-14.30	0.0000
BH	3	-32.15	0.8468	-37.97	0.0000
PEG	1	18.58	0.8468	21.94	0.0000
PEG	2	17.41	0.8468	20.56	0.0000
PEG	3	15.96	0.8468	18.84	0.0000
PEG-BH	1	10.99	0.8468	12.98	0.0000
PEG-BH	2	8.07	0.8468	9.53	0.0000
PEG-BH	3	7.01	0.8468	8.28	0.0000

POLY = BH
CONC = 2 subtracted from:

POLY	CONC	Difference of Means	SE of Difference	T-Value	Adjusted P-Value
BH	3	-20.05	0.8468	-23.68	0.0000
PEG	1	30.69	0.8468	36.24	0.0000
PEG	2	29.51	0.8468	34.85	0.0000
PEG	3	28.06	0.8468	33.14	0.0000
PEG-BH	1	23.09	0.8468	27.27	0.0000
PEG-BH	2	20.17	0.8468	23.82	0.0000
PEG-BH	3	19.12	0.8468	22.58	0.0000

POLY = BH
CONC = 3 subtracted from:

POLY	CONC	Difference of Means	SE of Difference	T-Value	Adjusted P-Value
PEG	1	50.73	0.8468	59.91	0.0000
PEG	2	49.56	0.8468	58.53	0.0000
PEG	3	48.11	0.8468	56.81	0.0000
PEG-BH	1	43.14	0.8468	50.95	0.0000
PEG-BH	2	40.22	0.8468	47.50	0.0000
PEG-BH	3	39.17	0.8468	46.25	0.0000

POLY = PEG
CONC = 1 subtracted from:

POLY	CONC	Difference of Means	SE of Difference	T-Value	Adjusted P-Value
PEG	2	-1.17	0.8468	-1.38	0.9005
PEG	3	-2.62	0.8468	-3.10	0.0648
PEG-BH	1	-7.59	0.8468	-8.96	0.0000
PEG-BH	2	-10.51	0.8468	-12.42	0.0000
PEG-BH	3	-11.57	0.8468	-13.66	0.0000

POLY = PEG
CONC = 2 subtracted from:

POLY	CONC	Difference of Means	SE of Difference	T-Value	Adjusted P-Value
PEG	3	-1.45	0.8468	-1.72	0.7348
PEG-BH	1	-6.42	0.8468	-7.58	0.0000
PEG-BH	2	-9.34	0.8468	-11.03	0.0000
PEG-BH	3	-10.39	0.8468	-12.27	0.0000

POLY = PEG
CONC = 3 subtracted from:

POLY	CONC	Difference of Means	SE of Difference	T-Value	Adjusted P-Value
PEG-BH	1	-4.967	0.8468	-5.87	0.0000
PEG-BH	2	-7.889	0.8468	-9.32	0.0000
PEG-BH	3	-8.941	0.8468	-10.56	0.0000

POLY = PEG-BH
CONC = 1 subtracted from:

POLY	CONC	Difference of Means	SE of Difference	T-Value	Adjusted P-Value
PEG-BH	2	-2.922	0.8468	-3.451	0.0248
PEG-BH	3	-3.974	0.8468	-4.693	0.0004

POLY = PEG-BH
CONC = 2 subtracted from:

POLY	CONC	Difference of Means	SE of Difference	T-Value	Adjusted P-Value
PEG-BH	3	-1.052	0.8468	-1.242	0.9440

Tukey Simultaneous Tests
Response Variable CELL VIABILITY
All Pairwise Comparisons among Levels of TIME*POLY*CONC
TIME = 6
POLY = BH
CONC = 1 subtracted from:

TIME	POLY	CONC	Difference of Means	SE of Difference	T-Value	Adjusted P-Value
6	BH	2	-4.43	1.694	-2.62	0.7653
6	BH	3	-9.38	1.694	-5.54	0.0003
6	PEG	1	16.63	1.694	9.82	0.0001
6	PEG	2	15.85	1.694	9.36	0.0001
6	PEG	3	14.38	1.694	8.49	0.0001
6	PEG-BH	1	13.51	1.694	7.98	0.0001
6	PEG-BH	2	8.67	1.694	5.12	0.0013
6	PEG-BH	3	6.74	1.694	3.98	0.0533
12	BH	1	12.11	1.694	7.15	0.0001
12	BH	2	0.31	1.694	0.18	1.0000
12	BH	3	-6.23	1.694	-3.68	0.1210
12	PEG	1	31.13	1.694	18.38	0.0001
12	PEG	2	29.72	1.694	17.55	0.0001
12	PEG	3	27.84	1.694	16.44	0.0001
12	PEG-BH	1	21.25	1.694	12.55	0.0001
12	PEG-BH	2	20.41	1.694	12.05	0.0001
12	PEG-BH	3	20.35	1.694	12.02	0.0001
24	BH	1	9.43	1.694	5.57	0.0003
24	BH	2	-1.75	1.694	-1.03	1.0000
24	BH	3	-16.08	1.694	-9.50	0.0001
24	PEG	1	29.16	1.694	17.22	0.0001
24	PEG	2	28.08	1.694	16.58	0.0001
24	PEG	3	27.91	1.694	16.48	0.0001
24	PEG-BH	1	20.64	1.694	12.19	0.0001

24	PEG-BH	2	18.59	1.694	10.98	0.0001
24	PEG-BH	3	17.11	1.694	10.10	0.0001
36	BH	1	8.69	1.694	5.13	0.0012
36	BH	2	-12.33	1.694	-7.28	0.0001
36	BH	3	-66.70	1.694	-39.39	0.0001
36	PEG	1	27.63	1.694	16.31	0.0001
36	PEG	2	26.20	1.694	15.47	0.0001
36	PEG	3	23.92	1.694	14.13	0.0001
36	PEG-BH	1	18.78	1.694	11.09	0.0001
36	PEG-BH	2	14.82	1.694	8.75	0.0001
36	PEG-BH	3	14.08	1.694	8.31	0.0001

TIME = 6
POLY = BH
CONC = 2 subtracted from:

TIME	POLY	CONC	Difference of Means	SE of Difference	T-Value	Adjusted P-Value
6	BH	3	-4.95	1.694	-2.92	0.5445
6	PEG	1	21.06	1.694	12.44	0.0001
6	PEG	2	20.28	1.694	11.98	0.0001
6	PEG	3	18.81	1.694	11.11	0.0001
6	PEG-BH	1	17.94	1.694	10.59	0.0001
6	PEG-BH	2	13.10	1.694	7.74	0.0001
6	PEG-BH	3	11.17	1.694	6.60	0.0001
12	BH	1	16.54	1.694	9.77	0.0001
12	BH	2	4.74	1.694	2.80	0.6365
12	BH	3	-1.80	1.694	-1.06	1.0000
12	PEG	1	35.56	1.694	21.00	0.0001
12	PEG	2	34.15	1.694	20.17	0.0001
12	PEG	3	32.27	1.694	19.05	0.0001
12	PEG-BH	1	25.68	1.694	15.16	0.0001
12	PEG-BH	2	24.84	1.694	14.67	0.0001
12	PEG-BH	3	24.78	1.694	14.63	0.0001
24	BH	1	13.86	1.694	8.18	0.0001
24	BH	2	2.68	1.694	1.58	0.9997
24	BH	3	-11.65	1.694	-6.88	0.0001
24	PEG	1	33.59	1.694	19.83	0.0001
24	PEG	2	32.51	1.694	19.20	0.0001
24	PEG	3	32.34	1.694	19.09	0.0001
24	PEG-BH	1	25.07	1.694	14.80	0.0001
24	PEG-BH	2	23.02	1.694	13.59	0.0001
24	PEG-BH	3	21.54	1.694	12.72	0.0001
36	BH	1	13.12	1.694	7.74	0.0001
36	BH	2	-7.90	1.694	-4.66	0.0062
36	BH	3	-62.28	1.694	-36.77	0.0001
36	PEG	1	32.06	1.694	18.93	0.0001
36	PEG	2	30.63	1.694	18.09	0.0001
36	PEG	3	28.35	1.694	16.74	0.0001
36	PEG-BH	1	23.21	1.694	13.70	0.0001
36	PEG-BH	2	19.25	1.694	11.36	0.0001
36	PEG-BH	3	18.51	1.694	10.93	0.0001

TIME = 6
POLY = BH
CONC = 3 subtracted from:

TIME	POLY	CONC	Difference of Means	SE of Difference	T-Value	Adjusted P-Value
6	PEG	1	26.01	1.694	15.36	0.0001
6	PEG	2	25.23	1.694	14.90	0.0001
6	PEG	3	23.75	1.694	14.03	0.0001
6	PEG-BH	1	22.89	1.694	13.52	0.0001
6	PEG-BH	2	18.05	1.694	10.66	0.0001
6	PEG-BH	3	16.12	1.694	9.52	0.0001
12	BH	1	21.49	1.694	12.69	0.0001
12	BH	2	9.69	1.694	5.72	0.0002
12	BH	3	3.15	1.694	1.86	0.9952
12	PEG	1	40.51	1.694	23.92	0.0001
12	PEG	2	39.10	1.694	23.09	0.0001
12	PEG	3	37.21	1.694	21.97	0.0001
12	PEG-BH	1	30.62	1.694	18.08	0.0001
12	PEG-BH	2	29.79	1.694	17.59	0.0001
12	PEG-BH	3	29.73	1.694	17.55	0.0001
24	BH	1	18.80	1.694	11.10	0.0001
24	BH	2	7.63	1.694	4.50	0.0106
24	BH	3	-6.71	1.694	-3.96	0.0568
24	PEG	1	38.53	1.694	22.75	0.0001
24	PEG	2	37.46	1.694	22.12	0.0001
24	PEG	3	37.28	1.694	22.02	0.0001
24	PEG-BH	1	30.01	1.694	17.72	0.0001
24	PEG-BH	2	27.97	1.694	16.51	0.0001
24	PEG-BH	3	26.48	1.694	15.64	0.0001
36	BH	1	18.06	1.694	10.67	0.0001
36	BH	2	-2.95	1.694	-1.74	0.9983
36	BH	3	-57.33	1.694	-33.85	0.0001
36	PEG	1	37.00	1.694	21.85	0.0001
36	PEG	2	35.58	1.694	21.01	0.0001
36	PEG	3	33.30	1.694	19.66	0.0001
36	PEG-BH	1	28.16	1.694	16.63	0.0001
36	PEG-BH	2	24.19	1.694	14.29	0.0001
36	PEG-BH	3	23.46	1.694	13.85	0.0001

TIME = 6
POLY = PEG
CONC = 1 subtracted from:

TIME	POLY	CONC	Difference of Means	SE of Difference	T-Value	Adjusted P-Value
6	PEG	2	-0.78	1.694	-0.46	1.0000
6	PEG	3	-2.25	1.694	-1.33	1.0000
6	PEG-BH	1	-3.12	1.694	-1.84	0.9958
6	PEG-BH	2	-7.96	1.694	-4.70	0.0055
6	PEG-BH	3	-9.89	1.694	-5.84	0.0001
12	BH	1	-4.52	1.694	-2.67	0.7289
12	BH	2	-16.32	1.694	-9.64	0.0001
12	BH	3	-22.86	1.694	-13.50	0.0001
12	PEG	1	14.50	1.694	8.56	0.0001
12	PEG	2	13.09	1.694	7.73	0.0001
12	PEG	3	11.21	1.694	6.62	0.0001
12	PEG-BH	1	4.62	1.694	2.73	0.6898
12	PEG-BH	2	3.78	1.694	2.23	0.9447
12	PEG-BH	3	3.72	1.694	2.20	0.9540

24	BH	1	-7.20	1.694	-4.25	0.0237
24	BH	2	-18.38	1.694	-10.85	0.0001
24	BH	3	-32.71	1.694	-19.32	0.0001
24	PEG	1	12.52	1.694	7.40	0.0001
24	PEG	2	11.45	1.694	6.76	0.0001
24	PEG	3	11.28	1.694	6.66	0.0001
24	PEG-BH	1	4.01	1.694	2.37	0.8987
24	PEG-BH	2	1.96	1.694	1.16	1.0000
24	PEG-BH	3	0.48	1.694	0.28	1.0000
36	BH	1	-7.94	1.694	-4.69	0.0057
36	BH	2	-28.96	1.694	-17.10	0.0001
36	BH	3	-83.34	1.694	-49.21	0.0001
36	PEG	1	11.00	1.694	6.49	0.0001
36	PEG	2	9.57	1.694	5.65	0.0002
36	PEG	3	7.29	1.694	4.31	0.0201
36	PEG-BH	1	2.15	1.694	1.27	1.0000
36	PEG-BH	2	-1.81	1.694	-1.07	1.0000
36	PEG-BH	3	-2.55	1.694	-1.51	0.9999

TIME = 6
POLY = PEG
CONC = 2 subtracted from:

TIME	POLY	CONC	Difference of Means	SE of Difference	T-Value	Adjusted P-Value
6	PEG	3	-1.48	1.694	-0.87	1.0000
6	PEG-BH	1	-2.34	1.694	-1.38	1.0000
6	PEG-BH	2	-7.18	1.694	-4.24	0.0245
6	PEG-BH	3	-9.11	1.694	-5.38	0.0005
12	BH	1	-3.74	1.694	-2.21	0.9502
12	BH	2	-15.54	1.694	-9.18	0.0001
12	BH	3	-22.08	1.694	-13.04	0.0001
12	PEG	1	15.28	1.694	9.02	0.0001
12	PEG	2	13.87	1.694	8.19	0.0001
12	PEG	3	11.98	1.694	7.08	0.0001
12	PEG-BH	1	5.39	1.694	3.18	0.3565
12	PEG-BH	2	4.56	1.694	2.69	0.7145
12	PEG-BH	3	4.50	1.694	2.65	0.7394
24	BH	1	-6.43	1.694	-3.79	0.0893
24	BH	2	-17.60	1.694	-10.39	0.0001
24	BH	3	-31.94	1.694	-18.86	0.0001
24	PEG	1	13.30	1.694	7.85	0.0001
24	PEG	2	12.23	1.694	7.22	0.0001
24	PEG	3	12.05	1.694	7.12	0.0001
24	PEG-BH	1	4.78	1.694	2.83	0.6165
24	PEG-BH	2	2.74	1.694	1.62	0.9996
24	PEG-BH	3	1.25	1.694	0.74	1.0000
36	BH	1	-7.17	1.694	-4.23	0.0252
36	BH	2	-28.18	1.694	-16.64	0.0001
36	BH	3	-82.56	1.694	-48.75	0.0001
36	PEG	1	11.77	1.694	6.95	0.0001
36	PEG	2	10.35	1.694	6.11	0.0001
36	PEG	3	8.07	1.694	4.76	0.0044
36	PEG-BH	1	2.93	1.694	1.73	0.9985
36	PEG-BH	2	-1.04	1.694	-0.61	1.0000
36	PEG-BH	3	-1.77	1.694	-1.05	1.0000

TIME = 6
POLY = PEG
CONC = 3 subtracted from:

TIME	POLY	CONC	Difference of Means	SE of Difference	T-Value	Adjusted P-Value
6	PEG-BH	1	-0.86	1.694	-0.51	1.0000
6	PEG-BH	2	-5.71	1.694	-3.37	0.2469
6	PEG-BH	3	-7.64	1.694	-4.51	0.0104
12	BH	1	-2.27	1.694	-1.34	1.0000
12	BH	2	-14.07	1.694	-8.31	0.0001
12	BH	3	-20.61	1.694	-12.17	0.0001
12	PEG	1	16.75	1.694	9.89	0.0001
12	PEG	2	15.35	1.694	9.06	0.0001
12	PEG	3	13.46	1.694	7.95	0.0001
12	PEG-BH	1	6.87	1.694	4.06	0.0430
12	PEG-BH	2	6.03	1.694	3.56	0.1605
12	PEG-BH	3	5.97	1.694	3.53	0.1748
24	BH	1	-4.95	1.694	-2.92	0.5429
24	BH	2	-16.13	1.694	-9.52	0.0001
24	BH	3	-30.46	1.694	-17.99	0.0001
24	PEG	1	14.78	1.694	8.73	0.0001
24	PEG	2	13.70	1.694	8.09	0.0001
24	PEG	3	13.53	1.694	7.99	0.0001
24	PEG-BH	1	6.26	1.694	3.70	0.1152
24	PEG-BH	2	4.21	1.694	2.49	0.8412
24	PEG-BH	3	2.73	1.694	1.61	0.9996
36	BH	1	-5.69	1.694	-3.36	0.2519
36	BH	2	-26.71	1.694	-15.77	0.0001
36	BH	3	-81.08	1.694	-47.88	0.0001
36	PEG	1	13.25	1.694	7.82	0.0001
36	PEG	2	11.82	1.694	6.98	0.0001
36	PEG	3	9.54	1.694	5.64	0.0002
36	PEG-BH	1	4.40	1.694	2.60	0.7757
36	PEG-BH	2	0.44	1.694	0.26	1.0000
36	PEG-BH	3	-0.30	1.694	-0.18	1.0000

TIME = 6
POLY = PEG-BH
CONC = 1 subtracted from:

TIME	POLY	CONC	Difference of Means	SE of Difference	T-Value	Adjusted P-Value
6	PEG-BH	2	-4.84	1.694	-2.86	0.5905
6	PEG-BH	3	-6.77	1.694	-4.00	0.0508
12	BH	1	-1.40	1.694	-0.83	1.0000
12	BH	2	-13.20	1.694	-7.80	0.0001
12	BH	3	-19.74	1.694	-11.66	0.0001
12	PEG	1	17.62	1.694	10.40	0.0001
12	PEG	2	16.21	1.694	9.57	0.0001
12	PEG	3	14.32	1.694	8.46	0.0001
12	PEG-BH	1	7.73	1.694	4.57	0.0086
12	PEG-BH	2	6.90	1.694	4.07	0.0409
12	PEG-BH	3	6.84	1.694	4.04	0.0454
24	BH	1	-4.09	1.694	-2.41	0.8789
24	BH	2	-15.26	1.694	-9.01	0.0001
24	BH	3	-29.59	1.694	-17.47	0.0001
24	PEG	1	15.64	1.694	9.24	0.0001
24	PEG	2	14.57	1.694	8.60	0.0001
24	PEG	3	14.40	1.694	8.50	0.0001

24	PEG-BH	1	7.13	1.694	4.21	0.0273
24	PEG-BH	2	5.08	1.694	3.00	0.4864
24	PEG-BH	3	3.59	1.694	2.12	0.9693
36	BH	1	-4.83	1.694	-2.85	0.5976
36	BH	2	-25.84	1.694	-15.26	0.0001
36	BH	3	-80.22	1.694	-47.37	0.0001
36	PEG	1	14.11	1.694	8.33	0.0001
36	PEG	2	12.69	1.694	7.49	0.0001
36	PEG	3	10.41	1.694	6.15	0.0001
36	PEG-BH	1	5.27	1.694	3.11	0.4065
36	PEG-BH	2	1.30	1.694	0.77	1.0000
36	PEG-BH	3	0.57	1.694	0.34	1.0000

TIME = 6
POLY = PEG-BH
CONC = 2 subtracted from:

TIME	POLY	CONC	Difference of Means	SE of Difference	T-Value	Adjusted P-Value
6	PEG-BH	3	-1.93	1.694	-1.14	1.0000
12	BH	1	3.44	1.694	2.03	0.9826
12	BH	2	-8.36	1.694	-4.94	0.0024
12	BH	3	-14.90	1.694	-8.80	0.0001
12	PEG	1	22.46	1.694	13.26	0.0001
12	PEG	2	21.05	1.694	12.43	0.0001
12	PEG	3	19.17	1.694	11.32	0.0001
12	PEG-BH	1	12.58	1.694	7.43	0.0001
12	PEG-BH	2	11.74	1.694	6.93	0.0001
12	PEG-BH	3	11.68	1.694	6.90	0.0001
24	BH	1	0.76	1.694	0.45	1.0000
24	BH	2	-10.42	1.694	-6.15	0.0001
24	BH	3	-24.75	1.694	-14.61	0.0001
24	PEG	1	20.49	1.694	12.10	0.0001
24	PEG	2	19.41	1.694	11.46	0.0001
24	PEG	3	19.24	1.694	11.36	0.0001
24	PEG-BH	1	11.97	1.694	7.07	0.0001
24	PEG-BH	2	9.92	1.694	5.86	0.0001
24	PEG-BH	3	8.44	1.694	4.98	0.0021
36	BH	1	0.02	1.694	0.01	1.0000
36	BH	2	-21.00	1.694	-12.40	0.0001
36	BH	3	-75.38	1.694	-44.51	0.0001
36	PEG	1	18.96	1.694	11.19	0.0001
36	PEG	2	17.53	1.694	10.35	0.0001
36	PEG	3	15.25	1.694	9.01	0.0001
36	PEG-BH	1	10.11	1.694	5.97	0.0001
36	PEG-BH	2	6.15	1.694	3.63	0.1363
36	PEG-BH	3	5.41	1.694	3.20	0.3493

TIME = 6
POLY = PEG-BH
CONC = 3 subtracted from:

TIME	POLY	CONC	Difference of Means	SE of Difference	T-Value	Adjusted P-Value
12	BH	1	5.37	1.694	3.17	0.3663
12	BH	2	-6.43	1.694	-3.80	0.0884
12	BH	3	-12.97	1.694	-7.66	0.0001
12	PEG	1	24.39	1.694	14.40	0.0001
12	PEG	2	22.98	1.694	13.57	0.0001

12	PEG	3	21.09	1.694	12.46	0.0001
12	PEG-BH	1	14.50	1.694	8.56	0.0001
12	PEG-BH	2	13.67	1.694	8.07	0.0001
12	PEG-BH	3	13.61	1.694	8.03	0.0001
24	BH	1	2.69	1.694	1.59	0.9997
24	BH	2	-8.49	1.694	-5.01	0.0018
24	BH	3	-22.82	1.694	-13.48	0.0001
24	PEG	1	22.41	1.694	13.23	0.0001
24	PEG	2	21.34	1.694	12.60	0.0001
24	PEG	3	21.17	1.694	12.50	0.0001
24	PEG-BH	1	13.90	1.694	8.21	0.0001
24	PEG-BH	2	11.85	1.694	7.00	0.0001
24	PEG-BH	3	10.37	1.694	6.12	0.0001
36	BH	1	1.94	1.694	1.15	1.0000
36	BH	2	-19.07	1.694	-11.26	0.0001
36	BH	3	-73.45	1.694	-43.37	0.0001
36	PEG	1	20.89	1.694	12.33	0.0001
36	PEG	2	19.46	1.694	11.49	0.0001
36	PEG	3	17.18	1.694	10.14	0.0001
36	PEG-BH	1	12.04	1.694	7.11	0.0001
36	PEG-BH	2	8.07	1.694	4.77	0.0043
36	PEG-BH	3	7.34	1.694	4.33	0.0184

TIME = 12
POLY = BH
CONC = 1 subtracted from:

TIME	POLY	CONC	Difference of Means	SE of Difference	T-Value	Adjusted P-Value
12	BH	2	-11.80	1.694	-6.97	0.0001
12	BH	3	-18.34	1.694	-10.83	0.0001
12	PEG	1	19.02	1.694	11.23	0.0001
12	PEG	2	17.61	1.694	10.40	0.0001
12	PEG	3	15.73	1.694	9.29	0.0001
12	PEG-BH	1	9.14	1.694	5.40	0.0005
12	PEG-BH	2	8.30	1.694	4.90	0.0027
12	PEG-BH	3	8.24	1.694	4.87	0.0031
24	BH	1	-2.68	1.694	-1.58	0.9997
24	BH	2	-13.86	1.694	-8.18	0.0001
24	BH	3	-28.19	1.694	-16.65	0.0001
24	PEG	1	17.05	1.694	10.07	0.0001
24	PEG	2	15.97	1.694	9.43	0.0001
24	PEG	3	15.80	1.694	9.33	0.0001
24	PEG-BH	1	8.53	1.694	5.04	0.0017
24	PEG-BH	2	6.48	1.694	3.83	0.0818
24	PEG-BH	3	5.00	1.694	2.95	0.5214
36	BH	1	-3.42	1.694	-2.02	0.9837
36	BH	2	-24.44	1.694	-14.43	0.0001
36	BH	3	-78.81	1.694	-46.54	0.0001
36	PEG	1	15.52	1.694	9.16	0.0001
36	PEG	2	14.09	1.694	8.32	0.0001
36	PEG	3	11.81	1.694	6.98	0.0001
36	PEG-BH	1	6.67	1.694	3.94	0.0602
36	PEG-BH	2	2.71	1.694	1.60	0.9996
36	PEG-BH	3	1.97	1.694	1.16	1.0000

TIME = 12
POLY = BH
CONC = 2 subtracted from:

TIME	POLY	CONC	Difference of Means	SE of Difference	T-Value	Adjusted P-Value
12	BH	3	-6.54	1.694	-3.86	0.0748
12	PEG	1	30.82	1.694	18.20	0.0001
12	PEG	2	29.41	1.694	17.37	0.0001
12	PEG	3	27.53	1.694	16.25	0.0001
12	PEG-BH	1	20.94	1.694	12.36	0.0001
12	PEG-BH	2	20.10	1.694	11.87	0.0001
12	PEG-BH	3	20.04	1.694	11.83	0.0001
24	BH	1	9.12	1.694	5.38	0.0005
24	BH	2	-2.06	1.694	-1.22	1.0000
24	BH	3	-16.39	1.694	-9.68	0.0001
24	PEG	1	28.85	1.694	17.03	0.0001
24	PEG	2	27.77	1.694	16.40	0.0001
24	PEG	3	27.60	1.694	16.30	0.0001
24	PEG-BH	1	20.33	1.694	12.00	0.0001
24	PEG-BH	2	18.28	1.694	10.79	0.0001
24	PEG-BH	3	16.80	1.694	9.92	0.0001
36	BH	1	8.38	1.694	4.95	0.0023
36	BH	2	-12.64	1.694	-7.46	0.0001
36	BH	3	-67.01	1.694	-39.57	0.0001
36	PEG	1	27.32	1.694	16.13	0.0001
36	PEG	2	25.89	1.694	15.29	0.0001
36	PEG	3	23.61	1.694	13.94	0.0001
36	PEG-BH	1	18.47	1.694	10.91	0.0001
36	PEG-BH	2	14.51	1.694	8.57	0.0001
36	PEG-BH	3	13.77	1.694	8.13	0.0001

TIME = 12
POLY = BH
CONC = 3 subtracted from:

TIME	POLY	CONC	Difference of Means	SE of Difference	T-Value	Adjusted P-Value
12	PEG	1	37.36	1.694	22.06	0.0001
12	PEG	2	35.95	1.694	21.23	0.0001
12	PEG	3	34.07	1.694	20.11	0.0001
12	PEG-BH	1	27.47	1.694	16.22	0.0001
12	PEG-BH	2	26.64	1.694	15.73	0.0001
12	PEG-BH	3	26.58	1.694	15.69	0.0001
24	BH	1	15.66	1.694	9.24	0.0001
24	BH	2	4.48	1.694	2.64	0.7460
24	BH	3	-9.85	1.694	-5.82	0.0001
24	PEG	1	35.38	1.694	20.89	0.0001
24	PEG	2	34.31	1.694	20.26	0.0001
24	PEG	3	34.14	1.694	20.16	0.0001
24	PEG-BH	1	26.87	1.694	15.86	0.0001
24	PEG-BH	2	24.82	1.694	14.66	0.0001
24	PEG-BH	3	23.34	1.694	13.78	0.0001
36	BH	1	14.91	1.694	8.81	0.0001
36	BH	2	-6.10	1.694	-3.60	0.1460
36	BH	3	-60.48	1.694	-35.71	0.0001
36	PEG	1	33.86	1.694	19.99	0.0001
36	PEG	2	32.43	1.694	19.15	0.0001
36	PEG	3	30.15	1.694	17.80	0.0001
36	PEG-BH	1	25.01	1.694	14.77	0.0001

36	PEG-BH	2	21.05	1.694	12.43	0.0001
36	PEG-BH	3	20.31	1.694	11.99	0.0001

TIME = 12
POLY = PEG
CONC = 1 subtracted from:

TIME	POLY	CONC	Difference of Means	SE of Difference	T-Value	Adjusted P-Value
12	PEG	2	-1.41	1.694	-0.83	1.0000
12	PEG	3	-3.29	1.694	-1.94	0.9905
12	PEG-BH	1	-9.88	1.694	-5.84	0.0001
12	PEG-BH	2	-10.72	1.694	-6.33	0.0001
12	PEG-BH	3	-10.78	1.694	-6.37	0.0001
24	BH	1	-21.70	1.694	-12.81	0.0001
24	BH	2	-32.88	1.694	-19.41	0.0001
24	BH	3	-47.21	1.694	-27.88	0.0001
24	PEG	1	-1.97	1.694	-1.17	1.0000
24	PEG	2	-3.05	1.694	-1.80	0.9971
24	PEG	3	-3.22	1.694	-1.90	0.9931
24	PEG-BH	1	-10.49	1.694	-6.19	0.0001
24	PEG-BH	2	-12.54	1.694	-7.40	0.0001
24	PEG-BH	3	-14.02	1.694	-8.28	0.0001
36	BH	1	-22.44	1.694	-13.25	0.0001
36	BH	2	-43.46	1.694	-25.66	0.0001
36	BH	3	-97.84	1.694	-57.77	0.0001
36	PEG	1	-3.50	1.694	-2.07	0.9779
36	PEG	2	-4.93	1.694	-2.91	0.5523
36	PEG	3	-7.21	1.694	-4.26	0.0235
36	PEG-BH	1	-12.35	1.694	-7.29	0.0001
36	PEG-BH	2	-16.31	1.694	-9.63	0.0001
36	PEG-BH	3	-17.05	1.694	-10.07	0.0001

TIME = 12
POLY = PEG
CONC = 2 subtracted from:

TIME	POLY	CONC	Difference of Means	SE of Difference	T-Value	Adjusted P-Value
12	PEG	3	-1.89	1.694	-1.11	1.0000
12	PEG-BH	1	-8.48	1.694	-5.01	0.0019
12	PEG-BH	2	-9.31	1.694	-5.50	0.0004
12	PEG-BH	3	-9.37	1.694	-5.54	0.0003
24	BH	1	-20.30	1.694	-11.98	0.0001
24	BH	2	-31.47	1.694	-18.58	0.0001
24	BH	3	-45.81	1.694	-27.05	0.0001
24	PEG	1	-0.57	1.694	-0.34	1.0000
24	PEG	2	-1.64	1.694	-0.97	1.0000
24	PEG	3	-1.82	1.694	-1.07	1.0000
24	PEG-BH	1	-9.09	1.694	-5.36	0.0005
24	PEG-BH	2	-11.13	1.694	-6.57	0.0001
24	PEG-BH	3	-12.62	1.694	-7.45	0.0001
36	BH	1	-21.04	1.694	-12.42	0.0001
36	BH	2	-42.05	1.694	-24.83	0.0001
36	BH	3	-96.43	1.694	-56.94	0.0001
36	PEG	1	-2.10	1.694	-1.24	1.0000
36	PEG	2	-3.52	1.694	-2.08	0.9761
36	PEG	3	-5.80	1.694	-3.43	0.2191
36	PEG-BH	1	-10.94	1.694	-6.46	0.0001

36	PEG-BH	2	-14.91	1.694	-8.80	0.0001
36	PEG-BH	3	-15.64	1.694	-9.24	0.0001

TIME = 12
POLY = PEG
CONC = 3 subtracted from:

TIME	POLY	CONC	Difference of Means	SE of Difference	T-Value	Adjusted P-Value
12	PEG-BH	1	-6.59	1.694	-3.89	0.0686
12	PEG-BH	2	-7.43	1.694	-4.38	0.0156
12	PEG-BH	3	-7.49	1.694	-4.42	0.0139
24	BH	1	-18.41	1.694	-10.87	0.0001
24	BH	2	-29.59	1.694	-17.47	0.0001
24	BH	3	-43.92	1.694	-25.93	0.0001
24	PEG	1	1.32	1.694	0.78	1.0000
24	PEG	2	0.24	1.694	0.14	1.0000
24	PEG	3	0.07	1.694	0.04	1.0000
24	PEG-BH	1	-7.20	1.694	-4.25	0.0239
24	PEG-BH	2	-9.25	1.694	-5.46	0.0004
24	PEG-BH	3	-10.73	1.694	-6.34	0.0001
36	BH	1	-19.15	1.694	-11.31	0.0001
36	BH	2	-40.16	1.694	-23.72	0.0001
36	BH	3	-94.54	1.694	-55.82	0.0001
36	PEG	1	-0.21	1.694	-0.12	1.0000
36	PEG	2	-1.64	1.694	-0.97	1.0000
36	PEG	3	-3.91	1.694	-2.31	0.9197
36	PEG-BH	1	-9.06	1.694	-5.35	0.0006
36	PEG-BH	2	-13.02	1.694	-7.69	0.0001
36	PEG-BH	3	-13.76	1.694	-8.12	0.0001

TIME = 12
POLY = PEG-BH
CONC = 1 subtracted from:

TIME	POLY	CONC	Difference of Means	SE of Difference	T-Value	Adjusted P-Value
12	PEG-BH	2	-0.84	1.694	-0.49	1.0000
12	PEG-BH	3	-0.90	1.694	-0.53	1.0000
24	BH	1	-11.82	1.694	-6.98	0.0001
24	BH	2	-23.00	1.694	-13.58	0.0001
24	BH	3	-37.33	1.694	-22.04	0.0001
24	PEG	1	7.91	1.694	4.67	0.0061
24	PEG	2	6.83	1.694	4.03	0.0457
24	PEG	3	6.66	1.694	3.93	0.0610
24	PEG-BH	1	-0.61	1.694	-0.36	1.0000
24	PEG-BH	2	-2.66	1.694	-1.57	0.9998
24	PEG-BH	3	-4.14	1.694	-2.44	0.8639
36	BH	1	-12.56	1.694	-7.42	0.0001
36	BH	2	-33.57	1.694	-19.82	0.0001
36	BH	3	-87.95	1.694	-51.93	0.0001
36	PEG	1	6.38	1.694	3.77	0.0958
36	PEG	2	4.95	1.694	2.93	0.5410
36	PEG	3	2.68	1.694	1.58	0.9997
36	PEG-BH	1	-2.47	1.694	-1.46	0.9999
36	PEG-BH	2	-6.43	1.694	-3.80	0.0889
36	PEG-BH	3	-7.16	1.694	-4.23	0.0254

TIME = 12
POLY = PEG-BH
CONC = 2 subtracted from:

TIME	POLY	CONC	Difference of Means	SE of Difference	T-Value	Adjusted P-Value
12	PEG-BH	3	-0.06	1.694	-0.04	1.0000
24	BH	1	-10.98	1.694	-6.48	0.0001
24	BH	2	-22.16	1.694	-13.08	0.0001
24	BH	3	-36.49	1.694	-21.55	0.0001
24	PEG	1	8.74	1.694	5.16	0.0011
24	PEG	2	7.67	1.694	4.53	0.0098
24	PEG	3	7.50	1.694	4.43	0.0136
24	PEG-BH	1	0.23	1.694	0.13	1.0000
24	PEG-BH	2	-1.82	1.694	-1.07	1.0000
24	PEG-BH	3	-3.30	1.694	-1.95	0.9901
36	BH	1	-11.72	1.694	-6.92	0.0001
36	BH	2	-32.74	1.694	-19.33	0.0001
36	BH	3	-87.12	1.694	-51.44	0.0001
36	PEG	1	7.22	1.694	4.26	0.0231
36	PEG	2	5.79	1.694	3.42	0.2225
36	PEG	3	3.51	1.694	2.07	0.9771
36	PEG-BH	1	-1.63	1.694	-0.96	1.0000
36	PEG-BH	2	-5.59	1.694	-3.30	0.2838
36	PEG-BH	3	-6.33	1.694	-3.74	0.1038

TIME = 12
POLY = PEG-BH
CONC = 3 subtracted from:

TIME	POLY	CONC	Difference of Means	SE of Difference	T-Value	Adjusted P-Value
24	BH	1	-10.92	1.694	-6.45	0.0001
24	BH	2	-22.10	1.694	-13.05	0.0001
24	BH	3	-36.43	1.694	-21.51	0.0001
24	PEG	1	8.81	1.694	5.20	0.0010
24	PEG	2	7.73	1.694	4.56	0.0087
24	PEG	3	7.56	1.694	4.46	0.0121
24	PEG-BH	1	0.29	1.694	0.17	1.0000
24	PEG-BH	2	-1.76	1.694	-1.04	1.0000
24	PEG-BH	3	-3.24	1.694	-1.91	0.9925
36	BH	1	-11.66	1.694	-6.89	0.0001
36	BH	2	-32.68	1.694	-19.29	0.0001
36	BH	3	-87.05	1.694	-51.40	0.0001
36	PEG	1	7.28	1.694	4.30	0.0206
36	PEG	2	5.85	1.694	3.46	0.2054
36	PEG	3	3.57	1.694	2.11	0.9715
36	PEG-BH	1	-1.57	1.694	-0.93	1.0000
36	PEG-BH	2	-5.53	1.694	-3.27	0.3049
36	PEG-BH	3	-6.27	1.694	-3.70	0.1139

TIME = 24
POLY = BH
CONC = 1 subtracted from:

TIME	POLY	CONC	Difference of Means	SE of Difference	T-Value	Adjusted P-Value
24	BH	2	-11.18	1.694	-6.60	0.0001
24	BH	3	-25.51	1.694	-15.06	0.0001

24	PEG	1	19.73	1.694	11.65	0.0001
24	PEG	2	18.65	1.694	11.01	0.0001
24	PEG	3	18.48	1.694	10.91	0.0001
24	PEG-BH	1	11.21	1.694	6.62	0.0001
24	PEG-BH	2	9.16	1.694	5.41	0.0005
24	PEG-BH	3	7.68	1.694	4.53	0.0096
36	BH	1	-0.74	1.694	-0.44	1.0000
36	BH	2	-21.76	1.694	-12.85	0.0001
36	BH	3	-76.13	1.694	-44.95	0.0001
36	PEG	1	18.20	1.694	10.75	0.0001
36	PEG	2	16.77	1.694	9.90	0.0001
36	PEG	3	14.49	1.694	8.56	0.0001
36	PEG-BH	1	9.35	1.694	5.52	0.0003
36	PEG-BH	2	5.39	1.694	3.18	0.3578
36	PEG-BH	3	4.65	1.694	2.75	0.6737

TIME = 24
POLY = BH
CONC = 2 subtracted from:

TIME	POLY	CONC	Difference of Means	SE of Difference	T-Value	Adjusted P-Value
24	BH	3	-14.33	1.694	-8.46	0.0001
24	PEG	1	30.91	1.694	18.25	0.0001
24	PEG	2	29.83	1.694	17.61	0.0001
24	PEG	3	29.66	1.694	17.51	0.0001
24	PEG-BH	1	22.39	1.694	13.22	0.0001
24	PEG-BH	2	20.34	1.694	12.01	0.0001
24	PEG-BH	3	18.86	1.694	11.13	0.0001
36	BH	1	10.44	1.694	6.16	0.0001
36	BH	2	-10.58	1.694	-6.25	0.0001
36	BH	3	-64.96	1.694	-38.35	0.0001
36	PEG	1	29.38	1.694	17.35	0.0001
36	PEG	2	27.95	1.694	16.50	0.0001
36	PEG	3	25.67	1.694	15.16	0.0001
36	PEG-BH	1	20.53	1.694	12.12	0.0001
36	PEG-BH	2	16.57	1.694	9.78	0.0001
36	PEG-BH	3	15.83	1.694	9.35	0.0001

TIME = 24
POLY = BH
CONC = 3 subtracted from:

TIME	POLY	CONC	Difference of Means	SE of Difference	T-Value	Adjusted P-Value
24	PEG	1	45.24	1.694	26.71	0.0001
24	PEG	2	44.16	1.694	26.08	0.0001
24	PEG	3	43.99	1.694	25.97	0.0001
24	PEG-BH	1	36.72	1.694	21.68	0.0001
24	PEG-BH	2	34.67	1.694	20.47	0.0001
24	PEG-BH	3	33.19	1.694	19.60	0.0001
36	BH	1	24.77	1.694	14.62	0.0001
36	BH	2	3.75	1.694	2.22	0.9489
36	BH	3	-50.62	1.694	-29.89	0.0001
36	PEG	1	43.71	1.694	25.81	0.0001
36	PEG	2	42.28	1.694	24.97	0.0001
36	PEG	3	40.00	1.694	23.62	0.0001
36	PEG-BH	1	34.86	1.694	20.58	0.0001
36	PEG-BH	2	30.90	1.694	18.24	0.0001

36	PEG-BH	3	30.16	1.694	17.81	0.0001

TIME = 24
POLY = PEG
CONC = 1 subtracted from:

TIME	POLY	CONC	Difference of Means	SE of Difference	T-Value	Adjusted P-Value
24	PEG	2	-1.08	1.694	-0.64	1.0000
24	PEG	3	-1.25	1.694	-0.74	1.0000
24	PEG-BH	1	-8.52	1.694	-5.03	0.0018
24	PEG-BH	2	-10.56	1.694	-6.24	0.0001
24	PEG-BH	3	-12.05	1.694	-7.11	0.0001
36	BH	1	-20.47	1.694	-12.09	0.0001
36	BH	2	-41.48	1.694	-24.49	0.0001
36	BH	3	-95.86	1.694	-56.60	0.0001
36	PEG	1	-1.53	1.694	-0.90	1.0000
36	PEG	2	-2.95	1.694	-1.74	0.9983
36	PEG	3	-5.23	1.694	-3.09	0.4202
36	PEG-BH	1	-10.38	1.694	-6.13	0.0001
36	PEG-BH	2	-14.34	1.694	-8.47	0.0001
36	PEG-BH	3	-15.07	1.694	-8.90	0.0001

TIME = 24
POLY = PEG
CONC = 2 subtracted from:

TIME	POLY	CONC	Difference of Means	SE of Difference	T-Value	Adjusted P-Value
24	PEG	3	-0.17	1.694	-0.10	1.0000
24	PEG-BH	1	-7.44	1.694	-4.39	0.0152
24	PEG-BH	2	-9.49	1.694	-5.60	0.0003
24	PEG-BH	3	-10.97	1.694	-6.48	0.0001
36	BH	1	-19.39	1.694	-11.45	0.0001
36	BH	2	-40.41	1.694	-23.86	0.0001
36	BH	3	-94.78	1.694	-55.97	0.0001
36	PEG	1	-0.45	1.694	-0.27	1.0000
36	PEG	2	-1.88	1.694	-1.11	1.0000
36	PEG	3	-4.16	1.694	-2.45	0.8583
36	PEG-BH	1	-9.30	1.694	-5.49	0.0004
36	PEG-BH	2	-13.26	1.694	-7.83	0.0001
36	PEG-BH	3	-14.00	1.694	-8.27	0.0001

TIME = 24
POLY = PEG
CONC = 3 subtracted from:

TIME	POLY	CONC	Difference of Means	SE of Difference	T-Value	Adjusted P-Value
24	PEG-BH	1	-7.27	1.694	-4.29	0.0209
24	PEG-BH	2	-9.32	1.694	-5.50	0.0003
24	PEG-BH	3	-10.80	1.694	-6.38	0.0001
36	BH	1	-19.22	1.694	-11.35	0.0001
36	BH	2	-40.24	1.694	-23.76	0.0001
36	BH	3	-94.61	1.694	-55.87	0.0001
36	PEG	1	-0.28	1.694	-0.17	1.0000
36	PEG	2	-1.71	1.694	-1.01	1.0000
36	PEG	3	-3.99	1.694	-2.35	0.9038

36	PEG-BH	1	-9.13	1.694	-5.39	0.0005
36	PEG-BH	2	-13.09	1.694	-7.73	0.0001
36	PEG-BH	3	-13.83	1.694	-8.16	0.0001

TIME = 24
POLY = PEG-BH
CONC = 1 subtracted from:

TIME	POLY	CONC	Difference of Means	SE of Difference	T-Value	Adjusted P-Value
24	PEG-BH	2	-2.05	1.694	-1.21	1.0000
24	PEG-BH	3	-3.53	1.694	-2.08	0.9755
36	BH	1	-11.95	1.694	-7.06	0.0001
36	BH	2	-32.97	1.694	-19.47	0.0001
36	BH	3	-87.34	1.694	-51.57	0.0001
36	PEG	1	6.99	1.694	4.13	0.0348
36	PEG	2	5.56	1.694	3.28	0.2946
36	PEG	3	3.28	1.694	1.94	0.9909
36	PEG-BH	1	-1.86	1.694	-1.10	1.0000
36	PEG-BH	2	-5.82	1.694	-3.44	0.2136
36	PEG-BH	3	-6.56	1.694	-3.87	0.0725

TIME = 24
POLY = PEG-BH
CONC = 2 subtracted from:

TIME	POLY	CONC	Difference of Means	SE of Difference	T-Value	Adjusted P-Value
24	PEG-BH	3	-1.48	1.694	-0.88	1.0000
36	BH	1	-9.91	1.694	-5.85	0.0001
36	BH	2	-30.92	1.694	-18.26	0.0001
36	BH	3	-85.30	1.694	-50.36	0.0001
36	PEG	1	9.04	1.694	5.34	0.0006
36	PEG	2	7.61	1.694	4.49	0.0110
36	PEG	3	5.33	1.694	3.15	0.3806
36	PEG-BH	1	0.19	1.694	0.11	1.0000
36	PEG-BH	2	-3.77	1.694	-2.23	0.9456
36	PEG-BH	3	-4.51	1.694	-2.66	0.7336

TIME = 24
POLY = PEG-BH
CONC = 3 subtracted from:

TIME	POLY	CONC	Difference of Means	SE of Difference	T-Value	Adjusted P-Value
36	BH	1	-8.42	1.694	-4.97	0.0021
36	BH	2	-29.44	1.694	-17.38	0.0001
36	BH	3	-83.81	1.694	-49.49	0.0001
36	PEG	1	10.52	1.694	6.21	0.0001
36	PEG	2	9.09	1.694	5.37	0.0005
36	PEG	3	6.81	1.694	4.02	0.0472
36	PEG-BH	1	1.67	1.694	0.99	1.0000
36	PEG-BH	2	-2.29	1.694	-1.35	1.0000
36	PEG-BH	3	-3.03	1.694	-1.79	0.9974

TIME = 36
POLY = BH
CONC = 1 subtracted from:

TIME	POLY	CONC	Difference of Means	SE of Difference	T-Value	Adjusted P-Value
36	BH	2	-21.01	1.694	-12.41	0.0001
36	BH	3	-75.39	1.694	-44.52	0.0001
36	PEG	1	18.94	1.694	11.18	0.0001
36	PEG	2	17.51	1.694	10.34	0.0001
36	PEG	3	15.24	1.694	9.00	0.0001
36	PEG-BH	1	10.09	1.694	5.96	0.0001
36	PEG-BH	2	6.13	1.694	3.62	0.1395
36	PEG-BH	3	5.40	1.694	3.19	0.3554

TIME = 36
POLY = BH
CONC = 2 subtracted from:

TIME	POLY	CONC	Difference of Means	SE of Difference	T-Value	Adjusted P-Value
36	BH	3	-54.38	1.694	-32.11	0.0001
36	PEG	1	39.96	1.694	23.59	0.0001
36	PEG	2	38.53	1.694	22.75	0.0001
36	PEG	3	36.25	1.694	21.40	0.0001
36	PEG-BH	1	31.11	1.694	18.37	0.0001
36	PEG-BH	2	27.14	1.694	16.03	0.0001
36	PEG-BH	3	26.41	1.694	15.59	0.0001

TIME = 36
POLY = BH
CONC = 3 subtracted from:

TIME	POLY	CONC	Difference of Means	SE of Difference	T-Value	Adjusted P-Value
36	PEG	1	94.33	1.694	55.70	0.0001
36	PEG	2	92.91	1.694	54.86	0.0001
36	PEG	3	90.63	1.694	53.51	0.0001
36	PEG-BH	1	85.49	1.694	50.48	0.0001
36	PEG-BH	2	81.52	1.694	48.14	0.0001
36	PEG-BH	3	80.79	1.694	47.70	0.0001

TIME = 36
POLY = PEG
CONC = 1 subtracted from:

TIME	POLY	CONC	Difference of Means	SE of Difference	T-Value	Adjusted P-Value
36	PEG	2	-1.43	1.694	-0.843	1.0000
36	PEG	3	-3.71	1.694	-2.188	0.9558
36	PEG-BH	1	-8.85	1.694	-5.225	0.0009
36	PEG-BH	2	-12.81	1.694	-7.564	0.0001
36	PEG-BH	3	-13.55	1.694	-7.999	0.0001

TIME = 36
POLY = PEG
CONC = 2 subtracted from:

TIME	POLY	CONC	Difference of Means	SE of Difference	T-Value	Adjusted P-Value
36	PEG	3	-2.28	1.694	-1.345	1.0000
36	PEG-BH	1	-7.42	1.694	-4.382	0.0158
36	PEG-BH	2	-11.38	1.694	-6.722	0.0001
36	PEG-BH	3	-12.12	1.694	-7.156	0.0001

TIME = 36
POLY = PEG
CONC = 3 subtracted from:

TIME	POLY	CONC	Difference of Means	SE of Difference	T-Value	Adjusted P-Value
36	PEG-BH	1	-5.142	1.694	-3.036	0.4587
36	PEG-BH	2	-9.105	1.694	-5.376	0.0005
36	PEG-BH	3	-9.841	1.694	-5.811	0.0002

TIME = 36
POLY = PEG-BH
CONC = 1 subtracted from:

TIME	POLY	CONC	Difference of Means	SE of Difference	T-Value	Adjusted P-Value
36	PEG-BH	2	-3.963	1.694	-2.340	0.9093
36	PEG-BH	3	-4.698	1.694	-2.774	0.6544

TIME = 36
POLY = PEG-BH
CONC = 2 subtracted from:

TIME	POLY	CONC	Difference of Means	SE of Difference	T-Value	Adjusted P-Value
36	PEG-BH	3	-0.7356	1.694	-0.4343	1.000

Residual Plots for CELL VIABILITY

Interaction Plot for CELL VIABILITY

A2. Residual Plots for Cell Viability

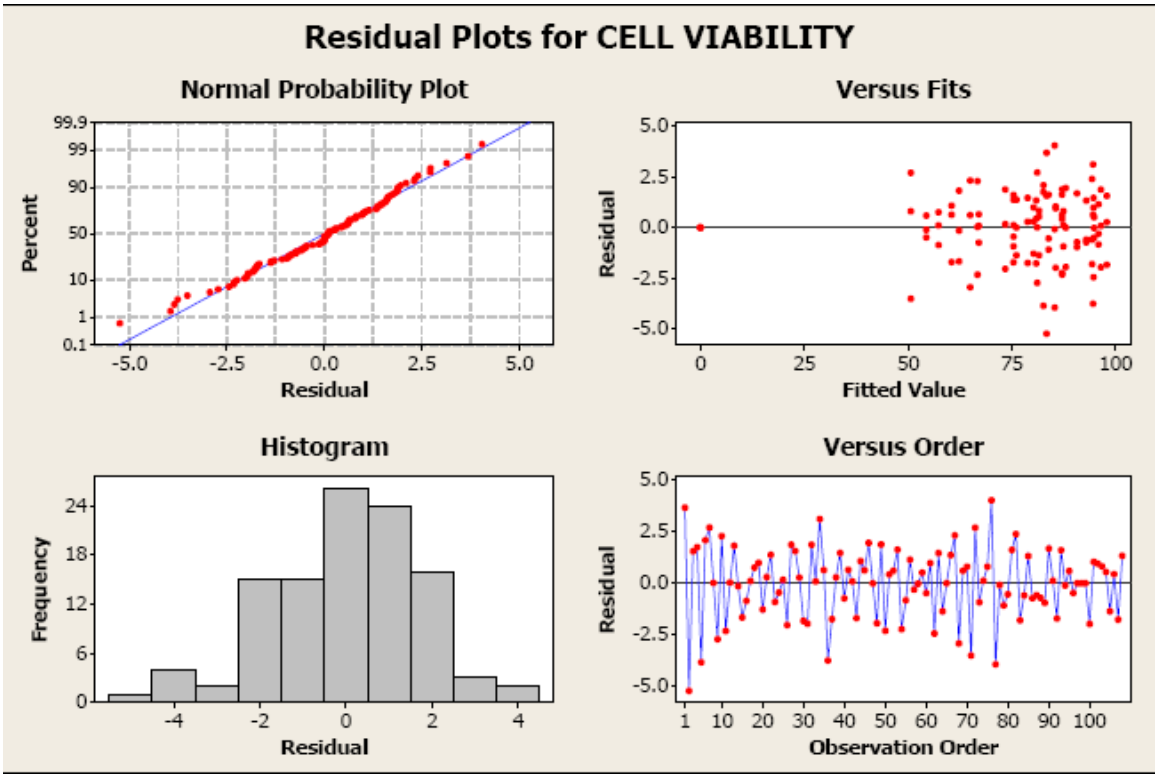

A3. Interaction Plot for Cell Viability

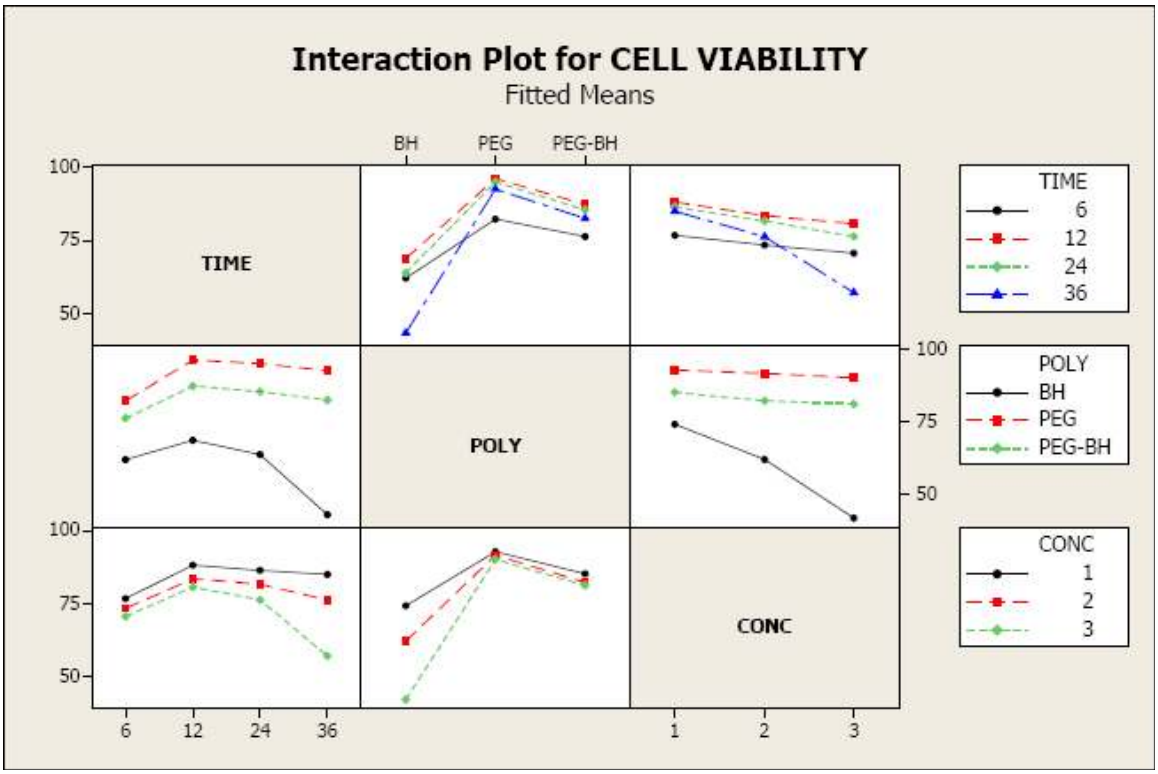

APPENDIX B

AUTHOR'S PERMISSION

From: Oleg Lukin (olukin@ccmsi.us)
To: Vinu Krishnan
Date: Thursday, November 8, 2007 4:34:27 AM
Subject: Re: Permission to use the dendrimer picture

Please use the picture with a reference to me,
Regards,
O. Lukin

-------- Original Message --------
From: "Vinu Krishnan" <vk11@uakron.edu>
To: olukin@ccmsi.us
Subject: Permission to use the dendrimer picture
Date: 07.11.2007 16:31

> Hi,
>
> My name is Vinu Krishnan, and I am currently here at the University of Akron doing my graduate research work on Dendrimers. I would like to get your permission to use the dendrimer picture you have uploaded on Wikipedia. The link is posted here.
>
> http://en.wikipedia.org/wiki/Dendrimer
>
> Please do let me know as soon as possible.
>
> Vinu Krishnan
> Graduate Research Assistant (Department of Polymer Science)
> Graduate Student (Biomaterials-Nanomedicine, Department of Biomedical Engineering)
> The University of Akron, Ohio
> www.uakron.edu